

# **Glycosylation of LRP6 regulates Wnt signaling**

Zur Erlangung des akademischen Grades eines

DOKTORS DER NATURWISSENSCHAFTEN

(Dr. rer. nat.)

Fakultät für Chemie und Biowissenschaften

Karlsruher Institut für Technologie (KIT) - Universitätsbereich

genehmigte

DISSERTATION

von

Diplom Biologe (KIT) Nico Andreas Braunegger

aus

Baden-Baden

Dekan: Prof. Dr. Peter Roesky  
Referent: Dr. Gary Davidson  
Korreferenten: Apl. Prof. Dr. Andrew Cato  
Priv. Doz. Dr. Ute Schepers

Tag der mündlichen Prüfung: 23.10.2015

I confirm that the presented thesis is an original work completed independently without inadmissible outside help. Any help or reference is stated in this thesis. Furthermore, I confirm that I obeyed the statutes of the University Karlsruhe (TH) especially with regard to good scientific practice.

Nico Andreas Braunegger, September 2015



# Abstract

---

The Wnt signaling pathway has been proven to be a key regulator for stem cell self-renewal, for cell proliferation and for differentiation. Through development and adult homeostasis, Wnt signaling is tightly controlled at many levels and by multiple mechanisms. While properly regulated Wnt signaling accounts for normal development and homeostasis, aberrant signaling leads to embryonic misdevelopment and diseases including carcinogenesis, diabetes type II and bone disease.

The Wnt co-receptor LRP6 is acting as a key regulator for transmission of the extracellular Wnt signal into the cell. LRP6 is therefore located at the cell surface. Subsequently, the binding of Wnt ligands to the LRP6 extracellular domain elicits multiple phosphorylation events on the LRP6 intracellular domain.

An unsolved issue in the field of Wnt/ $\beta$ -catenin signaling concerns the involvement of the asparagine-attached oligosaccharides (N-glycans) on the LRP6 extracellular domain in Wnt signaling. While it has been clearly shown that LRP5/6 generally need N-glycosylation to reach their destination, i.e. the cell surface, and that this process modulates Wnt signaling, only little is known about the N-glycosyltransferases mediating the oligosaccharide attachment and processing. Recently the N-glycan  $\beta$ -1,6-branch inducing MGAT-V, acting at an early step of N-glycan diversification, was shown to modulate Wnt signaling. However, the main diversifying N-glycosyltransferases which contribute to the length of the N-glycan antennae (GlcNAc transferases and galactose transferases) remain unknown.

In this study I provide the first evidence that an N-glycan antennae elongating GlcNAc transferase, B3GNT8, modulates canonical Wnt signaling by adding mass specifically to LRP6. My work supports a model where B3GNT8 modifies certain LRP6 subspecies to modulate their Golgi-to-surface transport. In addition, my study identifies for the first time a GlcNAc transferase that is involved in metabolic regulation of Wnt signaling. A model in which B3GNT8 promotes LRP6 Golgi-to-surface transport under the influence of metabolic processes is therefore proposed.

# Zusammenfassung

---

Der Wnt-Signalweg ist ein Schlüsselement in der Regulation von Stammzellen-Erneuerung, Zellproliferation und Differenzierung. Während der organismalen Entwicklung und während adulter Homöostaseprozesse ist der Wnt-Signalweg engmaschig auf mehreren Ebenen und durch mehrere Mechanismen kontrolliert. Während ein innerhalb homöostatischer Grenzen funktionierender Wnt-Signalweg zu normaler Entwicklung und normalen Homöostaseprozessen führt, führt abweichende Aktivierung zu embryonaler Fehlentwicklung und zu Krankheiten wie Krebs, Diabetes vom Typ II und Knochenkrankheiten.

Der Wnt Co-Rezeptor LRP6 agiert als Schlüsselregulator bei der Transmission der extrazellulären Wnt-Signale in die Zellen hinein. Aus diesem Grund ist LRP6 an der Zelloberfläche lokalisiert. Das Binden des Wnt Liganden an die extrazelluläre Domäne von LRP6 löst nachfolgend mehrere Phosphorylierungsereignisse an der intrazellulären Domäne von LRP6 aus.

Ein ungelöstes Sachverhalt im wissenschaftlichen Feld des Wnt-Signalwegs betrifft die Teilnahme der Asparagin-gebundenen Oligosaccharide (N-Glykane) auf der extrazellulären Domäne von LRP6 im Wnt-Signalweg. Während klar gezeigt werden konnte, dass LRP5/6 generell N-Glykosylierungen brauchen um ihren Zielort, die Zelloberfläche, zu erreichen und dass dieser Prozess das Wnt-Signaling moduliert, ist nur wenig bekannt über die N-Glykosyltransferasen, die das Anheften und die Prozessierung des Oligosaccharides ausführen. Kürzlich wurde der  $\beta$ -1,6-Verzweigung-induzierenden MGAT-V, welche an einer frühen Stufe der N-Glykan-Diversifizierung wirkt, eine Mitwirkung in der Modulation des Wnt-Signalwegs nachgewiesen. Jedoch bleiben die Hauptdiversifizierungsenzyme der N-Glykane im Wnt-Signalweg, die welche zur Länge der N-Glykan-Antennen beitragen (GlcNAc- und Galactosyl-Transferasen), unentdeckt.

In dieser Studie biete ich den ersten Beweis, dass eine N-Glykan-Antennen verlängernde GlcNAc-Transferase, B3GNT8, den Wnt-Signalweg moduliert durch das Hinzufügen von Masse spezifisch an LRP6. Meine Arbeit unterstützt ein Modell, in welchem B3GNT8 bestimmte LRP6-Subspezies modifiziert, um deren Transport vom Golgi zu der Zelloberfläche zu verstärken. Darüber hinaus identifiziert diese Studie zum ersten Mal eine GlcNAc-Transferase, B3GNT8, welche in die metabolische Regulierung des Wnt-Signalweges involviert ist. Deshalb wird ein Modell vorgeschlagen, in welcher B3GNT8 den Transport einer bestimmten LRP6-Subspezies vom Golgi zur Zelloberfläche unter dem Einfluss metabolischer Prozesse unterstützt.

# Content

---

Independence Declaration	I
Abstract	II
Zusammenfassung	III
Content	IV
Figure Index	VII
Table Index	IX
Abbreviations	X
<b>1. Introduction</b>	<b>1</b>
1.1 Wnt signaling	1
1.2 The known Wnt pathways	1
1.3 The mechanism of $\beta$ -catenin dependent Wnt signaling	3
1.4 The key components of canonical Wnt signaling	4
1.5 The Wnt co-receptor LRP6 - our field of interest	6
1.6 The N-glycosylation process	8
1.7 B3GNT8s role in N-glycosylation	13
1.8 N-glycosyltransferases and N-glycosylated pathway members in Wnt signaling	15
1.9 N-glycosylation of the Wnt co-receptor LRP6	16
<b>2. Aim of the Study</b>	<b>19</b>
<b>3. Results</b>	<b>20</b>
3.1 Identification of a GlcNAc transferase that covalently modifies LRP6 and stimulates Wnt signaling	20
3.2 B3GNT8 modifies endogenous Wnt signaling and promotes an LRP6 subspecies	22
3.3 LRP6 has 4 N-glycosylation sites that are highly conserved	24
3.4 B3GNT8 modifies the complex N-glycans of LRP6	24
3.5 B3GNT8 co-immunoprecipitates with LRP6	26
3.6 B3GNT8 acts at the level of the activated Wnt receptor complex	27
3.7 B3GNT8 specifically adds mass onto LRP6 to regulate Wnt signaling	30
3.8 B3GNT8 does not appear to modify LRP5	32
3.9 In HEK293 cells, B3GNT8 does not synergistically enhance the activity of B3GNT2 to stimulate Wnt signaling	33
3.10 B3GNT8 is required for LRP6 / Wnt signaling	34
3.11 B3GNT8 is sufficient to rescue LRP6 protein levels, Wnt signaling and cell proliferation	35
3.12 B3GNT8 LoF in HEK293 cells mainly influences Wnt signaling	36

3.13	B3GNT8 reduces Wnt/PCP signaling	42
3.14	B3GNT8 increases the cell surface levels of LRP6	43
3.15	The first two conserved LRP6 N-glycans are able to contact ligands	46
3.16	B3GNT8 acts in hexose induced Wnt signaling	48
4.	Discussion	54
4.1	The decision criteria for pursuing the characterization of B3GNT8	54
4.1.1	Identification of B3GNT8	54
4.2	Participation of B3GNT8 in Wnt signaling	55
4.2.1	Direct or indirect modification of the LRP6 N-glycans by B3GNT8	55
4.2.2	Participation of the B3GNT8-modified LRP6 in Wnt signaling	57
4.2.3	B3GNT8s enzymatic activity and Wnt pathway members	57
4.2.4	B3GNT2 and the modification of LRP6 and Wnt signaling in HEK293 cells	58
4.2.5	B3GNT8 siRNA gene silencing in LRP6/Wnt signaling	59
4.3	Functions of B3GNT8-modified LRP6 N-glycans	59
4.3.1	B3GNT8 in LRP6 Golgi-to-surface transport	59
4.3.2	B3GNT8 in LRP6/ligand interaction	60
4.3.3	B3GNT8 in signalosome endocytosis	61
4.4	B3GNT8 and other pathways	61
4.4.1	B3GNT8 and Wnt/PCP signaling	61
4.4.2	B3GNT8 and the N-glycosylation pathway	62
4.4.3	B3GNT8 and cell cycle	62
4.4.4	B3GNT8 siRNA gene silencing and Wnt, p53, TGF $\beta$ , Shh, FGF, and MAPK signaling pathway	62
4.5	LRP6 and B3GNT8 in metabolic regulation of Wnt signaling	63
4.5.1	LRP6 and hexose induced Wnt signaling	63
4.5.2	B3GNT8 and hexose induced Wnt signaling	64
4.6	Consequences of my study	65
5.	Materials and Methods	67
5.1	Methods	67
5.1.1	Maintenance of Cells	67
5.1.2	Transient ScreenfectA Transfection of Cell Lines for Overexpression Experiments	67
5.1.3	Transient Promofectin Transfection of Cell Lines for Overexpression Experiments	67
5.1.4	ScreenfectA Transfection of Cell Lines for siRNA Experiments	68
5.1.5	Cell Lysis for SDS-PAGE / Western Blotting	68
5.1.6	Bradford Assay	68

5.1.7	Sodium Dodecyl Sulfate – Polyacrylamide Gel Electrophoresis (SDS-PAGE)	68
5.1.8	Semi-Dry Western Blotting	69
5.1.9	Western Blotting with Trans Blot Turbo System	69
5.1.10	Blocking, Incubation with Primary and Secondary Antibodies, and Washing with the BioLane InSitu Hybridization Mashine	69
5.1.11	Blocking, Incubation with Primary and Secondary Antibodies, and Washing with the BioLane InSitu Hybridization Mashine	69
5.1.12	Transformation of Electro-competent Escherichia coli Strains	70
5.1.13	Transformation of Chemo-Competent Escherichia coli Strains	70
5.1.14	Plasmid Preparation with the PEQlab Mini-Prep Kits (peqlab)	70
5.1.15	Endonuclease Digestion of Plasmids and DNA	70
5.1.16	Luciferase Assays	71
5.1.17	Cell Surface Biotinylation	71
5.1.18	Immunoprecipitation	71
5.1.19	Polymerase Chain Reaction (PCR)	72
5.1.20	RNA Extraction	72
5.1.21	DNase I Digestion	72
5.1.22	Reverse Transcriptase PCR (RT-PCR)	72
5.1.23	Real Time PCR (qPCR)	72
5.1.24	RNAseq	73
5.1.25	Fixation of Cells in Formaldehyde	73
5.1.26	Peptide-N-Glycosidase F (PNGaseF) Digestion of LRP6	73
5.1.27	Endoglycosidase H Digestion of LRP6	73
5.1.28	Co-Immunoprecipitation	73
5.2	Materials	74
5.2.1	Consumables	74
5.2.2	Equipment	76
5.2.3	Buffers and Premixed Solutions	77
5.2.4	siRNA	78
5.2.5	Antibodies	79
5.2.6	RNAseq - target genes of different pathways	80
5.2.7	qPCR primer	83
5.2.8	Plasmids	83
	References	85
	Appendix	103
	Acknowledgements	108
	Dank	109
	Curriculum Vitae	110

# Figure Index

---

Figure 1:	The known Wnt pathways and their cellular response.	2
Figure 2:	ON state, OFF state and aberrant activation of Wnt/ $\beta$ -catenin signaling.	4
Figure 3:	Crystal structure of the <i>Xenopus laevis</i> Wnt8 in complex with the cysteine rich domain (CRD) of Frizzled8.	5
Figure 4:	Schematic view of LRP6 with a more detailed structure of the extracellular domain (ECD).	7
Figure 5:	The N-glycosylation process and the major N-glycan types.	12
Figure 6:	The Localization of B3GNT8 and products of B3GNT8s enzymatic function.	14
Figure 7:	Schematic view of LRP6 with a more detailed structure of the extracellular domain (ECD).	17
Figure 8:	Identification of B3GNT8.	21
Figure 9:	Only B3GNT8 modifies LRP6 and modulates Wnt signaling.	22
Figure 10:	B3GNT8 GoF stimulates exogenous and endogenous Wnt-signaling.	23
Figure 11:	Alignment of LRP6 from different species with LRP5.	24
Figure 12:	B3GNT8 modifies the N-glycans of LRP6.	25
Figure 13:	B3GNT8 modifies the complex N-glycans of LRP6.	26
Figure 14:	LRP6 co-immunoprecipitates with B3GNT8.	27
Figure 15:	B3GNT8 GoF acts at the level of the activated receptor complex.	28
Figure 16:	B3GNT8 LoF acts at the level of the activated receptor complex.	29
Figure 17:	B3GNT8 expression synergizes with Rab5 dependent Wnt stimulation.	30
Figure 18:	B3GNT8 specifically adds mass to LRP6 to regulate Wnt-signalling.	31
Figure 19:	LRP5 reduces B3GNT8 protein levels.	32
Figure 20:	Only B3GNT8 functionally modifies LRP6.	33
Figure 21:	B3GNT8 siRNA affects LRP6 and TOPFLASH.	35
Figure 22:	Rescue of B3GNT8 siRNA effects.	36
Figure 23:	Correlation analysis of samples for RNAseq confirms similarity for each condition.	37
Figure 24:	Three analysis identify Wnt signaling as differentially regulated by B3GNT8 LoF.	39
Figure 25:	RNAseq of Control siRNA vs. B3GNT8 siRNA treated HEK293T cells.	41
Figure 26:	B3GNT8 expression decreases Wnt/PCP signaling.	42
Figure 27:	B3GNT8 increases cell surface levels of LRP6.	43
Figure 28:	B3GNT8 co-localizes with and increases cell surface levels of LRP6.	46

Figure 29:	The first two conserved LRP6 N-glycans are in close spatial proximity to known MESD binding sites.	47
Figure 30:	FBS reduction increases TOPFLASH response and reduces LRP6 protein bands.	49
Figure 31:	Wnt-signaling and LRP6 react to glucose/glutamine reduction.	50
Figure 32:	B3GNT8 rescues upper LRP6 bands and TOPFLASH signaling in glucose/glutamine reduced media.	52
Figure 33:	Co-expression of B3GNT8 with LRP6 augments hexose sensitivity of TOPFLASH signaling in HEK293 cells.	53
Figure 34:	Model: B3GNT8 adds modifications to and enhances the cell surface transport of LRP6 under the influence of metabolic processes.	66
Supplementary Figure 1:	RNAseq, Principal Component Analysis	103

# Tables Index

---

Table1:	Abbreviations	X
Table 2:	Description of consumables	74
Table 3:	Description of equipment	76
Table 4:	Description of Buffers and Premixed Solutions	77
Table 5:	Description of siRNAs	78
Table 6:	Description of primary antibodies	79
Table 7:	Description of secondary antibodies	79
Table 8:	Description of target genes from different pathways	80
Table 9:	Description of qPCR primers	83
Table 10:	Description of plasmids used in this study	83
Supplementary Table 1:	Quality of raw reads after base calling	103
Supplementary Table 2:	Differentially regulated genes in B3GNT8 silenced HEK293 cells	104



# Abbreviations

---

<u>Abbreviation</u>	<u>Name</u>
APC	Adenomatous Polyposis Coli
APCDD1	Adenomatosis Polyposis Coli Down-Regulated 1
ATF2	Activating Transcription Factor 2
ATP	Adenosine-triphosphate
ATRA	All-trans retinoic acid
Axin	Axis inhibition protein
B3GNT	$\beta$ -1,3-N-acetylglucosaminyltransferase
BFDR	Benjamini False Discovery Rate Correction
BP	$\beta$ -propeller
BSA	Bovine serum albumin
C1q	Complement 1q
CAMKII	Calcium / Calmodulin Dependent Kinase II
CDG	congenital disorders of glycosylation
CDK	Cyclin dependent kinase
cDNA	complementary DANN
CK1	Casein kinase 1
CM	conditioned media
CoIP	Co-immunoprecipitation
COS-7	fibroblast-like monkey kidney cell line
CRD	Cysteine Rich Domain
CTLA-4	cytotoxic T-lymphocyte-associated Protein 4
Dkk	Dickkopf (german, means "big head")
DMEM	Dulbecco's Modified Eagle Medium
DMEM <sup>-/red</sup>	glutamine-free, glucose-reduced DMEM
DMSO	Dimethylsulfoxide
DPAGT1	Dolichyl-Phosphate N-Acetylglucosaminophosphotransferase 1
DTT	Dithiothreitol
Dvl	Dishevelled
EB	Elution Buffer
ECD	extracellular domain
ECL	Enhanced chemiluminescence
ECM	extracellular matrix
EDTA	Ethylenediaminetetraacetic acid
EGF-R	Epidermal Growth Factor Receptor
EndoH	endoglycosidase H
ER	Endoplasmic reticulum
FBS	Fetal Bovine Serum

FBS <sup>dial</sup>	dialyzed FBS
FGF	Fibroblast Growth Factor
FGFR	FGF Receptor
FLRT	fibronectin leucine rich transmembrane protein
Fz	Frizzled
Fzd	Frizzled
Gal	Galactose
GFAT	glutamine:fructose-6-phosphate amido transferase
GlcNAc	N-acetylglucosamine
GlcNAc-T	GlcNAc-Transferase
GLUT	Glucose transporter
GoF	gain-of-function
GSK3	Glycogen Synthase Kinase 3
HBP	hexosamine biosynthetic pathway
HCT15	Human colon adenocarcinoma cell line
HEK293T	Human embryonic kidney cells, immortalized, contain SV40 large T antigen
HFG	Helmholtz Forschungsgemeinschaft
HL60	Human promyelocytic leukemia cells
HRP	Horse Raddish Peroxidase
ICD	Intracellular domain
IGFBP	Insulin-like growth factor-binding protein
IGFR	Insulin-like Grotwh Factor Receptor
IgG	Immunglobulin G
J774.2	Mouse BALB/c monocyte macrophage cells
JNK	kinase
KEGG	Kyoto Encyclopedia of Genes and Genomes
KO	knock-out
LB	Luria Broth
LDLR	Low Density Lipoprotein Receptor
LoF	loss-of-function
LRP5/6	Low Density Lipoprotein Receptor Related Protein 5/6
LRP6 $\Delta$ C	truncated LRP6, lacks the ICD
LRP6 $\Delta$ E1-4	LRP6 construct with deleted YWTD $\beta$ -propeller/EGF modules
Man	Mannose
ManNAz	Azido-N acetylmannosamine
MAPK	Mitogen-activated protein kinases
Mbases	Megabases
MESD	Mesoderm development Candidate2
Mest/PEG1	Mesoderm Specific Transcript/Paternally expressed gene 1
MG132	proteasome inhibitor
MGAT-V	$\beta$ 1-6 N-acetylglucosaminyltransferase V
MMP	Matrix Metalloprotease
MO	Morpholino

MVB	Multivesicular Bodies
NDP-hexose	nucleotide diphosphate-activated hexose
ON	overnight
OST	oligosaccharyltransferase
pax2	paired box gene 2
PBS	Phosphate buffered saline
PCA	Principal Component analysis
PCP	planar cell polarity
PCR	Polymerase Chain Reaction
PDGFR	Platelet-derived growth factor receptor
Pen/Strep	Penicillin/Streptomycin
PF	cluster passing illumina chastitiy filter
PKC	Protein Kinase C
PMA	Phorbol 12-myristate 13-acetate
PNGaseF	Peptide-N-Glycosidase F
polyLacNAc	poly-N-acetyllactosamine
p-value	significance value
PVDF	Polyvinylidene fluoride
qPCR	Quantitative Real-time PCR
Rab5	small GTPase
rER	rough ER
RNA	Ribonucleic acid
ROCK	kinase
ROR2	neurotrophic tyrosine kinase, receptor-related 2
RT	Room Temperature
RT-PCR	Reverse Transkriptase-PCR
SDS-PAGE	Sodium dodecyl sulphate polyacrylamide gel electrophoresis
Shh	Sonic Hedgehog
siRNA	small interfering RNA
SNP	single nucleotide polymorphism
SOST	Sclerostin
TAC	Thesis Advisory Commitee
TbR	T-Brain
TBS	Tris-buffered saline
TCF/LEF	T-cell factor/Lymphoid enhancer-binding factor
Tf-R	Transferrin Receptor
TGF	Transfoming Growth Factor
TLB	triton lysis buffer
TOPFLASH	luciferase based reporter gene assay with TCF/LEF dependent promoter
Wnt	Wingless and Int
wt	wild-Type
$\beta$ -TrCP	E3 ubiquitin ligase

# 1. Introduction

---

## **1.1 Wnt signaling**

The Int1 gene was discovered to be an oncogene and was found to be related to the *Drosophila* Wg gene in 1982 by Nusse and Varmus. It took over a decade after this discovery to realize that the gene products of Int1 and Wg were part of a cellular signaling pathway, the so called Wnt pathway. Since then the Wnt pathway (or Wnt signaling) has proven to be a key regulator for stem cell self-renewal, for cell proliferation and for differentiation (Clevers, 2006; Logan and Nusse, 2004; Reya and Clevers, 2005). In embryonic development it is involved in primary body axis formation, in anteroposterior patterning, and in the organogenesis of limb, eye, skin, gut and liver (Kieckers and Niehrs, 2001; Yamaguchi, 2001). Also in adulthood, Wnt signaling regulates tissue homeostasis (Clevers and Nusse, 2012; MacDonald et al., 2009; Moon et al., 2004). Wnt signaling is tightly controlled at many levels and by multiple mechanisms. Aberrant Wnt signaling leads to defects in embryonic development as well as diseases including cancer, diabetes type II and bone disease (Lim and Nusse, 2013; Kim et al., 2013a; Polakis, 2012; Clevers and Nusse, 2012; Wray and Hartmann, 2012; Wang et al., 2012; Reya and Clevers, 2005; Peifer and Polakis, 2000; Polakis, 2000). Thus Wnt signaling is one of the most fundamental regulatory systems in all metazoan development and human pathogenesis. The regulation of Wnt signaling is therefore of profound relevance and research aimed at identifying the mechanisms used by cells to achieve this is highly active. Further insights into the mechanism of Wnt signaling regulation also holds promise for medical treatment of some major human diseases (Anastas and Moon, 2013).

Since Wnt signaling is highly evolutionarily conserved many model organisms are available for experimental studies. Invertebrate model organisms include the nematode *Caenorhabditis elegans* (Jackson and Eisenmann, 2012), the Cnidaria hydra (Hobmayer et al., 2000) and the fruit fly *Drosophila melanogaster* (Swarup and Verheyen, 2012). Vertebrate model organisms include *Xenopus spec.* (Kiecker and Niehrs, 2001), *Danio rerio* (Verkade and Heath, 2008) and *Mus musculus* (Wang et al., 2012). 30 years of experimentation with cell culture and model organisms have led to tremendous insights into the transduction and regulation that control the activity of the Wnt pathway.

## **1.2 The known Wnt pathways**

Wnt signaling is roughly divided into  $\beta$ -catenin dependent (canonical) and  $\beta$ -catenin independent (non-canonical) Wnt signaling (Cavallo et al., 1998) (fig. 1). The  $\beta$ -catenin

dependant pathway is the best characterised and uses the multifunctional  $\beta$ -catenin protein as a transcriptional co-activator. The levels of  $\beta$ -catenin are tightly regulated by its phosphorylation-dependent proteosomal degradation in the so-called  $\beta$ -catenin destruction complex (Logan and Nusse, 2004). Wnt receptor activation prevents this phosphorylation of  $\beta$ -catenin, allowing its accumulation in the cytoplasm, diffusion to the nucleus and activation of Wnt target genes. In addition to a Fzd receptor, LRP5/6 is required as a co-receptor for  $\beta$ -catenin dependent Wnt signaling.

The non-canonical Wnt signaling comprises the Wnt-Ca<sup>2+</sup>-pathway and planar cell polarity (PCP) signaling. PCP signaling is activated by binding of Wnts to Frizzled and further activates the small GTPases Rac and Rho. This consequently activates the kinases ROCK and JNK to regulate cytoskeleton rearrangement that regulate cell shape and cell migration. The PCP pathway requires the conserved signaling molecules Rac, Rho, Rock, JNK, Flamingo, Diego, Strabismus, Fat, and Prickle. But their detailed protein interactions have not been defined yet (Singh and Mlodzik, 2012).

Wnt-Ca<sup>2+</sup> signaling leads to calcium release, this activates calcineurin, the Calcium / Calmodulin Dependent Kinase II (CAMKII) and the Protein Kinase C (PKC) to regulate cell adhesion, migration, and cell destiny (De, 2011).

$\beta$ -catenin dependent Wnt signaling regulates induction and patterning of germ layers, controls the body axis formation, segment polarity, cell fate specification and cell proliferation (Logan and Nusse; 2004). Since the Wnt receptor LRP6 is the main topic of this study, the  $\beta$ -catenin dependent Wnt pathway will be discussed in detail in the next two paragraphs.

### The known Wnt pathways

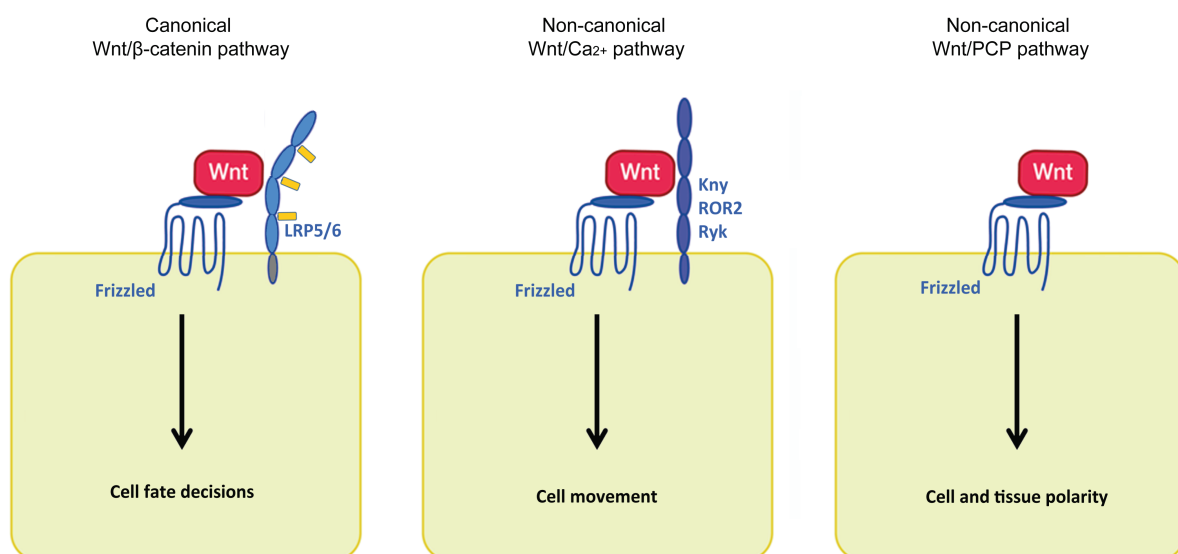


**Figure 1: The known Wnt pathways and their cellular response.**

The activation of either of the three known Wnt pathways depends on the particular combinations of Wnts, Frizzleds and co-receptors. For Wnt/ $\beta$ -catenin signaling binding of Wnts to LRP5/6 is a pre-requisite. Wnt/Ca<sup>2+</sup> signaling depends on the co-receptors Kny, ROR2

and Ryk. PCP signaling can be initiated by binding of particular Wnts to particular Frizzleds in the absence of co-receptors. The different pathways lead to different cellular responses. Modified after Logan and Nusse (2004).

### **1.3 The mechanism of $\beta$ -catenin dependent Wnt signaling**

Wnt/ $\beta$ -catenin can be represented by a simple ON/OFF model with or without Wnt, respectively (MacDonald et al., 2009; Logan and Nusse, 2004). In detail: at the surface of receiving cells Wnt ligands binds to both Fzd and Low Density Lipoprotein Receptor Related Proteins 5 or 6 (LRP5 or LRP6) to initiate signaling (fig. 2). In contrast to the other Wnt pathways, for  $\beta$ -catenin dependent signaling LRP5/6 is exclusively required in addition to the primary receptor Fzd (MacDonald and He, 2012a; He, 2004; Tamai et al., 2000). In the absence of a Wnt ligand cytosolic  $\beta$ -catenin is sequentially phosphorylated by the serine/threonine kinases Casein Kinase 1 alpha (CK1 $\alpha$ ) and Glycogen Synthase Kinase 3 (GSK3) to create a destruction recognition motif that is recognized by the E3 ubiquitin ligase  $\beta$ -TrCP and consequently ubiquitinated  $\beta$ -catenin is targeted for proteasomal degradation (Liu et al., 2002; Liu et al., 1999). GSK3, CK1 and  $\beta$ -catenin are part of the “ $\beta$ -catenin destruction complex” together with the scaffolding protein Axin and Adenomatous Polyposis Coli (APC) (Staos and Weis, 2013). When a Wnt ligand reaches a receiving cell it is incorporated into a ternary complex with Fzd and LRP5/6 which in turn recruits the scaffolding protein Dishevelled (Dvl) to Fzd (Gao and Chen, 2010). Large aggregates of Wnt receptors (called signalosomes) form as a result which leads to the phosphorylation of the PPPSP and CK1 sites in the intracellular domain (ICD) of LRP5/6. Consequently Axin is recruited to the phosphorylated LRP5/6 (Bilic et al., 2007; Tamai et al., 2004) and GSK3 is inactivated (Kim et al., 2013a; Pan et al., 2008a; Bilic et al., 2007; Cong, 2004). Through the phosphorylation of the LRP6 ICD GSK3 creates its own inhibitory substrate (Wu et al., 2009; Piao et al., 2008) thus providing a potential mechanism for activated Wnt receptors to directly inhibit the phosphorylation of  $\beta$ -catenin by GSK3. Another potential mechanism that has been proposed for GSK3 inhibition involves its sequestration into MVB's upon Wnt pathway activation (Taelman et al., 2010). Consequently,  $\beta$ -catenin is no longer degraded and is free to translocate into the nucleus where it binds to TCF/LEF transcription factors by replacing the transcription repressor Groucho and activates transcription of Wnt target genes. There are several well characterised Wnt target genes such as myc, cyclinD and Axin2 however the total number of Wnt target genes identified continues to grow, due to context and cell-specific Wnt signaling responses. Several Wnt target genes are themselves Wnt pathway components, highlighting the strong nature of feedback regulation (Lustig et al., 2002; Tetsu and McCormick, 1999; He et al., 1998). The exact mechanism by which the inactivation of the  $\beta$ -catenin destruction complex is achieved is not fully understood yet. Different studies support that either parts of the receptor complex or the whole complex is recruited to Fzd/LRP as a result of receptor activation events (Kim et al., 2013b; Li et al., 2012). Perturbations by e.g. mutation of pathway components can lead to aberrant activation (fig. 2).

A tight control of the level of  $\beta$ -catenin dependent Wnt signaling is important for tissues to function properly. Aberrant activation of Wnt signaling can lead e.g. to secondary axis formation or reduction in eye size in zebrafish (Chen et al., 2014). Several secreted and transmembrane activators and inhibitors exist to regulate Wnt signaling at the level of receptor activation, i.e. in addition to the Wnt-Fzd-LRP6 complex. Most of the Wnt signaling activators or inhibitors are highly conserved and many act at the level of LRP6, such as Wise/SOST (Itasaki et al., 2003; Li et al., 2005), IGFBP (Zhu et al., 2008), APCDD1 (Shimomura et al., 2010), Waif1 (Kagermeier-Schenk et al., 2011), ZNRF3m (Hao et al., 2012; Koo et al., 2012), C1q (Naito et al., 2012), Dickkopf (Dkk) (in vertebrates) (Bafico et al., 2001; Mao et al., 2001a) and R-spondin (Hao et al., 2012; Koo et al., 2012).

### Normal and dysregulated Wnt signaling

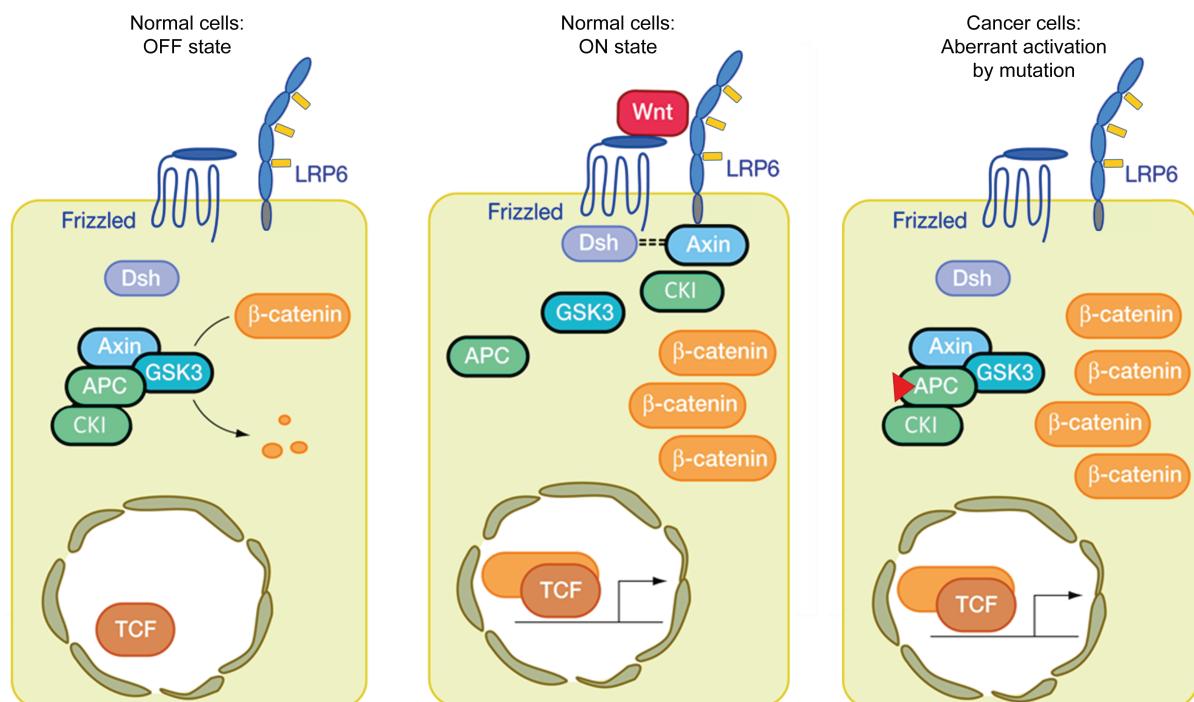


**Figure 2: ON state, OFF state and aberrant activation of Wnt/ $\beta$ -catenin signaling.**

Normal cells OFF state: In absence of the Wnt ligand, free  $\beta$ -catenin is constantly degraded by the so called  $\beta$ -catenin destruction complex consisting of Axin, GSK3, CK1 and APC.

Normal cells ON state: The Wnt ligand builds a ternary complex with Frizzleds and LRP5/6 which leads to inhibition of the  $\beta$ -catenin destruction complex by binding of Axin and Dsh to LRP5/6 and Frizzleds, respectively.  $\beta$ -catenin can accumulate and translocate into the nucleus where it acts as a co-activator together with the transcription factor TCF/LEF to induce Wnt target gene expression.

Cancer cells Aberrant activation: In absence of the Wnt ligand a mutation in APC or other pathway components (red triangle) inhibits the  $\beta$ -catenin destruction complex.  $\beta$ -catenin can accumulate and translocate into the nucleus where it starts expression of Wnt target genes as a co-activator together with the transcription factor TCF/LEF. Modified after Logan and Nusse (2004).

#### **1.4 The key components of canonical Wnt signaling**

The Wnt ligand is a family of secreted lipid-modified glycoproteins and comprises up to date 19 members. Wnts are lipid modified and thus are thought to be packaged and transported in lipoprotein particles or exosomes or within specific protein complexes (Gross and Boutros, 2013; Mulligan et al., 2012). Since it is very difficult to purify Wnts it is unknown where the



specificity of different Wnt ligands binding to its different receptors stems from. However, biochemical studies indicate that the binding of different Wnt/Fzd combinations to various co-receptors activates different signaling cascades (Niehrs, 2012; Angers and Moon, 2009; van Amerongen and Nusse, 2009). The most studied are Wnt1, Wnt 3a and Wnt8 and these are pre-dominantly involved in  $\beta$ -catenin dependent signaling. Additional to their lipid-modification Wnts can be N-glycosylated, in which some asparagine residues carry an N-linked oligosaccharide chain. Contrary to the lipid modification, the glycosylation sites fluctuate in the number and position on Wnts. The role of the N-glycosylation also is variable in the Wnt family: in several cellular contexts, replacement of N-glycosylation sites does not affect Wnt1-induced signaling, indicating that N-glycosylation is neither essential for signaling nor for secretion (Doubravska et al., 2011; Mason et al., 1992). This is supported by the position of one of the N-glycans on Wnt8, which sits right in the middle of the Wnt/Frizzled complex, and does not participate in Frizzled binding (Janda et al., 2012) (fig. 3). However, Wnt3a and Wnt5a N-glycosylation precedes the modification with a lipid and is important for proper Wnt secretion (Tang et al., 2012; Komekado et al., 2007; Kurayoshi et al., 2007).

### Crystal structure of Wnt8 in complex with Frizzled8-CRD

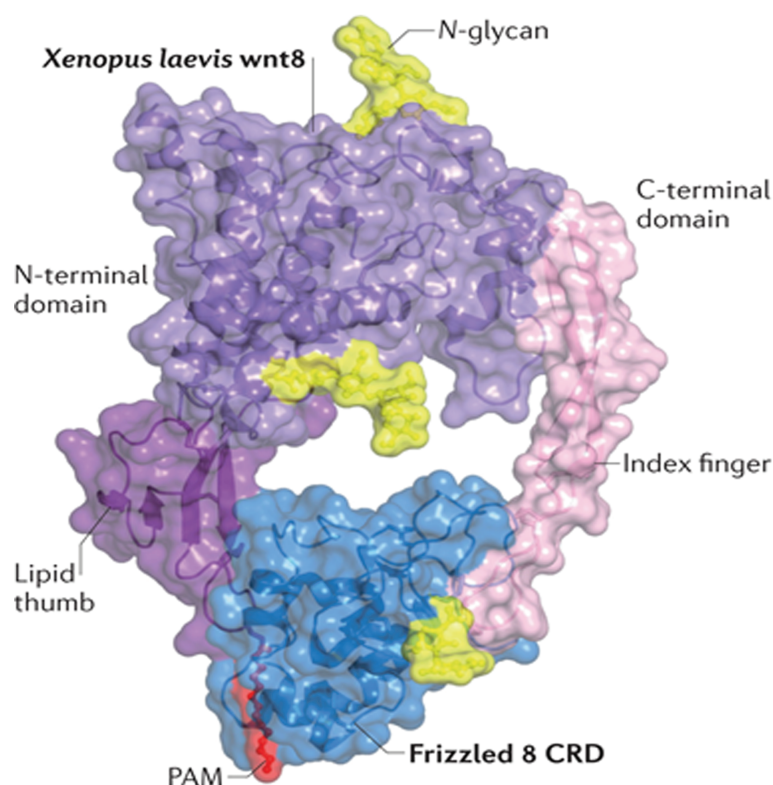


**Figure 3: Crystal structure of the *Xenopus laevis* Wnt8 in complex with the cysteine rich domain (CRD) of Frizzled8.**

The *Xenopus laevis* wnt8 is shown in purple, the N-terminal “lipid thumb” domain in deep purple, the C-terminal “index finger” domain in light pink and the palmitoleic acid (PAM) in red. The Frizzled 8 CRD is shown in blue. Rests of N-glycan are colored in yellow. Note the N-glycan rest of Wnt8 which is facing the Frizzled8 CRD but seems not to participate in binding. Modified after Niehrs (2012).



Fzd, the main Wnt receptor, is a seven-pass transmembrane glycoprotein. All family members possess an extracellular N-terminal Cysteine Rich Domain (CRD) and bind in an “index finger and thumb” conformation to Wnts (Janda et al., 2012). This ensures a high affinity and, at the same time, a specificity for the different Wnt/Fz combinations. Frizzleds share two highly conserved N-glycosylation sites and N-glycosylation mutants are retained in the ER (Milhem et al., 2014). But N-glycosylation mutants of Fzd8 and Secreted Frizzled Related Protein 3 (sFRP-3) exhibited an unchanged affinity for *Xenopus* Wnt8 (Dann et al., 2001).

$\beta$ -catenin is predominantly immobilized by cell membrane located cadherin. In absence of the Wnt ligand free  $\beta$ -catenin is constantly degraded. Upon Wnt binding  $\beta$ -catenin accumulates in the cytosol and then further translocates into the nucleus where it associates with TCF/LEF transcription factors.  $\beta$ -catenin is serine/threonine and tyrosine phosphorylated which modulates its stability (Valenta et al., 2012). Furthermore,  $\beta$ -catenin is O-glycosylated which regulates its transport into the nucleus and thus regulates its signaling activity (Sayat et al., 2008).

### **1.5 The Wnt co-receptor LRP6 - our field of interest**

Contrasting to the other Wnt pathways the co-receptor LRP5/6 is exclusively required in addition to the primary receptor Fzd in  $\beta$ -catenin dependent Wnt signaling (MacDonald and He, 2012a ; He, 2004; Tamai et al., 2000). LRP5/6 is therefore of great interest to the scientific field. LRP5/6 is a 1615/1613 amino acids single-span transmembrane protein and belongs to the Low Density Lipoprotein Receptor (LDLR) superfamily. Loss of the *Drosophila* orthologue arrow phenocopies the Wg mutant (Wehrli et al., 2000), which confirms it is essential for transduction of Wnt signaling. LRP5/6 is widely co-expressed during embryogenesis and in adults, which confirms their necessity for cell development and homeostasis (Kelly et al., 2004; Houston and Wylie, 2002; Dong et al., 1998; Hey et al., 1998). Unlike LRP5, expression of LRP6 alone in *Xenopus* embryos is sufficient to induce secondary axis formation. And LRP6<sup>-/-</sup> but not LRP5<sup>-/-</sup> mice are perinatal lethal (Kato et al., 2002; Pinson et al., 2000). This suggests that LRP6 is more active than LRP5 (He et al., 2004). On the other hand, LRP5 but not LRP6 is indispensable for adult bone homeostasis (He et al., 2004). But both LRP5 silencing and viable heterozygous LRP6<sup>+/-</sup> mice develop osteoporosis (low bone density) (Holmen et al., 2004). Since LRP6 seems more active than LRP5 in cell culture context, LRP6 is our labs field of interest and was used in all of my experiments except where indicated otherwise.

For Wnt signaling transduction, the phosphorylation of the intracellular domain (ICD) of LRP6 is crucial and has been subject of extensive studies (Niehrs and Shen, 2010). The modifications of the extracellular domain (ECD) are not so well characterized, which may be due to the difficulties associated with studying protein N-glycosylation (Winterhalter et al., 2013; Nie et al., 2013; Leymarie and Zaia, 2012; Wuhrer et al., 2011; Harvey et al., 2005). The

ECD of LRP6 mediates binding of Wnt ligands and antagonists (MacDonald and He, 2012). It comprises 1350aa and is modularized into four tandem  $\beta$ -propeller/EGF-like units (E1-E4) followed by three LDLR type A repeats (He et al., 2004) (fig. 4). Crystal structures of E1+E2 and E3+E4 showed the platform-like nature of these ligand-binding modules (Chu et al., 2013; Chen et al., 2011; Cheng et al., 2011a; Cheng et al., 2011b). LRP6 mutants lacking all of the tandem  $\beta$ -propeller(BP)/EGF-like units (LRP6 $\Delta$ E1-4) are constitutively active. Thus the ECD is important for tight control of Wnt signaling and prevents activation of the ICD in the unbound state. While Wnt1 prefers binding to BP1+BP2, Wnt3a binds to BP3+BP4 (Ettenberg et al., 2010; Bourhis et al., 2010). This indicates that LRP6 may bind multiple Wnt proteins simultaneously. Dkk1 binds to both BP1+BP2 and BP3+BP4, which supports the known broad inhibition spectrum of Dkk1 (Ettenberg et al., 2010). By binding to LRP6 Dkk1 interrupts Wnt/Fzd/LRP6 complexes (Semenov et al., 2008) and together with the Dkk1 receptor Kremen (Krm) initiates LRP6 removal from the cell surface (Mao et al., 2002a).

#### LRP6 - schematic view

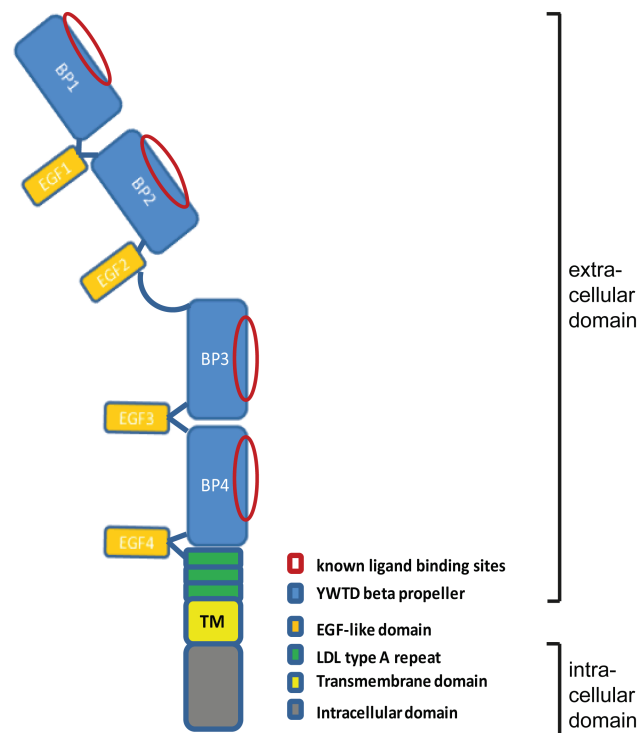


**Figure 4: Schematic view of LRP6 with a more detailed structure of the extracellular domain (ECD).**

The 4  $\beta$ -propellers of the type I transmembrane protein LRP6 are colored blue, EGF-like repeats in orange, LDL-type A repeats in green, the transmembrane domain is colored in yellow and the intracellular domain is colored in gray. Known ligand binding sites are marked by red ovals. The size is not in a realistic representation.

The maturation of the LRP6 ECD requires the formation of disulfide bonds and N-glycan attachment together with the correct folding of a complex set of alternating helices, turns and  $\beta$ -strands to form the 4 six-bladed  $\beta$ -propellers typical for LRPs. The LRP6 chaperone MESD (Mesoderm Development Candidate 2) both assists in folding of these highly complex domains and escorts properly folded LRP6 from the ER to Golgi. By doing so MESD prevents

premature LRP6 aggregation and improper disulfide bond formation (Hsieh et al., 2003). The ER exit of LRP6 is also reported to be controlled by palmytoylation at two Cysteines in the ICD (C1394 and C1399) close to the transmembrane domain, which helps to tilt the transmembrane domain properly with respect to the ER membrane in order to prevent a hydrophobic mismatch and thus ER retention (Abrami et al., 2008b). Mest/PEG1 (Mesoderm Specific Transcript/Paternally expressed gene 1), which reduces LRP6 N-glycosylation levels, leads to ER retention of LRP6 (Jung et al. 2011), highlighting the importance of N-glycosylation for LRP6 maturation. N-glycosylation stabilizes proteins and makes them more soluble in aqueous solutions, thus it protects them against proteases and is important for the accomplishment of the various tasks a protein fulfills (Gabijs, 2009). When LRP6 protein is analyzed by SDS-PAGE/Immunoblotting two bands are detected: a low molecular weight form and a high molecular weight form. These LRP6 forms are low N-glycosylated and highly N-glycosylated forms and are thought to be immature, ER-localized and mature, Golgi-transited receptor, respectively (Jung et al., 2011; Khan et al., 2007; Hsieh et al., 2003). Improper N-glycosylation prevents normal ER-to-surface transport of LRP6 and inhibits Wnt/ $\beta$ -catenin signaling (Jung et al., 2011). Hence, N-glycosylation is an important modification of LRP6 in order for LRP6 to reach the cell surface. Therefore I will introduce the N-glycosylation process in the next paragraph.

### **1.6 The N-glycosylation process**

For proper protein folding proteins in the secretory route need N-glycosylation (Roth et al., 2008; Ellgaard and Helenius, 2003; Roth, 2002). The N-glycosylation pathway is a highly ordered, complex set of enzymatic modifications that results in the decoration of secreted and transmembrane proteins with specific N-glycan chains. All N-glycans are synthesized through the same pathway and share a mutual core glycan structure. The core N-glycan structure consists of two N-acetylglucosamine (GlcNAc) and three mannoses (Man), which is attached to asparagine residues within conserved Asn-X-Ser/Thr motifs on proteins in the ER via a dolichol-attached intermediate. This core N-glycan structure is then further modified in the Golgi by a diverse set of glycosyltransferases, resulting in a great variety of N-glycan structures (Drickamer and Taylor, 2006). The maturation of N-glycans from the oligosaccharide precursor to high-mannose-, complex- or hybrid-types increases diversity and thus functionality of the proteome to a degree unmatched by any other post-translational modification (Walsh, 2006; Trombetta, 2003; Spiro, 2002; Burda and Aebi, 1999).

The biosynthesis of N-glycans can thus be simplified into three major steps (fig. 5):

- 1) Synthesis of the dolichol-attached oligosaccharide precursor
- 2) Transfer of the oligosaccharide precursor to a new-forming protein
- 3) Processing of the oligosaccharide precursor (trimming and then elongation/branching events to diversify the structural nature of the glycan chains)

The N-glycosylation of proteins begins in the rough ER (rER) as a co-translational process (Zuber and Roth, 2009; Burda and Aebi, 1999). It starts with the formation of the dolichol-linked oligosaccharide precursor. Dolichol consists of repeating isoprene units and acts as a lipid anchor that attaches the oligosaccharide precursor to the ER membrane. The assembly of the oligosaccharide precursor can be divided into two stages: The cytoplasmic-ER-face stage and the ER-luminal stage. In the first stage, GlcNAc is attached to the dolichol anchor by the the Dolichyl-Phosphate N-Acetylglucosaminophosphotransferase 1 (DPAGT1) through a pyrophosphate unit, one phosphate being originally attached to dolichol and the second from the nucleotide sugar, UDP-GlcNAc (Drickamer and Taylor, 2006). By the addition of various sugars, the oligosaccharide chain extends to form the oligosaccharide precursor which is made up of 2 GlcNAc, 9 mannose and 3 glucose molecules. After the addition of the last of the three GlcNAc the precursor is ready to be transferred onto a new forming polypeptide. In the second stage, the dolichol-linked oligosaccharide is flipped into the lumen of the ER. There, the precursor is co-translationally transferred *en bloc* to an Asparagine or Arginine of an Asp/Arg-X-Ser/Thr/Cys recognition motif by the multisubunit oligosaccharyltransferase (OST), which forms a complex with the Sec61 translocon and an associated ribosome (Chavan and Lennarz, 2006; Kelleher and Gilmore, 2006). The transfer of the oligosaccharide precursor to a nascent peptide is driven by the cleavage of the pyrophosphate bond between the dolichol and the glycan which releases energy. Three conditions must be fulfilled before a glycan is transferred onto an asparagine (or arginine):

1. The asparagine has to be located in a specific consensus sequence (Asn/Arg-X-Ser/Thr/Cys, X≠P) of a target protein (i.e. a cell surface or secreted protein) (Mellquist et al., 1998). This consensus sequence is also called asparagine sequon.
2. The asparagine has to be exposed on the surface of the protein being synthesized and not buried in a 3D-structure.
3. The asparagine must be located in the luminal side of the ER (Drickamer and Taylor, 2006).

The biosynthetic N-glycosylation process and the resulting oligosaccharide precursor are evolutionarily conserved from yeast to mammals. The presence of the oligosaccharide precursor aids in proper protein folding and thus the rER is the main quality control center for protein folding in living cells (Roth et al., 2010). It is noteworthy that the vesico-tubular clusters of the pre-Golgi intermediates also house quality control machinery (Fan et al., 2003; Zuber et al., 2001; Zuber et al., 2000; Bannykh et al., 1996; Lucocq et al., 1986). Golgi entry of newly synthesized proteins is only achieved after passage through these quality control machineries. Quality control of folding is important for cells since folding disorders can result in pathological loss-of-function (LoF) or gain-of-function (GoF) (Roth, 2010).

The next step in N-glycosylation is the pre-trimming of the oligosaccharide precursor in the ER/pre-Golgi, which signals the correct protein folding (fig. 5). The trimming of the oligosaccharide precursor is a complex process. After transfer of the completed oligosaccharide precursor onto an asparagine of an ER-lumen-exposed peptide, three

glucose residues are removed from the precursor. This pre-trimming in the ER requires the concerted action of the (exo-)Glucosidases I, II and III, which prevents further interaction of the oligosaccharide with the oligosaccharyltransferase (Kalz- Fuller et al., 1995; Hettkamp et al., 1984; Brada and Dubach, 1984; Burns and Touster, 1982). From here on, the involved enzymes start to be distributed between rER to pre-Golgi, since glucosidase II was detected throughout the rER, in the smooth ER and in vesiculo-tubular clusters (Zuber et al., 2000; Roth et al., 1990; Lucocq et al., 1986). In general, di-glucosylated oligosaccharides generated by Glucosidase I represent a glyco-code that allows for further translocation in the secretory route and thus for further N-glycan processing. Mono-glucosylated oligosaccharides represent a glyco-code promoting protein folding through the calnexin/calreticulin cycle, i.e. the misfolded protein-response for dislocation from the ER and subsequent degradation (Roth, 2010; Hammond et al., 1994; Hebert et al., 1995). These oligosaccharide precursor trimming reactions are known to be conserved from yeast to higher eukaryotes (Roth, 1987; Kornfeld and Kornfeld, 1985). If the protein is properly folded the oligosaccharide precursor is further trimmed by Mannosidase I and II (Roth, 2002; Roth et al., 2010). It has been shown that the removal of both the glucose and some of the mannoses are important for the protein quality control (Roth et al., 2010).

In the Golgi, the next step involves further removal and addition of sugar residues by glycosidases and glycosyltransferases, respectively. In the cis-Golgi, mannosidases completely or partially remove the four mannose in  $\alpha$ -1,2 linkages. Subsequently, glycosyltransferases of the medial Golgi add sugar residues to the core glycan (which consists of 2 GlcNAc and 3 mannose), initiating the synthesis of the three main types of N-glycans: high mannose types, complex types and hybrid types N-glycans (Roth et al., 2010; Drickamer and Taylor, 2006; Roth, 2002) (fig.5).

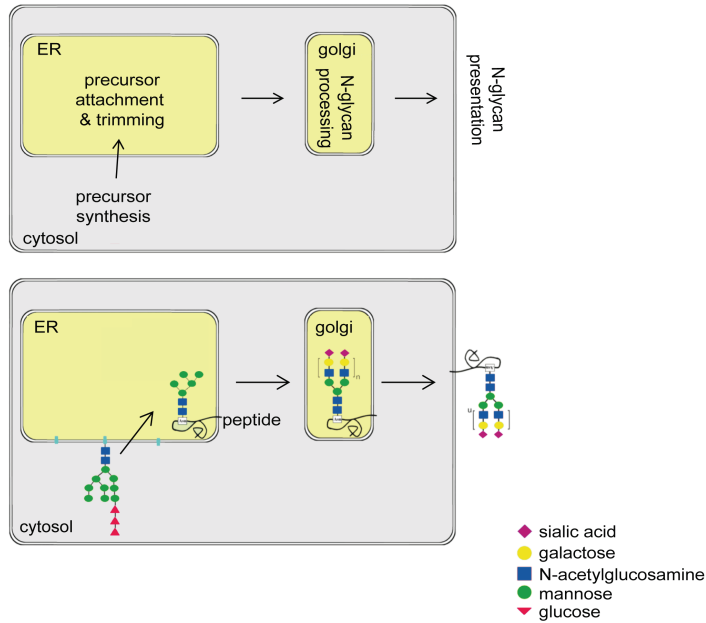
High-mannose N-glycans: High-mannose N-glycans are made of two GlcNAc with many attached mannose residues.

Complex N-glycans: As implicated by their name, complex oligosaccharides can contain almost every possible number of saccharide types and saccharides. The GlcNAc transferase B3GNT8, which is being analyzed in this study, is involved in the construction of complex N-glycans. Synthesis of complex N-glycans happens primarily in the Golgi. Here, GlcNAc-T I transfers a GlcNAc to the Man- $\alpha$ -1,3 arm of Man<sub>5</sub>GlcNAc<sub>2</sub>-Asn-X creating a  $\beta$ -1,2 linkage. B3GNT8 prefers the  $\beta$ -1,2-arm. Then the mannosidase II-mediated removal of two mannose units forms the substrate for GlcNAc-T II, which then transfers GlcNAc to the Man- $\alpha$ -1,6 arm to create a  $\beta$ -1,2 linkage. When GlcNAc-T I and mannosidase II have acted as described above, a second antenna can be formed by GlcNAc-T II and GlcNAc-T III to VI as well as the core fucosyltransferases may act. The action of GlcNAc-T I is required for the actions of GlcNAc-T II, III and IV, mannosidase II and the core alpha-1,6-fucosyltransferase. However, GlcNAc-T V and VI require, in addition to GlcNAc-T I, the prior action of GlcNAc-T II (Schachter 2000). The GlcNAc-transferases MgatI, -II, -IV and V can increase the number of antenna (Lau et al., 2007). Complex N-glycans share the N-acetylactosamine (LacNAc)

structure which is a disaccharide consisting of N-acetylglucosamine (GlcNAc) and galactose (Gal). Multiple alternating additions of Gal and GlcNAc by galactosyl transferases and GlcNAc transferases respectively can form long poly-LacNAc chains on complex N-glycans. The GlcNAc transferase B3GNT8 belongs to the LacNAc synthesizing group of enzymes (Seko and Yamashita, 2008) (for detailed description see next paragraph). GlcNAc transferases and galactosyl transferases act in successive steps to elongate glycan chains on the same protein. For this reason GlcNAc transferases and galactosyl transferases localize to the same compartments and physically associate. GlcNAc transferases and galactosyltransferases share this common localization with many other glycosyltransferases in organisms from *Saccharomyces cerevisiae* to *Homo sapiens* (de Graffenried and Bertozzi 2004; Giraudou and Maccioni 2003a; Bieberich et al. 2002; Moremen 2002; Giraudou et al. 2001; Jungmann et al. 1999; Jungmann and Munro 1998; Nilsson et al. 1994). Two mechanisms may account for the proper localization of these type II single transmembrane-spanning glycosyltransferases: the first is called the “bilayer thickness” model, because it has been proposed that different glycosyltransferases sort according to the size of their transmembrane domains and the size of the local membrane thickness (Mitra et al. 2004; Bretscher and Munro 1993). The second is referred to as the “kin recognition” model, where it has been proposed that glycosyltransferases in the same compartment form complexes and are thus excluded from Golgi-to-surface moving vesicles (Opat et al. 2000; Nilsson et al. 1993; Machamer 1991). These models are not mutually exclusive: the membrane thickness could contribute to the localization of enzyme complexes while enzyme complexes could establish domains in a particular membrane (Lee et al., 2009).

A

### The N-glycosylation process



B

### Products of N-glycosylation

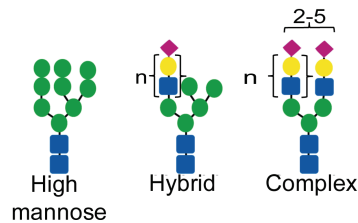


**Figure 5: The N-glycosylation process and the major N-glycan types.**

A. Upper panel: schematic view, lower panel: molecular view. An oligo-saccharide precursor is flipped into the lumen of the ER and an oligo-saccharide transferase attaches it to an asparagine or arginine residue of the target protein. The precursor is then modified and decorated with a more elaborate set of sugars and branches by a large number of different glycosyltransferases.

B. The N-glycosylation process leads to high-mannose, complex, or hybrid type N-glycans. For the complex type N-glycans one example is shown. The amount of polyLacNAc (n) can vary on each antenna.

Hybrid N-glycans: The third type of N-glycans is the hybrid type. As the name implicates hybrid types are made up of mannose residues on one branch while on the other branch LacNAc units form a complex branch. For synthesis of hybrid N-glycans GlcNAc-T III must act on the product of GlcNAc-T I before mannosidase II. Then the pathway is committed to hybrid structures since Mannosidase II will not find a substrate on bisected oligosaccharides (the reverse action leads to complex N-glycans). The amounts of GlcNAc-T III and mannosidase II in cells directs the N-glycan biosynthetic pathway towards hybrid or complex type N-glycans (Schachter, 2000).



The three aforementioned N-glycan pathways towards high mannose, complex and hybrid type are conserved in prokaryotes as well as in archaea (Dell et al., 2010). The difference between prokaryotes/archaea and eukaryotes is the final N-glycan structure. In prokaryotes and archaea the N-glycan structure does not differ much from the initial oligosaccharide precursor. However in eukaryotes, the oligosaccharide precursor is extensively modified while being transported from ER to cell surface (Drickamer and Taylor, 2006). As mentioned before, the peptide attachment of the oligosaccharide precursor as well as its processing into high mannose/hybrid/complex N-glycans is important for proteins like the Wnt co-receptor LRP6 to reach its destination, i.e. the cell surface (Khan et al., 2007, Hsieh et al., 2003). Although this is known since more than a decade, up to date no specific N-glycosyltransferase has been identified that is involved in controlling the transport of the Wnt co-receptor LRP6. While it is easy to hypothesize that the GlcNAc-to-dolichol transferase DPAGT1 or the precursor-transferring OST are involved in LRP6 transport by exerting a global effect on the complex N-glycans of LRP6, it is harder to predict which Gal- or GlcNAc-transferase modifies the nature of the N-glycan chains. B3GNT8, that was identified in this study, is involved in the elongation of LacNAc units of complex N-glycans.

### **1.7 B3GNT8s role in N-glycosylation**

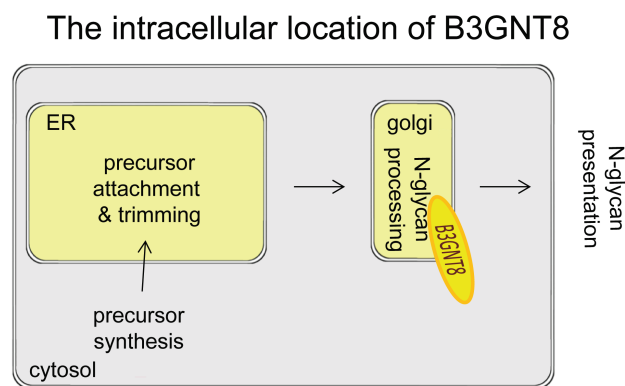
The B3GNT family comprises nine members: iGnT, B3GNT2, -3, -4, -5, -6, -7, -8 and -9. Their sequences are highly homologous and some of their activities have been characterized. The members iGnT, B3GNT2, -3, -4, and -8 mediate poly-LacNAc synthesis (Ishida et al., 2005; Shiraishi et al., 2001; Sasaki et al., 1997). Furthermore, B3GNT3 is also involved in the synthesis of O-glycan core 1 structures (Yeh et al., 2001). The non-LacNAc-synthesizing enzymes B3GNT5, -6, and -7 mediate the synthesis of lactotriose (Togayachi et al., 2001), core 3 O-glycans (Iwai et al., 2002) and the keratan sulfate backbone (Seko and Yamashita, 2004; Kataoka and Huh, 2002), respectively. B3GNT2 and -8 are the main poly-LacNAc synthesizing glycosyltransferases in humans and thus are thought to be localized in the Golgi (Qiu et al. 2011). The substrate specificities of the B3GNT family members can explain which members are involved in the addition of  $\beta$ 1,3-linked GlcNAc to specific glycoconjugates. However their involvement in the elongation of oligo- or poly-LacNAc units on multi-antennary N-glycans is not yet fully understood.

B3GNT8, is poorly characterized in comparison to the other members of the family. It comprises 397 amino acids and the transmembrane region is located at the N-terminus making B3GNT8 a type II protein. In SDS-PAGE / Immunoblotting B3GNT8 shows up as two bands at approximately 43kDa, since B3GNT8 is itself N-glycosylated. Most of B3GNT8s characteristic features are drawn from *in vitro* studies. In a  $Mn^{2+}$ -dependent manner, B3GNT8 selectively transfers GlcNAc from UDP-GlcNAc onto galactose of tetra- or penta-antennary N-glycans with or without core fucose (Ishida et al., 2005). To transfer GlcNAc from UDP-GlcNAc onto galactose, the divalent metal-binding motif of B3GNT8 interacts with



the phosphate group of the nucleotide donor through coordination of a divalent cation such as  $Mn^{2+}$ . While DDD is the conserved metal binding-motif in other B3GNT enzymes, the divalent metal-binding motif in B3GNT8 is QDD (Hiruma et al., 2004; Iwai et al., 2002; Togayachi et al., 2001; Shiraishi et al., 2001). The *in vitro* action of B3GNT8 on tetra-antennary N-glycans yields two products: one with a GlcNAc on a Gal residue of the  $\beta$ 1,2 branch, and the other with a GlcNAc on a Gal residue of the  $\beta$ 1,6 branch. However, *in vitro* studies have shown that B3GNT8 prefers the  $\beta$ 1,2 branch over the  $\beta$ 1,6 branch (fig. 6). Furthermore, it was shown *in vitro* that the specificity of B3GNT8 is similar to that of B3GNT2. B3GNT8 and B3GNT2 have been demonstrated to interact in COS-7 cells and form a heterocomplex *in vitro* with enhanced enzymatic activity of B3GNT2 (Seko and Yamashita, 2008).

A



B

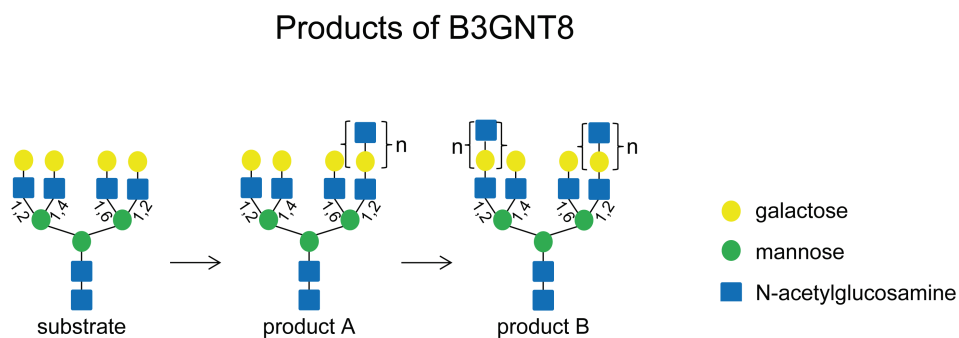


**Figure 6: The Localization of B3GNT8 and products of B3GNT8s enzymatic function.**

A. B3GNT8 is localized in the Golgi according to the GeneCards Humand Genes Database. This is based on the localization of family members, the enzymatic function in the N-glycosylation process and signal sequence.

B. B3GNT8 GlcNAcylates galactose residues on the  $\beta$ 1,2-branch of mainly tetra-antennary (lesser penta-antennary) N-glycans. As the n indicates, the alternating addition of GlcNAc and galactose by B3GNT8 and an yet unknown galactosyltransferase creates the repeating polyLacNAc units that are typical for complex N-glycans. B3GNT8 is one of five family members involved in polyLacNAc synthesis. The final N-glycan structure will be "capped" with sialic acid (not shown).

The tissue expression of B3GNT8 is highest in pancreas, spleen, small intestine and bone marrow. Real time-PCR showed no expression in heart, prostate, adult or fetal brain and colon. However, in colon cancer it is highly up-regulated (as is LRP6). In HCT15 human colon cancer cells, exogenous B3GNT8 enhanced the cell surface expression of poly-LacNAc and

beta-1-6-branched N-glycans (Ishida et al., 2005), confirming that it is involved in the synthesis of poly-LacNAc units. In Hep2 cells, gain-of-function (GoF) or loss-of-function (LoF) of B3GNT8 increases or decreases respectively cell proliferation and invasion. Furthermore, mRNA and protein levels of B3GNT8, MMP2/9 and TGF-1 $\beta$  are positively coupled, confirming its relevance for cancer. However, MMP-2 is a non-glycosylated protein. Thus the correlation with MMP2 is likely to be indirect (Shen et al. 2011). In nude mice B3GNT8 GoF and LoF modulate tumor growth (Hua et al., 2012).

### **1.8 N-glycosyltransferases and N-glycosylated pathway members in Wnt signaling**

Recently the N-glycan branching enzyme  $\beta$ 1,6 N-acetylglucosaminyltransferase V (MGAT-V), was shown to modulate Wnt signaling. MGAT-V acts at an early step of N-glycan modification by inducing  $\beta$ 1,6-branching of the trimmed oligosaccharide (Guo et al., 2014). However, it is not known how MGAT-V modulates Wnt signaling and if it acts directly on a component of the pathway.

The dolichol-phosphate GlcNAc-transferase DPAGT1 is a Wnt target gene (Sengupta et al., 2010) and had been reported to modulate canonical Wnt signaling in human squamous carcinoma cell lines (Jamal et al., 2012). The authors hypothesize that DPAGT1 facilitates changes in the glycosylation pattern of Wnt3a and LRP5/6 although this has not been confirmed. This has still to be shown.

The principal diversifying N-glycosyl transferases that contribute to lengthening of N-glycan antennae (i.e. GlcNAc transferases and galactose transferases) are not known. The reason for this is the difficulties which the structural study of N-glycans bears (Winterhalter et al., 2013; Nie et al., 2013; Leymarie and Zai, 2012; Wuhrer et al, 2011; Harvey et al. 2005).

There are nineteen different Wnt ligands and, although all of them are N-glycosylated, there are variations in both the number and position of N-glycosylation sites, indicating that the role of Wnts N-glycosylation is not evolutionary conserved (Tanaka et al., 2002). In support of this, deletion of Wnt1 N-glycosylation sites does not affect signaling (Xiaofang et al., 2012; Doubravska et al., 2011; Mason et al., 1992) and the N-glycan of Wnt8 does not participate in Fzd8-binding, although it is located in the gap between a Wnt/Fzd complex (Janda et al., 2012). On the contrary, for Wnt3a and Wnt5a N-glycosylation is important for secretion but not for action (Tang et al., 2012; Komekado et al., 2007; Kurayoshi et al., 2007).

$\beta$ -catenin is O-glycosylated which regulates its transport into the nucleus and thus regulates its signaling activity (Sayat et al., 2008).

Frizzleds share two highly conserved N-glycosylation sites and Frz harboring mutations in these sites are retained in the ER (Milhem et al., 2014). Although N-glycosylation is important for Fzd Golgi-to-surface transport and can be regulated by the ER-resident protein

Shisa (Yamamoto et al. 2005), the N-glycans seem not to participate in the interaction with Wnts (Janda et al., 2012).

The regulation of Wnt signaling by metabolic processes is also connected to N-glycosylation. In two macrophage cell lines (J774.2 and RAW264.7) Wnt signaling is positively coupled to glucose and L-glutamine supply changes (Anagnostou and Shepherd, 2008). Both L-glutamine and glucose are used in the hexosamine biosynthetic pathway (HBP) to produce nucleotide diphosphate-activated hexoses (NDP-hexoses), e.g. for N-glycosylation. The authors demonstrated that the glucose and L-glutamine mediated change in Wnt signaling was caused by N-glycosylation of Wnt pathway members upstream of GSK3. It has been suggested that this is regulated in part via N-glycosylation-dependent LRP6 Golgi-to-surface transport (Jung et al., 2011; Anagnostou and Shepherd, 2008).

### **1.9 N-glycosylation of the Wnt co-receptor LRP6**

LRP6 needs N-glycosylation to reach its destination at the cell surface (Khan et al., 2007, Hsieh et al., 2003). The nature of the N-glycans needed is however not clear. Seven of the ten possible N-glycosylation sites in LRP6 have been demonstrated to carry N-glycans (Cheng et al., 2012; Chen et al., 2011; Khan et al., 2007). All are located in BP or EGF-like domains (fig. 7): None of the LRP6 mutations associated with early CAD (coronary artery disease), late-onset AD, OPPG (osteoporosis-pseudoglioma syndrome), FEVR (familial exudative vitreoretinopathy), or HBM (high bone mass, for LRP5) disease have been associated with known LRP6 N-glycosylation sites (Chen et al., 2011). There is a single nucleotide polymorphism (SNP) known for amino acid 281 (N-glycan #3) but no links to a disease.

LRP6 can be detected as two bands of different molecular weight in western-blot. The lower molecular weight band represents the immature LRP6 that is located in the endoplasmatic reticulum (ER), whereas the higher molecular weight band represents the mature LRP6 at the cell surface (Hsieh et al., 2003). The higher molecular weight of the mature, membrane located LRP6-proteins is thought to result from glycan modification of LRP6 in the Golgi, during the later stages of the N-glycosylation pathway (Hsieh et al., 2003). When subjected to PNGase F treatment (which cleaves all N-glycans, regardless of their structure) both LRP6 bands are downshifted, indicating that both LRP6 species corresponding to these bands are N-glycosylated (Khan et al., 2007). The same group subjected the LRP6' N-glycosylation-process to treatment with tunicamycin: tunicamycin blocks the transfer of GlcNAc-1-phosphate to dolichol-monophosphate (the ER-anchor of the oligosaccharide precursor) by inhibition of the GlcNAc-1-P-Transferase (Eckert et al., 1998). Thus, it inhibits the formation of all N-glycans. This treatment phenocopied the PNGaseF treatment confirming that both LRP6 bands differ solely in N-glycosylation. This is consistent with a co-translational attachment of the oligosaccharide precursor. The lower molecular weight form of LRP6 is cleaved by endoglycosidase H and is resistant to neuraminidase. In contrast, the higher molecular weight form of LRP6 is resistant to digestion with endoglycosidase H and sensitive

to neuraminidase digestion. This indicates that the higher molecular weight fraction of LRP6 represents receptor that has transited through the Golgi, while the lower molecular weight form of LRP6 represents the fraction of receptor retained in the ER (Khan et al., 2007; Hsieh et al., 2003). Since endoglycosidase H cleaves high-mannose and some hybrid-types of N-glycans, the mature form of LRP6 contains only complex-type N-glycans and/or hybrid-types but no high mannose types. The cleavage of sialic acid by neuraminidase clearly supports this, since the sialic acid “cap” is found solely on complex- and hybrid-types.

### Putative N-glycan sites of LRP6

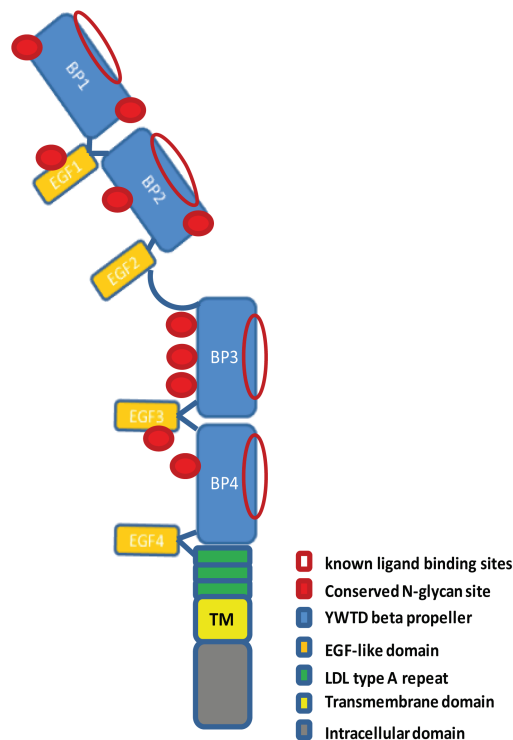


**Figure 7: Schematic view of LRP6 with a more detailed structure of the extracellular domain (ECD).**

Scheme of LRP6, with red filled circles indicating the position of putative N-glycan sites (BP1: amino acids #42, #81, EGF-like repeat 1: #281, BP2: #433 & #486, BP3: #692, #859, #865, EGF-like repeat 3: #926, BP4: #1039). Dark red ovals show known ligand binding sites. The 4  $\beta$ -propellers of LRP6 are colored blue, EGF-like repeats in orange, LDL-type A repeats in green, the transmembrane domain is colored in yellow and the intracellular domain is colored in gray. The size is not in a realistic representation. Note the close spatial proximity of some N-glycan sites to known ligand binding sites.

A disturbance of the LRP6' N-glycosylation process leads to translocation problems. In the ER, molecular chaperones check newly synthesized proteins for correct folding. Since attachment of the oligosaccharide precursor is co-translational, folding sometimes depends on it. LRP6 requires the chaperone MESD and in its absence LRP6 forms aggregates in the ER (Koduri and Blacklow, 2007; Li et al., 2006; Culi et al., 2004; Culi and Mann, 2003). All LDLR family members consist of at least one BP domain, which is followed by a linker and an EGF-like repeat. MESD is specifically required for the maturation of these tandem BP-EGF-like repeats and aids in attachment of the oligosaccharide precursor to LRP6 (Culi et al., 2004). This highlights the importance of the attachment of the precursor for LRP6 ER-to-Golgi transport. Furthermore, Mest/PEG1 (Mesoderm Specific Transcript/Paternally expressed

gene 1), which inhibits the processing of the oligosaccharide precursor on LRP6, leads to intracellular retention of LRP6 (Jung et al. 2011). This highlights the importance of the N-glycan processing or maturation for the LRP6 Golgi-to-surface transport. Therefore defects in LRP6 N-glycosylation are likely to constitute the known effects of LRP6 cell surface absence like neonatal lethality, abnormalities of skeleton/central nervous system/mammary gland/and heart, and the Wnt-deficiency phenotypes seen in mice (Joiner et al., 2013).

The identification of B3GNT8 as a novel LRP6 glycosyltransferase is the first reported link between a specific glycosylation pathway component and Wnt receptor regulation and will provide a foundation for future research into this highly complex process.

## 2. Aims of the Study

---

The aims of this study are as follows:

1. Identify the importance of the N-glycosylation sites in LRP6 of different species together with the functionally redundant LRP5 for  $\beta$ -catenin-dependent Wnt signaling
2. Identify N-glycosyl transferases that modify both LRP6 and Wnt signaling using a Medaka cDNA expression library and cell culture based screening experiments
3. For any glycosyltransferase gene(s) identified from this screen, characterize in detail the modification of LRP6
4. For this glycosyltransferase gene, provide a detailed characterization of any potential requirement especially for Wnt signaling, but also for other pathways
5. Functionally characterize the action of the identified glycosyltransferase on LRP6 and N-glycosylated members of the  $\beta$ -catenin-dependent Wnt pathway

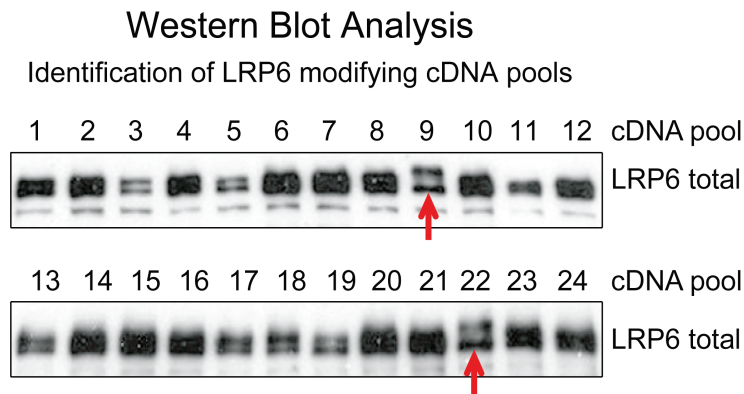
## 3. Results

---

### **3.1 Identification of a GlcNAc transferase that covalently modifies LRP6 and stimulates Wnt signaling**

I screened a medaka cDNA library for regulatory modifiers of the Wnt co-receptor LRP6 and used SDS-PAGE LRP6 immunoblotting as well as TOPFLASH reporter assays as read-outs to identify suitable candidates for further characterisation. The medaka cDNA library was prepared in collaboration with Jochen Wittbrodt (COS, Heidelberg University) and consists of approximately 20.000 unique, full length, sequence verified and annotated medaka clones made from RNA extracted from medaka eggs and early stage embryos. In order to simplify the screening process, 24 cDNA clones were combined from the original library of individually arrayed clones and these cDNA pools prepared as transfection ready plasmid DNA samples. In total 740 pools of potential LRP6 modifiers were prepared in this way. As in former screening approaches performed in our lab (Zhang et al, 2015; Chen et al, 2014; Davidson et al., 2009; Davidson et al., 2005), the read out of this gain-of-function expression-screen was the detection of LRP6 in SDS-PAGE/Immunoblotting and in my screen I focused on modifiers that would alter the migration characteristics of the mature upper LRP6 band. I identified a pool of 24 cDNAs that covalently added mass to the upper LRP6 band, resulting in a clear upshift after Western Blot detection (fig. 8 A, upper arrow). A secondary screen using the single cDNAs from this pool identified a member of the  $\beta$ -1,3-N-acetylglucosaminyl transferase (B3GNT) family, named B3GNT8 (fig. 8 B). There are 9 members of the B3GNT family in total, numbered in the order of their identification. This B3GNT8 is a recently identified member and relatively uncharacterized.

A



B

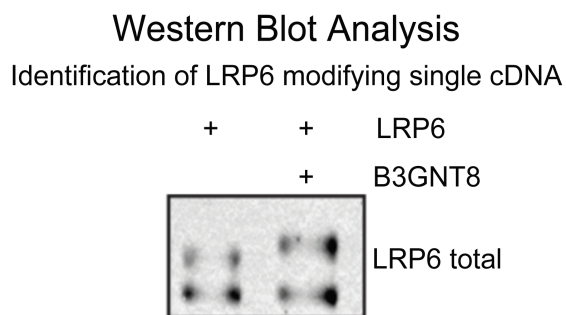


**Figure 8: Identification of B3GNT8.**

A. SDS-PAGE/WB of cell lysates from the primary screen. 120 ng of the cDNA pools (5 ng of single cDNA clone) were co-transfected with 10ng myc-LRP6 and cell lysates harvested 20 hours post-transfection. An anti-myc antibody was used to detect total LRP6. A cDNA within one pool conferred covalent modification of LRP6, visualised as an up-shift (arrow).

B. A secondary screen identified the individual cDNA clone as the glycosyl transferase B3GNT8.

In addition to B3GNT8, three other potential LRP6 glycosyltransferase genes have been identified that promoted an upshift of the mature form of LRP6; two in the screen I performed and two that were identified in a previous screening experiment that used a different cDNA library as the source of potential modifiers (one representative example: fig. 8 A, lower arrow). All four of these glycosyltransferases were then tested for their ability to regulate LRP6/Wnt signaling using the TOPFLASH Wnt reporter assay. The TOPFLASH reporter construct encodes a firefly luciferase under transcriptional control of 7x TCF/LEF transcriptional response elements. This TCF/LEF element, with the DNA binding sequences (A/T)(A/T)CAA(A/T)G and TTCAAAG for TCF and LEF respectively (Gustavson et al., 2004), is activated by  $\beta$ -catenin. A construct harboring the renilla luciferase under a thymidine kinase promoter served as a control for transfection efficiency and cell viability and was used to normalize TOPFLASH values. Initial TOPFLASH reporter assays and SDS-PAGE / Immunoblotting showed that only B3GNT8 had the ability to both modify LRP6 and modulate Wnt signaling. I then performed a titration experiment using B3GNT8 and, in addition, B3GNT7, one of the additional glycosyltransferase hits that shares highest similarity to B3GNT8, and ST3GAL3, a sialic acid transferase that conferred a smaller up-shift to LRP6



than B3GNT8 (fig. 9). These experiments confirmed that only B3GNT8 can functionally modify LRP6 and that it can do so in a dose-dependent manner (fig. 9).

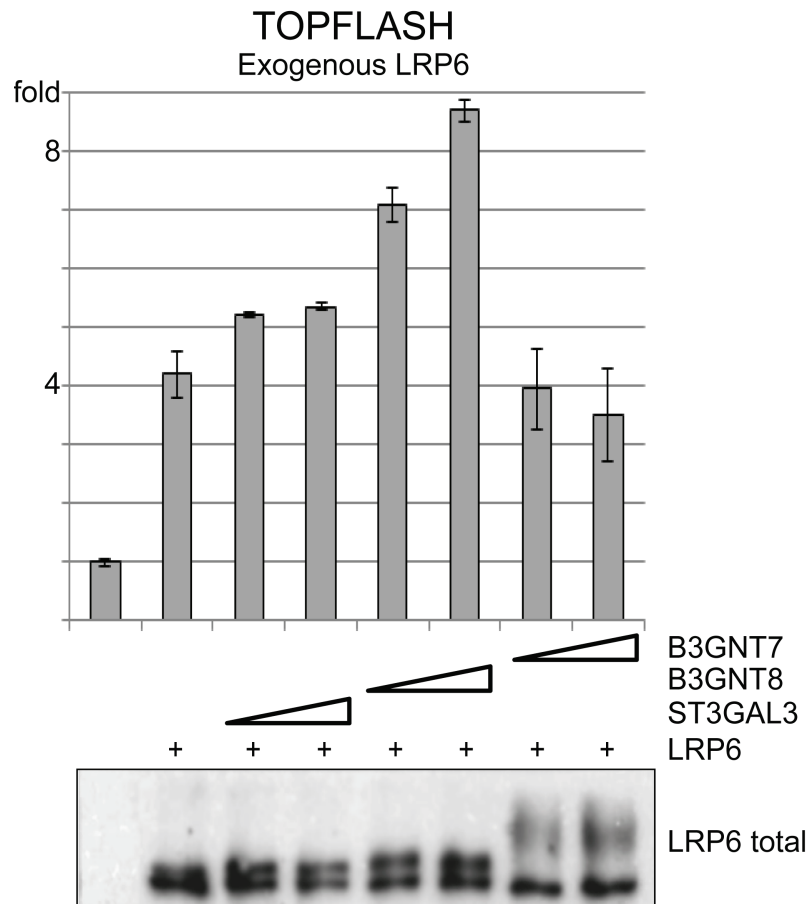


**Figure 9: Only B3GNT8 modifies LRP6 and modulates Wnt signaling.**

HEK293T cells in 96well format were co-transfected with TOPFLASH luciferase Wnt reporter (20ng), thymidine kinase-renilla reporter (4ng), LRP6 (20ng) and with increasing concentrations of B3GNT8 or B3GNT7 (10, and 15ng). Cells were harvested 24h later in 1% triton lysis buffer for Western Blot or passive lysis buffer (Promega) for Luciferase assay. Anti-myc antibody was employed to detect LRP6. Note that B3GNT7 promotes significant modification of LRP6 but, unlike B3GNT8, has no functional effect on signaling.

### **3.2 B3GNT8 modifies endogenous Wnt signaling and promotes an LRP6 subspecies**

The results presented above rely on over-expressed LRP6, which are present at non-physiological levels and therefore are more susceptible to artifactual results. In order to test the effect of B3GNT8 under more physiologically relevant conditions I performed TOPFLASH reporter assays as well as SDS-PAGE/Western Blot analysis without co-expressing LRP6. Non-B3GNT8 transfected cells were taken as controls. B3GNT8 also promoted a dose-dependent activation of Wnt signaling in the absence of co-expressed LRP6 (fig. 10 B). Importantly, the dose-dependent activation of Wnt signaling by B3GNT8 was accompanied by a small but clear upshift of the mature form of endogenous LRP6 (fig. 10 B, lower panel). Two independent LRP6 antibodies were used to demonstrate this effect of B3GNT8 on endogenous LRP6 and each showed the presence of higher molecular weight forms of mature, cell surface LRP6, corresponding to the upper bands. Moreover, the increasing

phosphorylation at the first PPPSP site (serine 1490) on endogenous LRP6, which is generally regarded as the first sign for activated Wnt signaling, confirmed the activation of LRP6 itself, in addition to Wnt signaling (fig. 10 B, upper panel). This indicates that the up-shift of the endogenous mature form of LRP6 that was promoted by B3GNT8 was responsible for the activation of Wnt signaling.

In order to more clearly detect the different endogenous LRP6 subspecies to B3GNT8, I used 12% SDS-polyacrylamide gels with extended run-times. In contrast to lower percentage SDS polyacrylamide gels the 12% gel maintains the proper definition of all LRP6 bands but needed longer run-times. Careful examination of the results shows that the upshift of exogenous LRP6 corresponds to the strengthening of a pre-existing endogenous third upper band (fig. 10 B, lower panel, red arrow). This third endogenous band was also detectable with the anti-Sp1490 antibody (fig. 10 B, upper panel). This indicates that the cell surface LRP6 consists of different LRP6 sub-species.

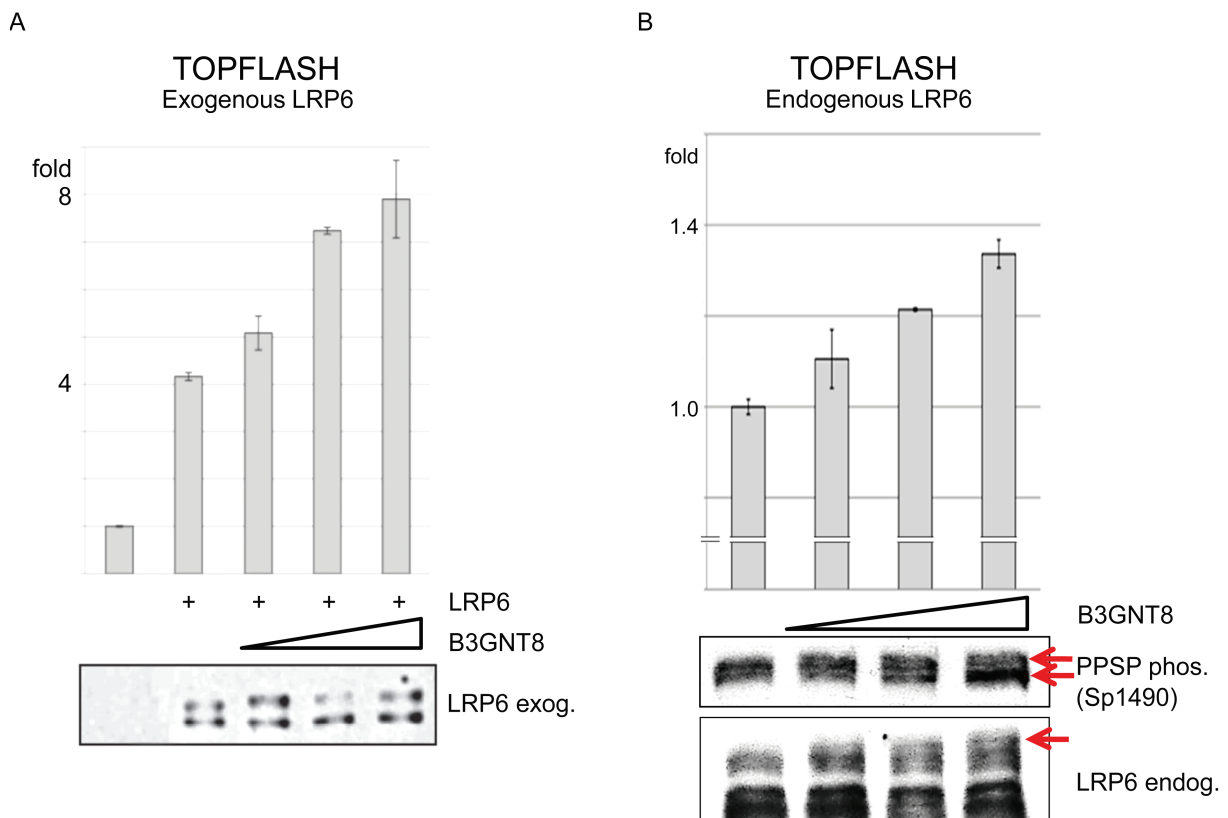


**Figure 10: B3GNT8 GoF stimulates exogenous and endogenous Wnt-signalling.**

A. TOPFLASH reporter assay (upper graph) and WB of overexpressed LRP6 from lysates of HEK293T cells transfected as indicated. Myc-tagged LRP6 (20ng) was transfected alone or with increasing concentrations of B3GNT8 (10ng, 15ng, 20ng). Total cell lysates were harvested 24 hours post-transfection in 1% triton lysis buffer for Western Blot or passive lysis buffer (Promega) for luciferase assay.  $\alpha$ -LRP6 (T1479) was used to detect total LRP6.

B. As in A, but without LRP6 co-overexpression. TOPFLASH reporter assay in HEK293 cells with increasing amounts of transfected B3GNT8 (10ng, 15ng, 20ng). For the Western Blots, 12% SDS-polyacrylamide gels and extended run-times were used to separate the different endogenous LRP6 species (distinct bands). Anti-T1479 Ab was used to detect total LRP6 (LRP6 endog.). Note the progressively stronger appearance of a third upper band with increasing amounts of B3GNT8 (lower red arrow). An antibody detecting phospho-Serine-1490 (Sp1490) was used to detect LRP6 PPSP phosphorylation status. Note the increase in signal intensity (middle red arrow) as well as the appearance of an additional "upper" band (upper red arrow) detected by the Sp1490 Ab.

### 3.3 LRP6 has 4 N-glycosylation sites that are highly conserved

The Wnt co-receptor LRP6 harbours 10 Asp/Arg-X-Ser/Thr putative N-glycosylation sites. My multiple sequence alignment using Clustal O (1.2.1) software of *homo sapiens*, *mus musculus*, *xenopus tropicalis*, and *danio rerio* LRP5/6 demonstrates that eight of these N-glycosylation sites are highly conserved in vertebrates. If the *drosophila melanogaster* LRP6 homolog Arrow is included in the alignment, only 4 evolutionarily conserved N-glycosylation sites appear (sites #2, #5, #6, and #8, corresponding to Asn81, Asn486, Asn692, and Asn865, respectively). These 4 sites (fig. 11 and fig. 29 A, labelled as 1 to 4) are located exclusively in the  $\beta$ -propeller domains. All four evolutionarily conserved N-glycosylation sites are located within the YWTD propeller/ $\beta$ -sheet domains referred to as BP1-4; one each in BP domains 1 and 2 and two in BP domain 3 (see fig. 11).

#### Highly Conserved N-glycosylation sites 1-4 in LRP6 of different species

075581	LRP6_HUMAN	51	EDAAAVDFVFSHGLI-- <b>Y</b> WSDVSEEA <b>I</b> K <b>R</b> TE <b>F</b> N <b>K</b> T <b>E</b> -----SVQNVVVSGLLSPDGLACD	BP1
075197	LRP5_HUMAN	63	EDAAAVDFQFSKGAV-- <b>Y</b> WTDVSEEA <b>I</b> K <b>Q</b> T <b>Y</b> L <b>N</b> Q <b>T</b> E-----A-AVQNVVISGLVSPDGLACD	
B5L5I6	LRP6_DANRE	51	EDAAAVDYIYAQGLI-- <b>Y</b> WSDVSEEA <b>S</b> I <b>K</b> R <b>T</b> L <b>F</b> NG <b>S</b> A-----PSGVQTTVISGLASPDGLACD	
088572	LRP6_MOUSE	51	EDAAAVDFVFGHGLI-- <b>Y</b> WSDVSEEA <b>I</b> K <b>R</b> TE <b>F</b> N <b>K</b> S <b>E</b> -----SVQNVVVSGLLSPDGLACD	
F6YLU8	LRP6_XENTR	52	EDAAAVDFVFFRGLI-- <b>Y</b> WSDVSEEA <b>I</b> K <b>R</b> I <b>D</b> F <b>N</b> K <b>T</b> S-----SSHDVVVISGLLSPDGLACD	
Q9NHE9	ARRO_DROME	119	AEAMAIDFYAKNLV-- <b>C</b> W <b>T</b> D <b>S</b> G <b>R</b> E <b>I</b> I <b>E</b> C <b>A</b> Q <b>T</b> N <b>S</b> S <b>A</b> L <b>Q</b> P <b>L</b> L <b>R</b> A <b>P</b> Q <b>T</b> V <b>I</b> S <b>T</b> G <b>L</b> D <b>K</b> E <b>P</b> E <b>G</b> L <b>A</b> M <b>D</b>	
...				
075581	LRP6_HUMAN	460	<b>M</b> Y <b>W</b> T <b>D</b> W <b>G</b> E---IP <b>K</b> I <b>E</b> R <b>A</b> A <b>L</b> D <b>G</b> S <b>D</b> R <b>V</b> V <b>L</b> V <b>N</b> T <b>S</b> L <b>G</b> W <b>P</b> N <b>G</b> L <b>A</b> L <b>D</b> Y <b>D</b> E <b>G</b> K <b>I</b> Y <b>W</b> G <b>D</b> A <b>K</b> T <b>D</b> K <b>I</b> E <b>V</b> M <b>N</b>	BP2
075197	LRP5_HUMAN	473	<b>M</b> Y <b>W</b> T <b>D</b> W <b>G</b> E---N <b>P</b> K <b>I</b> E <b>C</b> A <b>N</b> L <b>D</b> Q <b>E</b> R <b>R</b> V <b>L</b> V <b>N</b> A <b>S</b> L <b>G</b> W <b>P</b> N <b>G</b> L <b>A</b> L <b>D</b> L <b>Q</b> E <b>G</b> K <b>L</b> Y <b>W</b> G <b>D</b> A <b>K</b> T <b>D</b> K <b>I</b> E <b>V</b> I <b>N</b>	
B5L5I6	LRP6_DANRE	464	<b>M</b> Y <b>W</b> T <b>D</b> W <b>G</b> E---V <b>P</b> K <b>I</b> E <b>R</b> A <b>A</b> L <b>D</b> G <b>S</b> Q <b>R</b> M <b>V</b> M <b>V</b> N <b>T</b> S <b>L</b> G <b>W</b> P <b>N</b> G <b>L</b> A <b>L</b> D <b>Y</b> S <b>E</b> R <b>K</b> I <b>Y</b> W <b>G</b> D <b>A</b> K <b>T</b> D <b>V</b> I <b>E</b> V <b>M</b> E	
088572	LRP6_MOUSE	460	<b>M</b> Y <b>W</b> T <b>D</b> W <b>G</b> E---IP <b>K</b> I <b>E</b> R <b>A</b> A <b>L</b> D <b>G</b> S <b>D</b> R <b>V</b> V <b>L</b> V <b>N</b> T <b>S</b> L <b>G</b> W <b>P</b> N <b>G</b> L <b>A</b> L <b>D</b> Y <b>D</b> E <b>G</b> T <b>I</b> Y <b>W</b> G <b>D</b> A <b>K</b> T <b>D</b> K <b>I</b> E <b>V</b> M <b>N</b>	
F6YLU8	LRP6_XENTR	461	<b>M</b> Y <b>W</b> T <b>D</b> W <b>G</b> E---IP <b>K</b> I <b>E</b> R <b>A</b> A <b>M</b> D <b>G</b> S <b>D</b> R <b>I</b> L <b>V</b> N <b>T</b> S <b>L</b> G <b>W</b> P <b>N</b> G <b>L</b> A <b>L</b> D <b>Y</b> A <b>E</b> G <b>K</b> I <b>Y</b> W <b>G</b> D <b>A</b> K <b>T</b> D <b>K</b> I <b>E</b> V <b>M</b> T	
Q9NHE9	ARRO_DROME	534	<b>M</b> F <b>W</b> S <b>D</b> W <b>N</b> E---R <b>K</b> P <b>K</b> V <b>E</b> R <b>A</b> S <b>L</b> D <b>G</b> S <b>E</b> R <b>V</b> V <b>L</b> V <b>S</b> E <b>N</b> L <b>G</b> W <b>P</b> N <b>G</b> I <b>A</b> L <b>D</b> I <b>E</b> A <b>K</b> A <b>I</b> Y <b>W</b> C <b>D</b> G <b>K</b> T <b>D</b> K <b>I</b> E <b>V</b> A <b>N</b>	
...				
075581	LRP6_HUMAN	638	RRADIRRI <b>S</b> L <b>E</b> T <b>N</b> ---N <b>N</b> N <b>V</b> A <b>I</b> P <b>L</b> T <b>G</b> V <b>K</b> E <b>A</b> S <b>A</b> L <b>D</b> F <b>D</b> V <b>T</b> D <b>N</b> R <b>I</b> <b>Y</b> W <b>T</b> D <b>I</b> S <b>L</b> K <b>T</b> I <b>S</b> R <b>A</b> E <b>F</b> M <b>N</b> G <b>S</b>	BP3
075197	LRP5_HUMAN	651	SRAAIHRIS <b>L</b> E <b>T</b> N---N <b>N</b> D <b>V</b> A <b>I</b> P <b>L</b> T <b>G</b> V <b>K</b> E <b>A</b> S <b>A</b> L <b>D</b> F <b>D</b> V <b>S</b> N <b>N</b> H <b>I</b> <b>Y</b> W <b>T</b> D <b>V</b> S <b>L</b> K <b>T</b> I <b>S</b> R <b>A</b> E <b>F</b> M <b>N</b> G <b>S</b>	
B5L5I6	LRP6_DANRE	642	RHTDIRRIS <b>L</b> E <b>T</b> N---N <b>N</b> N <b>V</b> A <b>I</b> P <b>L</b> T <b>G</b> V <b>K</b> E <b>A</b> S <b>A</b> L <b>D</b> F <b>D</b> I <b>T</b> D <b>N</b> R <b>I</b> <b>Y</b> W <b>T</b> D <b>I</b> T <b>L</b> K <b>T</b> I <b>S</b> R <b>A</b> E <b>F</b> M <b>N</b> G <b>S</b>	
088572	LRP6_MOUSE	638	RRADIRRIS <b>L</b> E <b>T</b> N---N <b>N</b> N <b>V</b> A <b>I</b> P <b>L</b> T <b>G</b> V <b>K</b> E <b>A</b> S <b>A</b> L <b>D</b> F <b>D</b> V <b>T</b> D <b>N</b> R <b>I</b> <b>Y</b> W <b>T</b> D <b>I</b> S <b>L</b> K <b>T</b> I <b>S</b> R <b>A</b> E <b>F</b> M <b>N</b> G <b>S</b>	
F6YLU8	LRP6_XENTR	639	RRADIRRIS <b>L</b> E <b>T</b> S---N <b>S</b> H <b>V</b> A <b>I</b> P <b>L</b> T <b>G</b> V <b>K</b> E <b>A</b> S <b>A</b> L <b>D</b> F <b>D</b> V <b>T</b> D <b>N</b> R <b>I</b> <b>Y</b> W <b>T</b> D <b>V</b> S <b>L</b> K <b>T</b> I <b>S</b> R <b>A</b> E <b>F</b> M <b>N</b> G <b>S</b>	
Q9NHE9	ARRO_DROME	714	RQEHIGRISIE <b>Y</b> E <b>G</b> N <b>H</b> N <b>D</b> E <b>R</b> I <b>P</b> F <b>K</b> D <b>V</b> R <b>D</b> A <b>H</b> A <b>L</b> D <b>V</b> S <b>V</b> A <b>E</b> R <b>R</b> I <b>Y</b> W <b>T</b> D <b>Q</b> K <b>S</b> K <b>C</b> I <b>F</b> R <b>A</b> E <b>F</b> L <b>I</b> N <b>G</b> S	
...				
075581	LRP6_HUMAN	814	LI <b>E</b> S <b>S</b> N <b>M</b> L <b>G</b> L <b>N</b> R <b>E</b> -VI <b>A</b> D <b>D</b> L <b>P</b> H <b>P</b> F <b>G</b> L <b>T</b> Q <b>Y</b> Q <b>D</b> Y <b>I</b> <b>Y</b> W <b>T</b> D <b>W</b> S <b>R</b> R <b>S</b> I <b>E</b> R <b>A</b> N <b>K</b> T <b>S</b> G <b>N</b> R <b>T</b> I <b>I</b> Q <b>H</b>	BP4
075197	LRP5_HUMAN	827	MI <b>E</b> S <b>S</b> N <b>M</b> L <b>G</b> Q <b>E</b> R <b>V</b> -VI <b>A</b> D <b>D</b> L <b>P</b> H <b>P</b> F <b>G</b> L <b>T</b> Q <b>Y</b> S <b>D</b> Y <b>I</b> <b>Y</b> W <b>T</b> D <b>W</b> N <b>L</b> H <b>S</b> I <b>E</b> R <b>A</b> D <b>K</b> T <b>S</b> G <b>N</b> R <b>T</b> I <b>I</b> Q <b>H</b>	
B5L5I6	LRP6_DANRE	818	LI <b>E</b> S <b>S</b> N <b>M</b> L <b>G</b> L <b>E</b> R <b>E</b> -VI <b>A</b> D <b>D</b> L <b>P</b> H <b>P</b> F <b>G</b> L <b>T</b> Q <b>Y</b> Q <b>D</b> Y <b>I</b> <b>Y</b> W <b>T</b> D <b>W</b> S <b>Q</b> R <b>S</b> I <b>E</b> R <b>A</b> N <b>K</b> T <b>S</b> G <b>N</b> R <b>T</b> I <b>I</b> Q <b>H</b>	
088572	LRP6_MOUSE	814	LI <b>E</b> S <b>S</b> D <b>M</b> L <b>G</b> L <b>N</b> R <b>E</b> -VI <b>A</b> D <b>D</b> L <b>P</b> H <b>P</b> F <b>G</b> L <b>T</b> Q <b>Y</b> Q <b>D</b> Y <b>I</b> <b>Y</b> W <b>T</b> D <b>W</b> S <b>R</b> R <b>S</b> I <b>E</b> R <b>A</b> N <b>K</b> T <b>S</b> G <b>N</b> R <b>T</b> I <b>I</b> Q <b>H</b>	
F6YLU8	LRP6_XENTR	815	LI <b>E</b> S <b>S</b> N <b>M</b> L <b>G</b> L <b>D</b> R <b>V</b> -VI <b>A</b> D <b>D</b> L <b>P</b> H <b>P</b> F <b>G</b> L <b>T</b> Q <b>Y</b> Q <b>D</b> Y <b>I</b> <b>Y</b> W <b>T</b> D <b>W</b> S <b>Q</b> R <b>S</b> I <b>E</b> R <b>A</b> N <b>K</b> T <b>S</b> G <b>N</b> R <b>T</b> I <b>I</b> Q <b>H</b>	
Q9NHE9	ARRO_DROME	893	K <b>I</b> E <b>S</b> A <b>D</b> W <b>D</b> G <b>K</b> K <b>R</b> Q <b>I</b> L <b>V</b> G <b>S</b> D <b>M</b> D <b>E</b> P <b>Y</b> A <b>V</b> S <b>L</b> Y <b>Q</b> D <b>Y</b> V <b>Y</b> W <b>S</b> D <b>W</b> N <b>T</b> G <b>D</b> I <b>E</b> R <b>V</b> H <b>K</b> T <b>T</b> G <b>N</b> R <b>S</b> L <b>V</b> H <b>S</b> G	
...				

Figure 11: Alignment of LRP6 from different species with LRP5.

Alignment of *homo sapiens* LRP6, *homo sapiens* LRP5, *danio rerio* LRP6, *mus musculus* LRP6, *xenopus tropicalis* LRP6, and *drosophila melanogaster* LRP6. In every line the uniprot identifier is given before the gene\_species abbreviation together with the number of the line starting amino acid. The YWTD BP /  $\beta$ -sheet motif of the  $\beta$ -propeller domains 1-3 (BP1-3) preceding the conserved N-glycosylation site is colored magenta/blue, respectively. Highly conserved N-glycosylation sites are boxed red. Interspersed amino acids are abbreviated by three dots.

### 3.4 B3GNT8 modifies the complex N-glycans of LRP6

Considering B3GNT8 is predicted to modify pre-existing N-glycan chains, I next asked what type of LRP6 N-glycan chains are modified by using specific inhibitors of N-glycosylation as well as enzymes that cleave different types of N-glycan chains. To this end I added a well-

known global inhibitor of N-glycosylation, tunicamycin, to LRP6 and B3GNT8 transfected HEK293 cells. Tunicamycin inhibits N-glycosylation by being incorporated instead of the very first GlcNAc of the new forming oligosaccharide precursor (Eckert et al., 1998). Thereby it inhibits all subsequent steps of N-glycosylation. In SDS-PAGE/Immunoblotting, tunicamycin reduces all LRP6 forms to one single, fast migrating band indicating that all LRP6 subspecies differ predominantly in their N-glycans (Khan et al., 2007). In agreement with these findings, SDS-PAGE/Immunoblot analysis of LRP6 from tunicamycin treated cells confirmed the down shift of both LRP6 bands. The SDS-PAGE/Immunoblotting also revealed that B3GNT8 was not able to modify LRP6 after the tunicamycin treatment, indicating that B3GNT8 modifies pre-existing N-glycans on LRP6 (fig. 12 A). The decrease in total LRP6 after tunicamycin treatment is reportedly due to deregulation of quality control mechanisms (Khan et al., 2007).

Next, I treated cells with an N-glycan dissociation agent to test if this removes the glycan chains of B3GNT8-modified LRP6. I subjected Western Blot-ready lysates from LRP6 and B3GNT8 transfected HEK293 cells to peptide:N-glycosidaseF (PNGaseF) treatment which removes all types of N-glycans. Un-modified LRP6 was used as control. As expected, PNGase F down shifted both LRP6 bands. In line with my expectations, PNGaseF also completely removed the B3GNT8-mediated modification of LRP6 (fig. 12 B). From these experiments I could confirm that B3GNT8 indeed modifies the N-glycans of LRP6.

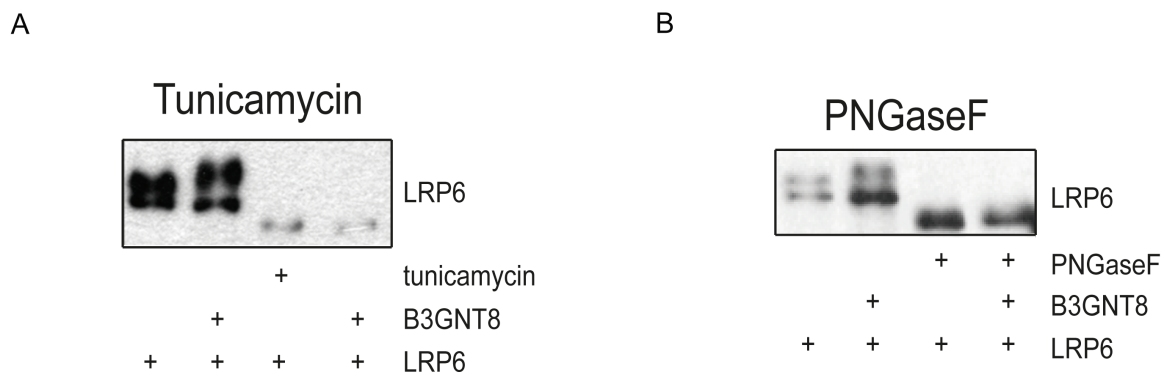


**Figure 12: B3GNT8 modifies the N-glycans of LRP6.**

A. Western Blots of lysates from HEK293T cells in 96-wells transfected with LRP6 (20ng) and B3GNT8 (15ng) and harvested 24 hours later. 3.5h post-transfection, 0.1µg tunicamycin was added per 96well.

B. As in A, but PNGaseF was added to lysates in Laemmli loading buffer for 2h at 37°C.

The N-glycans of LRP6 are all thought to be processed from high mannose precursors into complex- or hybrid-types (Khan et al., 2007). I used endoglycosidase H (EndoH), which removes only high mannose and some hybrid N-glycans but not complex-types, to confirm that B3GNT8 acts on complex N-glycans which is its substrate. I subjected Western Blot lysates from LRP6 and B3GNT8 transfected HEK293 cells to endoglycosidase H treatment and in SDS-PAGE / Immunoblot analysis, the lower LRP6 band could be down-shifted (fig. 13 A). The down-shift of the lower LRP6 band is consistent with the co-translational attachment of

the mannose-rich oligosaccharide precursor to immature LRP6 forms. Neither the unmodified nor the B3GNT8-modified upper LRP6 band was downshifted. The stability of the upper LRP6 bands to EndoH treatment confirms that all precursors are processed into complex-types and that B3GNT8 acts on these complex-type N-glycans.

Complex N-glycans uniquely possess a terminal sialic acid residue (the so-called “cap”) on each of their antennae. The exoglycosidase neuraminidase cleaves specifically this last sialic acid of all types of glycans and the complex type N-glycans of LRP6 have been shown to be sensitive to neuraminidase treatment (Hsieh et al., 2003). To confirm that B3GNT8 acts on the complex N-glycans of LRP6 I administered neuraminidase to whole cell lysates from LRP6 and B3GNT8 transfected HEK293 cells. Un-modified LRP6 served as control. The exoglycosidases galactosidase and N-acetylglucosaminase were administered as controls to exclude unspecific addition of galactose or N-acetylglucosamine. Non-exoglycosidase treated samples were loaded on both sides of the SDS-polyacrylamide gel to make the small downshift visible. Neuraminidase conferred the same downshift to the upper LRP6 band both with and without B3GNT8s modification (fig. 13 B, samples “N”, note the decrease in distance between upper and lower LRP6 band). In line with my expectations, the galactosidase and N-acetylglucosaminase treated samples showed no effect. This strongly suggests that B3GNT8 modifies complex N-glycans on the ECD of LRP6.

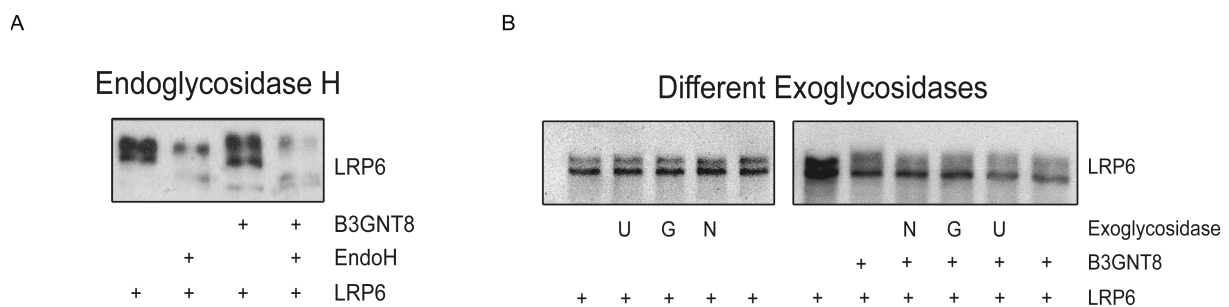


**Figure 13: B3GNT8 modifies the complex N-glycans of LRP6.**

A. Western Blots of lysates from HEK293T cells in 96-wells transfected with LRP6 (20ng) and B3GNT8 (15ng) and harvested 24 hours later. Endo H was added to lysates for 2h at 37°C. Note that the lower bands, but not the upper bands, of LRP6 are endoglycosidase H sensitive. An anti-myc antibody was used to detect total LRP6.

B. As in a, but Neuraminidase (N), Galactosidase (G), or N-Acetylglucosaminase (U) was added to lysates in Laemmli loading buffer for 2h at 37°C. Note the small decrease of distance between upper and lower LRP6 bands with Neuraminidase.

### **3.5 B3GNT8 co-immunoprecipitates with LRP6**

In order to test if B3GNT8 and LRP6 interact physically I performed co-immunoprecipitation experiments where antiFLAG-antibody coupled beads are used to enrich FLAG-tagged proteins and their binding partners. FLAG-tagged B3GNT8 was used as bait from LRP6 and FLAG-B3GNT8 transfected HEK293T cell lysates. The N-glycosylated Dickkopf3 (DKK3) protein and the non-glycosylated Glycogen Synthase Kinase 3 (GSK3) were used as secretory (ER/Golgi-transiting) and cytosolic (non-ER/Golgi-transiting) control, respectively. In line with expectations, B3GNT8 co-immunoprecipitated with LRP6 (fig. 14, upper panel). However

B3GNT8 did not co-immunoprecipitate with DKK3 and GSK3. This result confirms that LRP6 and B3GNT8 physically interact, which is in line with the finding that LRP6 is a substrate for B3GNT8.

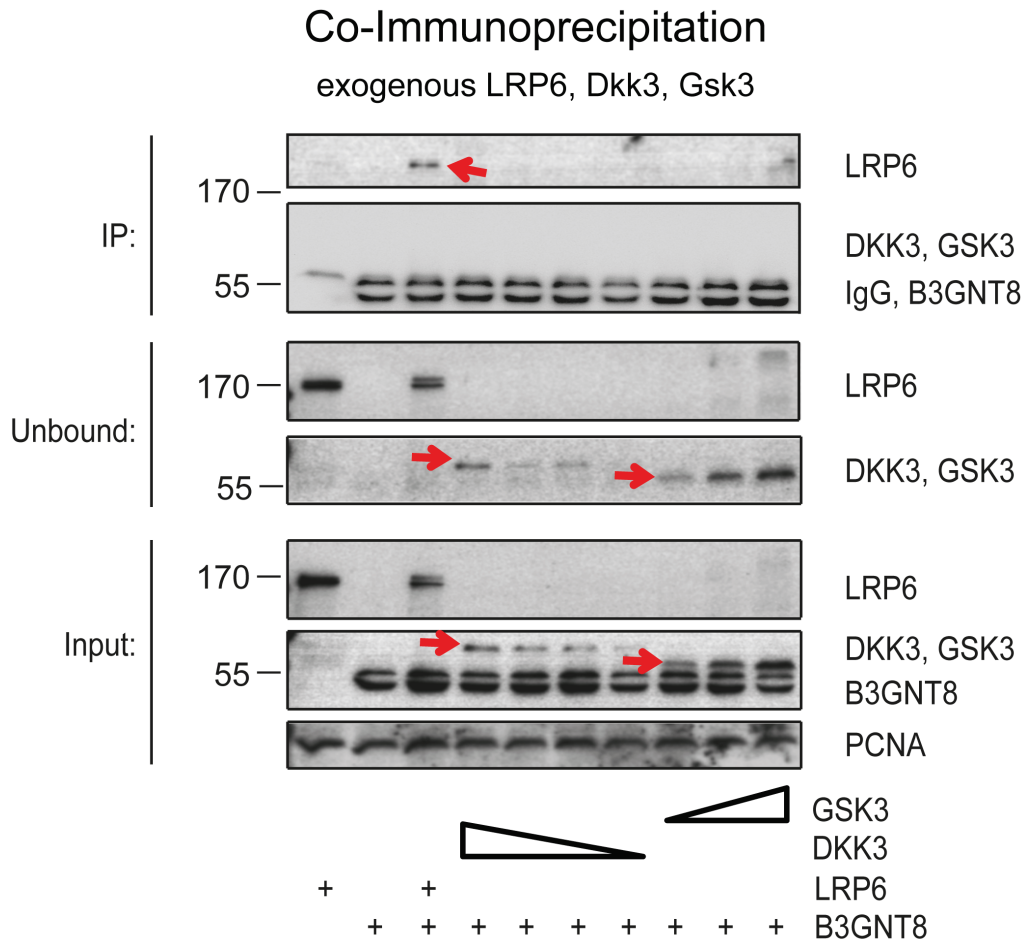


**Figure 14: LRP6 co-immunoprecipitates with B3GNT8.**

Western Blots of lysates from HEK293T cells transfected with combinations of LRP6::6myc (600ng), DKK3-V5 (60, 40, 30, and 24ng), GSK3-myc (300, 600, and 1200ng), and B3GNT8::FLAG (450ng) in 6 well format. Whole cell lysates were harvested 24hours past transfection and co-immunoprecipitated with anti-FLAG agarose beads. Anti-Myc antibody was employed to detect LRP6, and GSK3, B3GNT8 was detected by an anti-FLAG antibody, DKK3 was detected by an anti-V5 antibody. Note that the IgG band is just above the two B3GNT8 bands. Note that DKK3 and GSK3 are above the B3GNT8 and the IgG bands.

### **3.6 B3GNT8 acts at the level of the activated Wnt receptor complex**

To gain insights into where B3GNT8 functions to activate Wnt signaling I performed an epistasis experiment by over-expressing different pathway components to activate signaling at different levels and asked to what degree co-expression of B3GNT8 enhanced this further. Wnt3a was applied as conditioned media (CM) in order to focus on Wnt reception at the cell surface and avoid any potential effects during the Wnt synthesis and secretion route. The TOPFLASH reporter alone served as control for B3GNT8s baseline activity. In TOPFLASH assays, B3GNT8 showed synergies together with the Wnt receptor complex or the so called signalosome members Wnt3a, LRP6, Dsh, and CK1 $\gamma$  (fig. 15, synergies are indicated by stars



according to their p-value). No enhancement by B3GNT8 was seen if the pathway was activated by  $\beta$ -catenin, which acts further downstream in Wnt signal transduction. This indicates that the modification of LRP6 acts at the level of the activated signalosome.

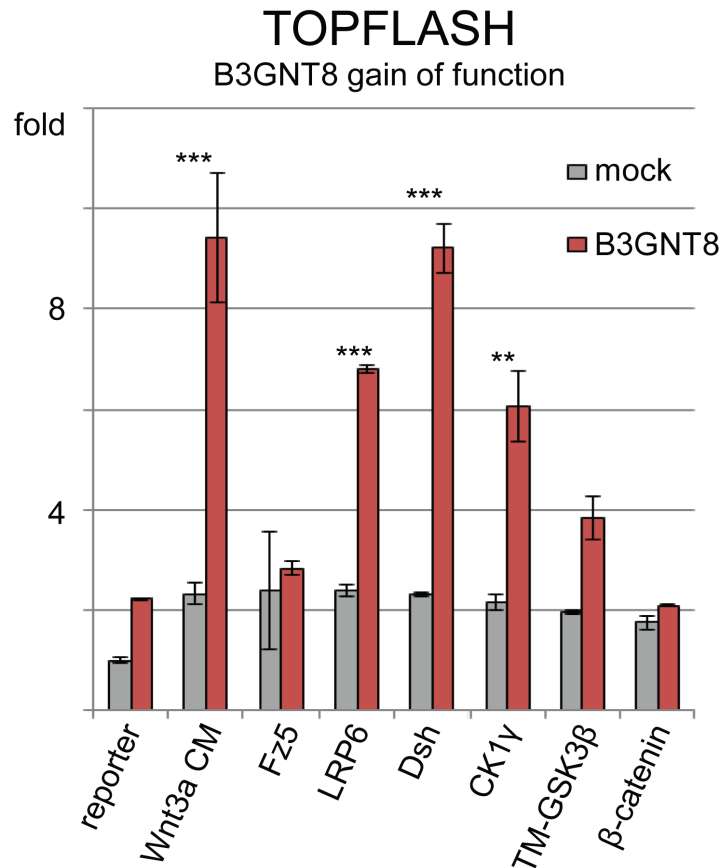


**Figure 15: B3GNT8 GoF acts at the level of the activated receptor complex.**

HEK293T cells were co-transfected with the Wnt-reporter TOPFLASH (20ng), thymidine kinase-renilla reporter (4ng), Fz5 (50ng), LRP6 (7ng), Dsh (20ng), CK1 $\gamma$  (10ng), transmembrane(TM)-GSK3 (30ng), beta-catenin (20ng), and LacZ (mock) or B3GNT8 (15ng) per 96well. Wnt3a or Dkk1-conditioned medium was added (5ul or 70ul O.N., respectively). The cells were harvested 24h past transfection in passive lysis buffer (Promega). P-values for synergies (compared to difference in signaling of reporter w/o B3GNT8): \* $\leq$ 0.05, \*\* $\leq$ 0.01, \*\*\* $\leq$ 0.001.

To support the B3GNT8 GoF epistasis experiments I performed B3GNT8 LoF epistasis experiments. One day after transfection of HEK293 cells with B3GNT8 siRNA I transiently transfected the same cells with canonical pathway members. The TOPFLASH reporter alone served as control for B3GNT8s silencing, which, as expected, reduced basal Wnt signaling about 2-fold (fig. 16). The inhibition of Wnt signaling by B3GNT8 siRNA was however more significant if the pathway was activated by Wnt3a-CM or LRP6 and, to lesser extent by Dvl (fig. 16). As for B3GNT8 GoF, B3GNT8 siRNA had no significant effect on Wnt signaling activity if the pathway was activated at the level of  $\beta$ -catenin. I interpret this as a confirmation that the modification of LRP6 acts at the receptor complex level and not downstream.

## TOPFLASH B3GNT8 loss of function

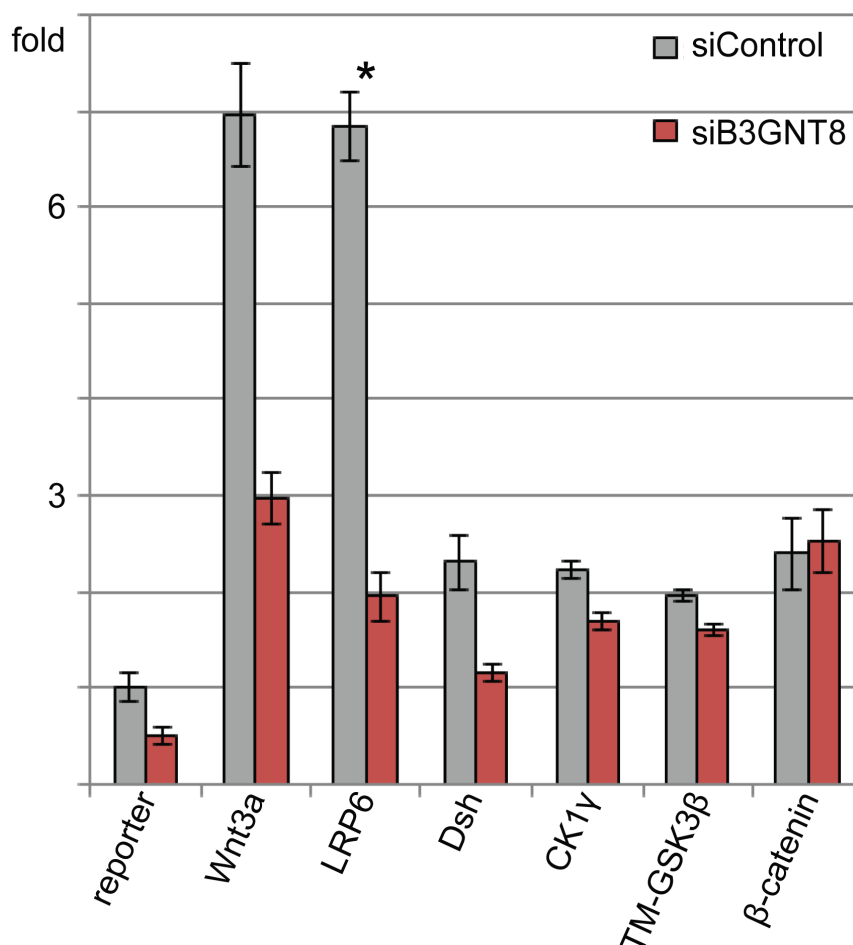


**Figure 16: B3GNT8 LoF acts at the level of the activated receptor complex.**

On day 1, HEK293T cells were subjected to siRNA (siControl or siB3GNT8, 20pmol each) mediated gene silencing. On day 2, the same cells were co-transfected with the Wnt-reporter TOPFLASH (20ng), thymidin kinase-renilla reporter (4ng), Wnt3a (20ng), LRP6 (20ng), Dsh (20ng), CK1g (10ng), the constitutively active transmembrane(TM)-GSK3 (30ng), beta-catenin (20ng), and LacZ (mock) or B3GNT8 (15ng) per 96well. Harvest was done as described above. P-values for synergies (compared to difference in signaling of reporter w/o B3GNT8): \* $\leq 0.05$ .

Activated signalosomes are thought to be endocytosed in a Rab5 dependent manner. Rab5 defines the site of entry into early endosomes and modulates Wnt signaling depending on the cell type (Dasgupta et. al, 2005; Rives et al., 2006; Seto and Bellen, 2006). Rab4 and Rab11 mediate the fast and the slow recycling, respectively, but are not thought to modulate Wnt signaling (Kikuchi et al. 2006). In TOPFLASH luciferase reporter assays I tested increasing concentrations of the Rab proteins 4, 5, and 11 for their effects on the B3GNT8 mediated Wnt stimulus. The TOPFLASH reporter alone was used to control for B3GNT8s activity. While Rab11 did not increase Wnt signaling Rab4 enhanced signaling about 2-fold, similar to the effect of B3GNT8 (fig. 17). However, Rab4 and B3GNT8 co-expression led to a merely additive effect. Rab4 enhances exosomal shuttling of endogenous Wg proteins in *Drosophila* (Gross et al., 2012). To me this suggests that the increase in TOPFLASH response upon Rab4 expression may reflect an enhanced exosomal shuttling of Wnt. The early



endosome marker Rab5 lead to a 3-fold activation of Wnt signaling and, strikingly, co-expression of B3GNT8 lead to a synergistic enhancement at higher Rab5 levels. This result suggests that B3GNT8s modification of LRP6 acts at the level of the activated signalosome.

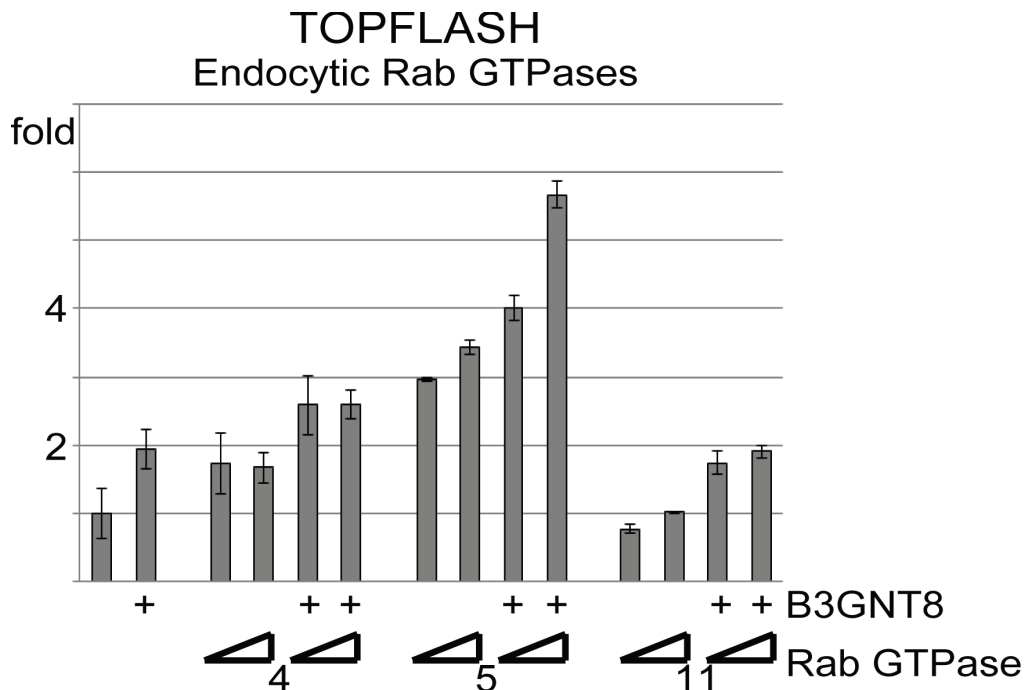


**Figure 17: B3GNT8 expression synergizes with Rab5 dependent Wnt stimulation.**

B3GNT8 sensitizes the Rab5 induced Wnt signalling. TOPFLASH reporter assay using HEK293T cells treated cotransfected with increasing concentrations the endocytosis related proteins Rab4 (5, 10, 20ng), Rab5 (1, 2, 4ng) and Rab11 (5, 10, 20ng) either with or without 15ng B3GNT8. Cell lysates were harvested 20 hours post-transfection for Luciferase activity measurement. Note the steepened increase in Wnt signaling when B3GNT8 is co-transfected with Rab5.

### **3.7 B3GNT8 specifically adds mass onto LRP6 to regulate Wnt signaling**

I tested the ability of B3GNT8 to functionally modify a truncated LRP6 (LRP6ΔE1-4) that lacks most of its extracellular domain and thus lacks all N-glycosylation sites. Although LRP6ΔE1-4 is constitutively active (Mao et al., 2004), its activity can still be enhanced by addition of Wnt medium or co-expression of LRP6 kinases such as CK1γ (Davidson et al., 2005). LRP6ΔC, which lacks most of the intracellular domain but still possesses its extracellular domain and thus all N-glycosylation sites, was used as control in addition to wild-type LRP6. In contrast to LRP6ΔE1-4, LRP6ΔC should be modified (up-shifted protein band) by B3GNT8 but should not be able to activate Wnt signaling since it's missing its intracellular domain. In line with my expectations, B3GNT8 modified wild type LRP6 and LRP6ΔC in the immunoblot assays while the LRP6ΔE1-4 bands remained uninfluenced (fig. 18 A). In agreement with my hypothesis that B3GNT8 activates Wnt signaling by modifying the N-glycans of LRP6, B3GNT8 was however not able to stimulate LRP6ΔE1-4 activated Wnt signaling, as it did with the wild type LRP6 (fig. 18 A, graph). As expected LRP6ΔC decreased Wnt signaling and B3GNT8 did not counteract this dominant-negative effect. This is consistent with a positive role in Wnt signaling for B3GNT8 mediated modification of LRP6 N-glycan chains.

N-glycosylated canonical Wnt pathway members comprise LRPs, Wnts, and Frizzleds. To verify the above results, I tested if B3GNT8 can covalently modify other N-glycosylated Wnt pathway members than LRP6. Wnt3a and Frizzled5 were readily available in our lab and have been tested for their activity in Wnt/TOPFLASH signaling. LRP6 served as control for B3GNT8s activity. I transiently transfected HEK293T cells with LRP6, Wnt3a, and Frizzled5 either with or without B3GNT8 for SDS-PAGE/Immunoblot assays. As expected, B3GNT8 solely up-shifted LRP6 (fig. 18 B). From the above mentioned experiments I conclude that the mass addition to LRP6 is the cause of B3GNT8s Wnt stimulus.

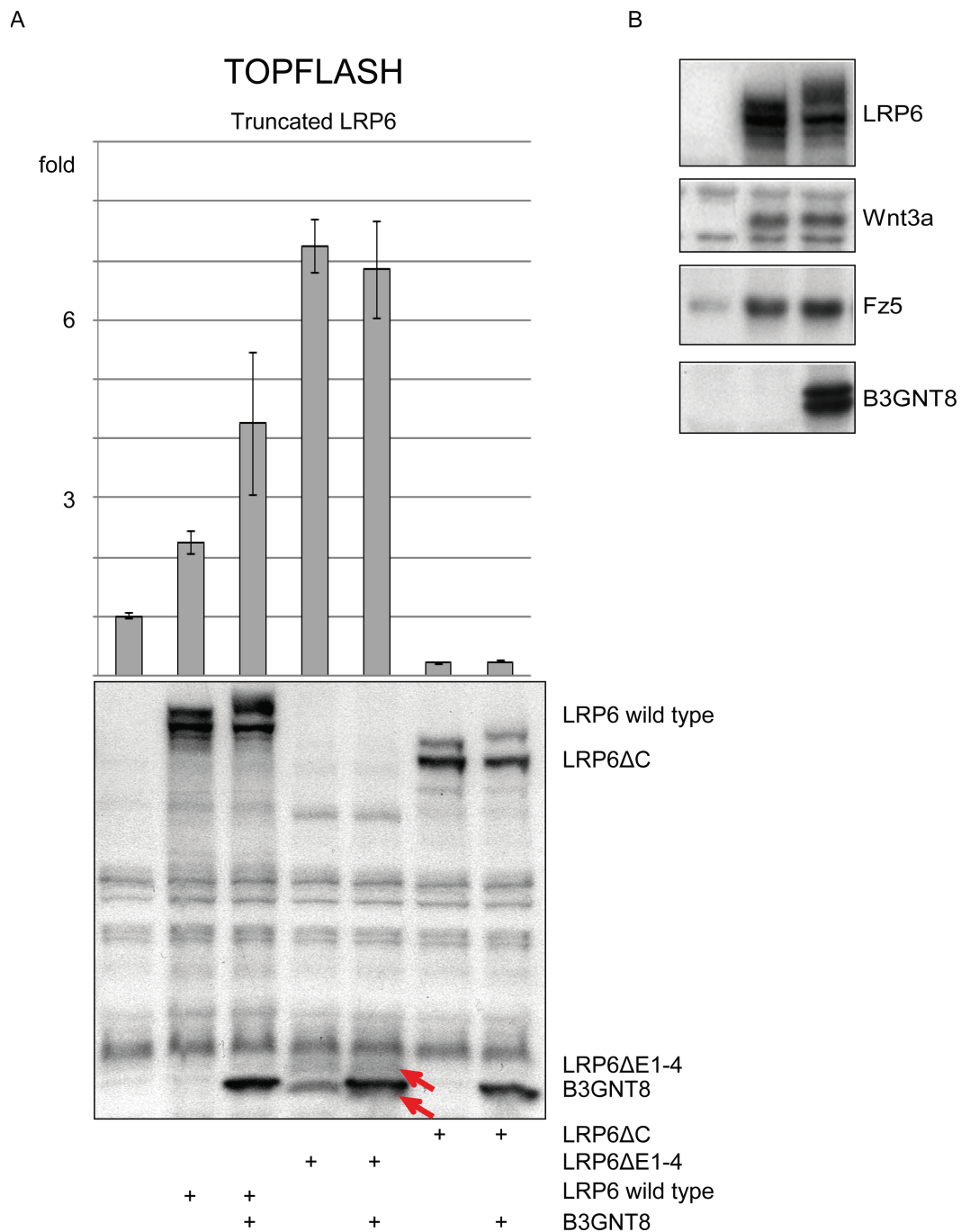


**Figure 18: B3GNT8 specifically adds mass to LRP6 to regulate Wnt-signalling.**

A. HEK293T cells were co-transfected with TOPFLASH luciferase (20ng), thymidine kinase-renilla reporter (4ng) and the indicated LRP6 construct (each 20ng) and w/o B3GNT8 (15ng). Cells were harvested 24h later in 1% triton lysis buffer for Western Blot or passive lysis buffer (Promega) for luciferase assay. Anti-myc and anti-Flag antibodies were employed to detect the LRP6 construct, anti-Flag was used to

detect B3GNT8. Note that the lower LRP6 $\Delta$ E1-4 band is on the height of B3GNT8. Note that the stimulation of Wnt signaling stops with LRP6 $\Delta$ E1-4.

B. Western Blots of lysates from HEK293T cells co-transfected with LRP6 (20ng), Frizzled5 (20ng), Wnt3a (5ng), and LacZ (Mock) or B3GNT8 (15ng). Whole cell lysates were harvested 20hours past transfection in 1% triton lysis buffer. An anti-myc antibody was employed to detect LRP6, an anti-V5 antibody was used to detect Frizzled5 and Wnt3a. Note that B3GNT8 up-shifts solely LRP6.

### **3.8 B3GNT8 does not appear to modify LRP5**

Considering LRP5 and LRP6 function redundantly I tested the ability of B3GNT8 to modify LRP5. To this purpose I co-expressed increasing amounts of LRP5, with or without B3GNT8. LRP6 expression served as a functional control for B3GNT8 activity. While LRP6 expression stabilized B3GNT8 (fig. 19, compare first and last lane), a strong reduction of B3GNT8 appeared, whenever LRP5 was co-expressed (compare lane 1 and 3). B3GNT8 was not able to confer mass upon LRP5. Although LRP5 and -6 expression is driven by the same promoter, LRP5 is either translated at much lower levels, leading to weaker protein bands, or the Myc-epitope is less accessible to the antibody. In contrast to LRP6, the upper LRP5 band is stronger than the lower band, suggesting that LRP5 N-glycan processing may be more efficient. This shows that in the canonical Wnt pathway B3GNT8 acts mainly on LRP6.

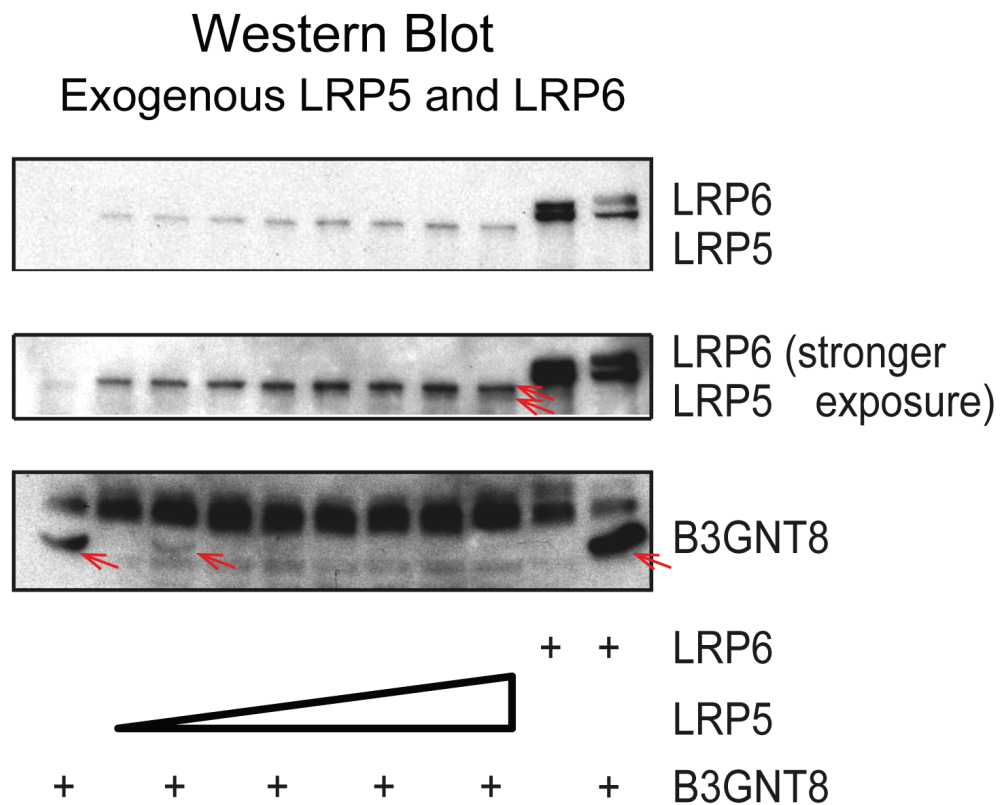


**Figure 19: B3GNT8 does not modify LRP5 and LRP5 reduces B3GNT8 protein levels.**

Western Blots of lysates from HEK293T cells transfected with LRP6::myc (20ng) or LRP5::myc (20, 40, 60, or 80ng), and B3GNT8-FLAG (25ng) or LacZ (mock) in 96 well format. Whole cell lysates were harvested 20hours past transfection in 1% triton lysis buffer. Anti-FLAG antibody was employed to detect B3GNT8, LRP5 and LRP6 were detected with anti-myc antibody. The unspecific band above B3GNT8 may serve as loading control. Note that B3GNT8 protein levels decreases with introduction of LRP5 (lowest band in lower panel).

### 3.9 In HEK293 cells, B3GNT8 does not synergistically enhance the activity of B3GNT2 to stimulate Wnt signaling

It was shown that B3GNT8 synergistically enhances in vitro the activity of and co-immunopurifies in COS-7 cells with its family member B3GNT2 (Seko and Yamashita, 2008). I therefore asked if the covalent mass addition to LRP6 in HEK293T cells might be rather through B3GNT2 than B3GNT8. I therefore isolated the B3GNT2 construct from our annotated medaka cDNA library and transfected increasing amounts in HEK293T cells either with or without B3GNT8. LRP6 together with B3GNT8 alone served as a control for B3GNT8s activity. Although B3GNT2 activated Wnt signaling in a dose-dependent manner it has no effect on the modification of LRP6 as seen by SDS-PAGE/Western Blot analysis (fig. 20). Moreover, the combination of B3GNT2 and B3GNT8 resulted merely in an additive TOPFLASH increase (fig. 20, graph). Since our lab is interested in the effects of protein modifiers on the Wnt co-receptor LRP6 I decided not to investigate further the effect B3GNT2 in Wnt signaling. To me this result indicates that the enhancement of B3GNT2 activity by the mere presence of B3GNT8 does not happen in HEK293T cells.

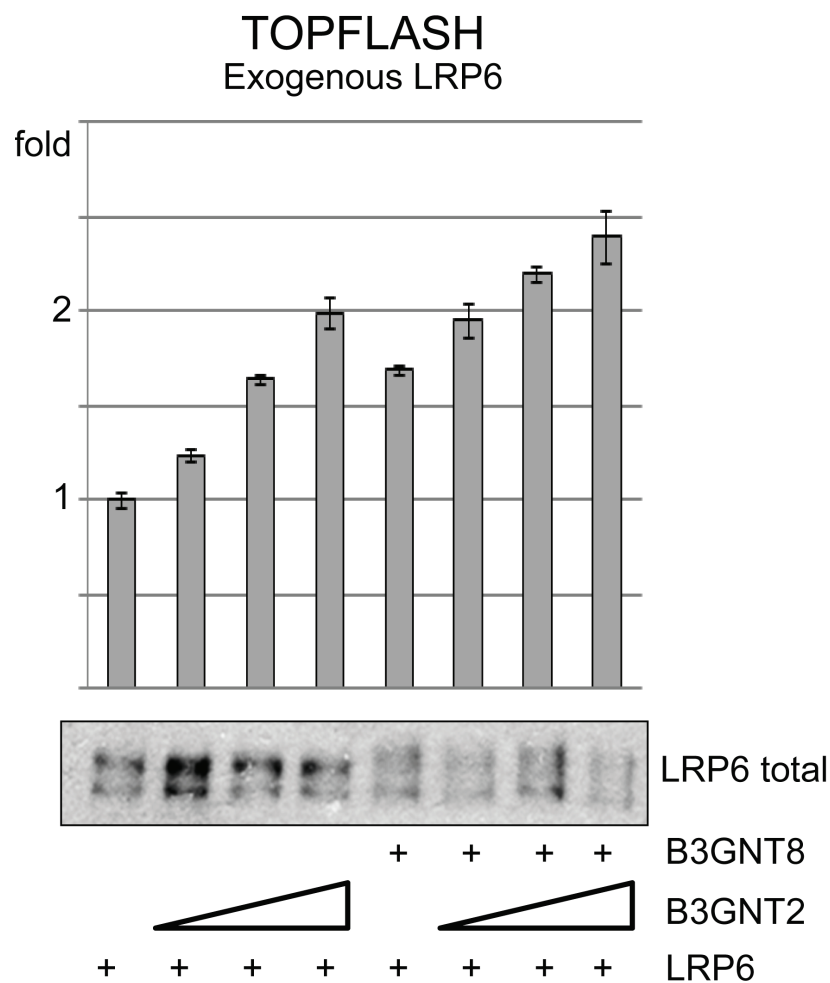


**Figure 20: Only B3GNT8 functionally modifies LRP6.**

HEK293T cells in 96well format were co-transfected with TOPFLASH luciferase Wnt reporter (20ng), thymidine kinase-renilla (4ng), LRP6 (each 20ng) and with increasing concentrations of B3GNT2 (5, 10, and 15ng) either in the presence or absence of B3GNT8 (15ng). Cells were harvested 24h later in 1% triton lysis buffer for Western Blot or passive lysis buffer (Promega) for Luciferase assay. Anti-myc antibody

was employed to detect LRP6. Note that B3GNT2 dose-dependently stimulates Wnt signaling, but neither alone nor in combination with B3GNT8 up-shifts LRP6 in Western Blot.

### **3.10 B3GNT8 is required for LRP6 / Wnt signaling**

To investigate the requirement of B3GNT8 for LRP6/Wnt signaling I performed B3GNT8 gene silencing (siRNA) experiments. TOPFLASH and SDS-PAGE/Immunoblot assays on LRP6 protein were performed after a 48h knock down (siRNA) of the B3GNT8 gene, which was previously shown to be the optimal time (not shown). Time course experiments for B3GNT8 silencing also showed that the knock down was stable for at least 4 days. For the loss-of-function (LoF) experiments the siRNA was transfected on day 1 and on day 2 TOPFLASH, B3GNT8 and mock pDNA constructs were transfected. LRP6 knock down (siRNA) was used as a positive control for Wnt signaling inhibition and for proper identification of the LRP6 protein in SDS-PAGE/Immunoblotting. Non-targeting siRNA (siControl) was used to control for the transfection procedure. In TOPFLASH assays B3GNT8 knockdown significantly reduced Wnt signaling, although it did not reach the level of the LRP6 knock down (fig. 21 A, graph). SDS-PAGE/Immunoblotting analysis showed a slight downregulation of LRP6 total protein and a clear decrease in phosphorylation of the LRP6 Serine at position 1490 (fig. 21 A, upper and middle panel). The decrease in the level of S1490 phosphorylation corresponded approximately with the decrease in Wnt signaling (both approx. -45%). Quantitative real-time PCR showed that the B3GNT8 LoF did not decrease LRP6 on transcriptional levels (fig. 21 B). The LRP6 protein decrease must therefore happen post-transcriptionally. LRP6 and B3GNT8 knockdown have been reported to reduce cell proliferation (Hua et al., 2012; Keramati et al., 2009) and I confirmed this effect in HEK293T cells (fig. 21 C). Cell proliferation analysis as well as qPCR analysis of B3GNT8 mRNA levels confirmed knockdown by siRNA targeting B3GNT8 (fig. 21 B, C).

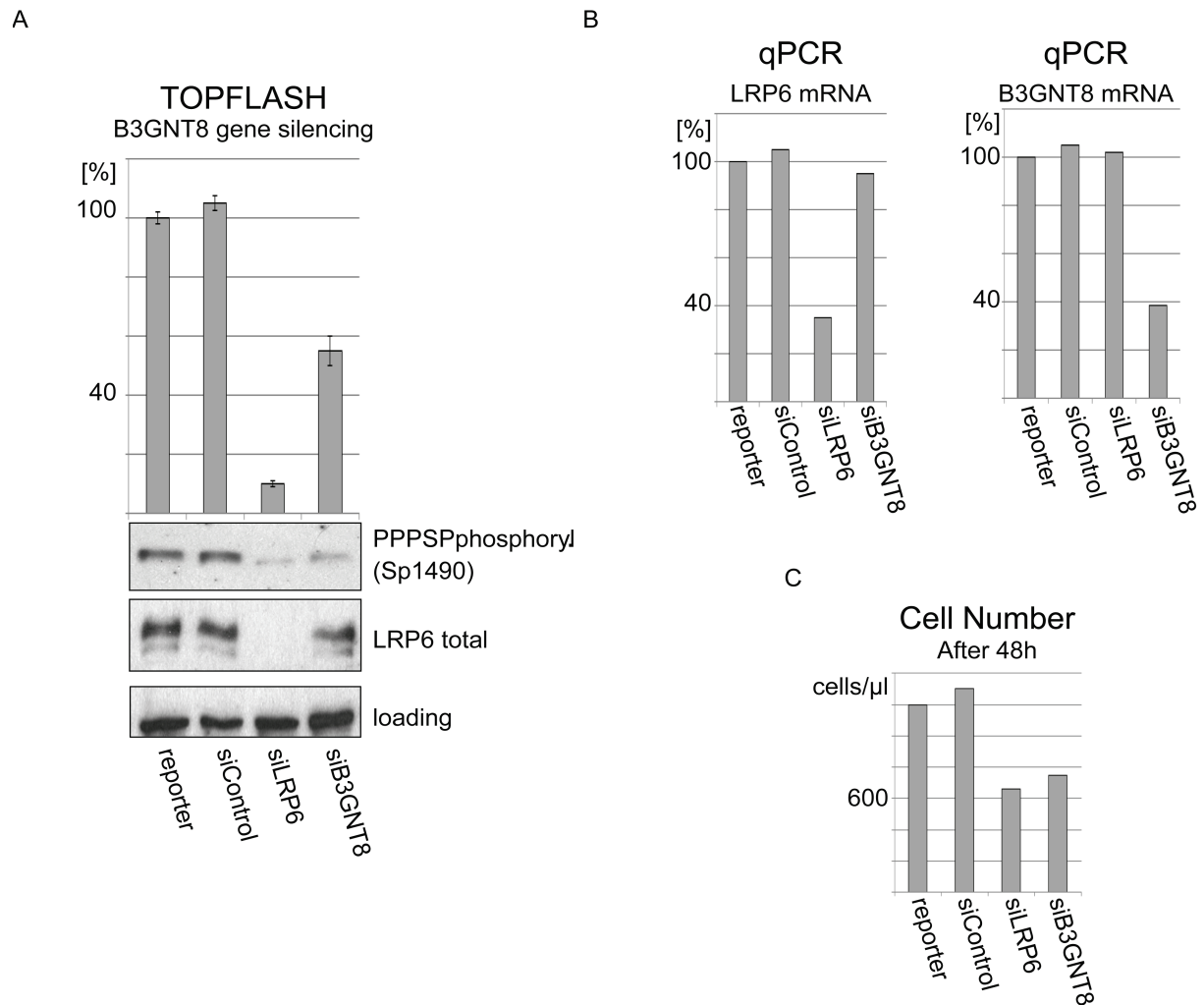


**Figure 21: B3GNT8 siRNA affects LRP6 and TOPFLASH.**

A. TOPFLASH assay and Western Blots of HEK293T cell lysates 48 hours after siRNA transfection. HEK293T cells were transfected with 20pmol of the indicated siRNA and, 24h later, transfected with TOPFLASH reporters (20ng) and thymidine kinase renilla reporter (4ng). Wnt3a-CM was added to make the PPSP phosphorylation visible.  $\alpha$ -LRP6\_T1479 was used to detect total LRP6. Anti-LRP6\_Sp1490 was used to detect phosphorylation of the Serine at position 1490, to monitor Wnt pathway regulation at receptor complex level. Note that B3GNT8 siRNA LoF results in significant reduction of both Wnt signaling and LRP6 (siB3GNT8).

B. Cells from the same transfection as in A were subjected to qPCR. Note that B3GNT8 knock down does not influence LRP6 mRNA levels, and vice versa.

C. Cells from the same transfection as in A have been detached via trypsinisation and counted. Note that the reported decrease of cell proliferation upon B3GNT8 knock down can be observed (siB3GNT8).

### **3.11 B3GNT8 is sufficient to rescue LRP6 protein levels, Wnt signaling and cell proliferation**

In order to confirm the specificity of the B3GNT8 silencing and its apparent requirement for Wnt signaling, I performed a rescue experiment using medaka B3GNT8, which is not targeted by the B3GNT8 siRNA used. I therefore first silenced the B3GNT8 gene by siRNA transfection in HEK293T cells and the next day I transfected exogenous medaka B3GNT8 in the same cells. In TOPFLASH assays B3GNT8 siRNA caused a 2-fold reduction in Wnt signaling that was completely rescued by exogenous B3GNT8 (fig. 22 A, graph). LRP6 protein levels were reduced by B3GNT8 siRNA and this could also be rescued, as seen in SDS-PAGE/Immunoblotting (fig. 22 A, panels below graph). This confirms B3GNT8 is required for the maintenance of correct LRP6 levels and Wnt/ $\beta$ -catenin signaling. The Epidermal Growth



Factor Receptor (EGF-R), the Transferrin Receptor (Tf-R), and Wnt3a served as controls since these proteins are also subject to N-glycosylation. The fact that neither the B3GNT8 LoF nor rescue influenced protein amounts of the EGF-R, the Tf-R and Wnt3a adds to the specificity of B3GNT8 for LRP6 (fig. 22 A, panels). B3GNT8 siRNA, as expected, reduced the proliferation rate of cells and this was also rescued by subsequent co-expression of medaka B3GNT8 (fig. 22 B and C). These results confirm that B3GNT8 is required for LRP6/Wnt signaling.

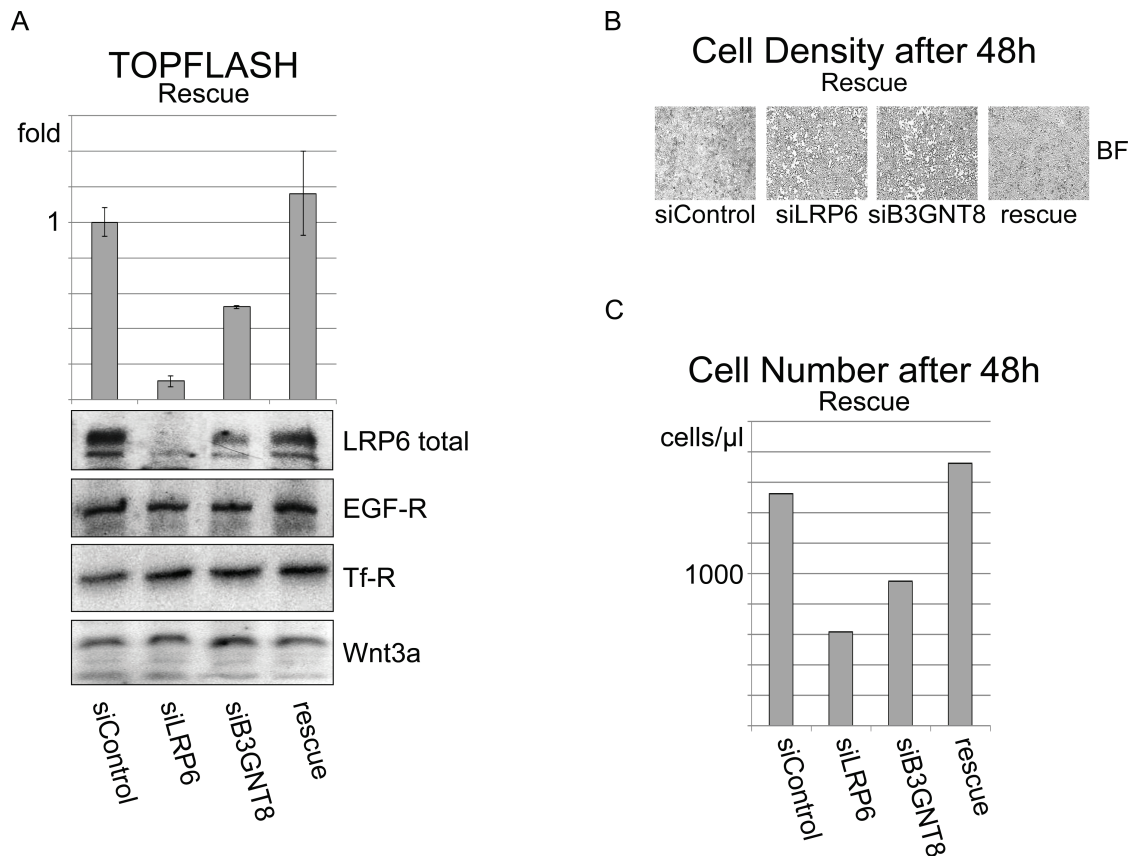


**Figure 22: Rescue of B3GNT8 siRNA effects.**

A. TOPFLASH assay and Western Blots of HEK293T cell lysates 40 hours after siRNA transfection.  $\alpha$ -LRP6\_T1479 was used to detect total LRP6, anti-EGFR antibody, was used to detect the epidermal growth factor receptor (EGFR), and anti-TfR antibody detected the Transferrin receptor, a well-defined cell membrane control, and anti-Wnt3a antibody was used to detect Wnt3a. HEK293T cells were transfected with 20pmol of the indicated siRNA and, 24h later, transfected with TOPFLASH reporters (20ng), thymidine kinase renilla reporter(4ng) with or without Medaka B3GNT8 (15ng). Note that B3GNT8 siRNA LoF results in significant reduction of both Wnt signaling and LRP6 (siB3GNT8), and these effects are rescued upon reintroduction of exogenous B3GNT8 (rescue).

B. Cells from the same transfection as in A were light microscopied (BF) to monitor proliferation. Note that the reported decrease of cell proliferation upon B3GNT8 knock down can be observed (siB3GNT8), and this is used as an additional control for the successful knock down of B3GNT8 together with the qPCR (not shown) and the TOPFLASH assay. Note that reintroduction of B3GNT8 rescues the siRNA effects (rescue).

C. The cells from B have been detached via trypsinisation and counted.

### **3.12 B3GNT8 LoF in HEK293 cells mainly influences Wnt signaling**

After finding that B3GNT8 is required for LRP6/Wnt signaling I asked if B3GNT8 affects other signaling pathways. To this end I carried out a global transcriptional analysis which is a deep sequencing assay (RNAseq) in cooperation with Dr. Olivier Armant (KIT), who did the RNAseq. I produced biological triplicates of Control-siRNA or B3GNT8-siRNA (LoF) treated

HEK293 cells and controlled the efficacy of the B3GNT8 knock down by quantitative real-time PCR (fig. 23 A). The RNAseq samples showed no sign of degradation (RNA index number >8). The sequencing resulted in more than 48 million pairs of 50 nucleotides long reads per sample with a mean Phred quality score >35. The reads were mapped against the human genome (GRCh37) using known exon junctions (Ensembl release 75). The correlation analysis via heat mapping confirmed the data consistency for each experimental condition (fig. 23 B). The reduction of MMP2 expression and the increase in TIMP-2 expression reported as a consequence of B3GNT8 silencing (Hua et al., 2012) was also observed in our RNAseq analysis, thus validating the experimental procedure (-32% and +26% in this RNAseq experiment, respectively).

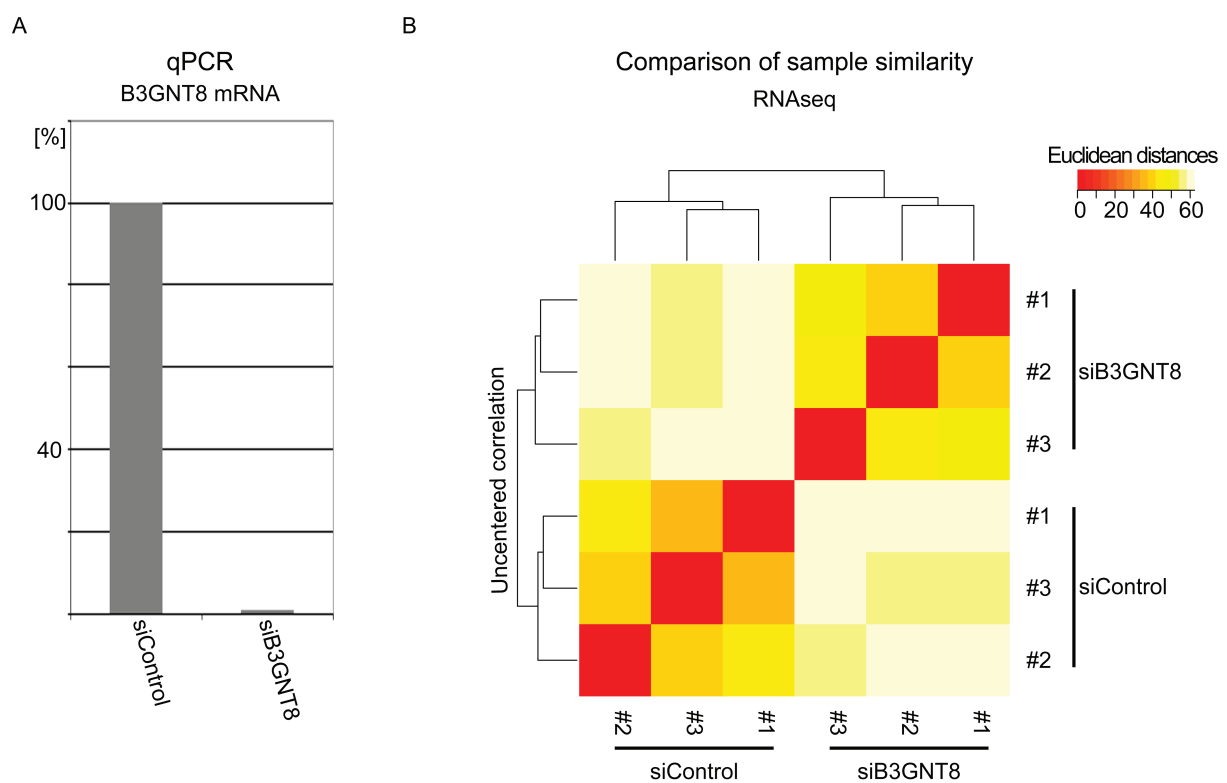


**Figure 23: Correlation analysis of samples for RNAseq confirms similarity for each condition.**

A. One representative example of a qPCR of Control siRNA versus B3GNT8 siRNA treated HEK293T cells for the RNAseq.

B. Control siRNA versus B3GNT8 siRNA. Cells were seeded at day one in 6 well plates and transfected with 100pmol of the siRNA (siControl or siB3GNT8). On day two the medium was exchanged. On day three, cells were lysed in peqGold RNA pure, and RNA was precipitated. RNA concentrations were adjusted with Nanodrop 1000 Spectrophotometer. qPCR confirmed the knock down (not shown). Heat mapping of sample triplets was done by Dr. Olivier Armant (KIT).

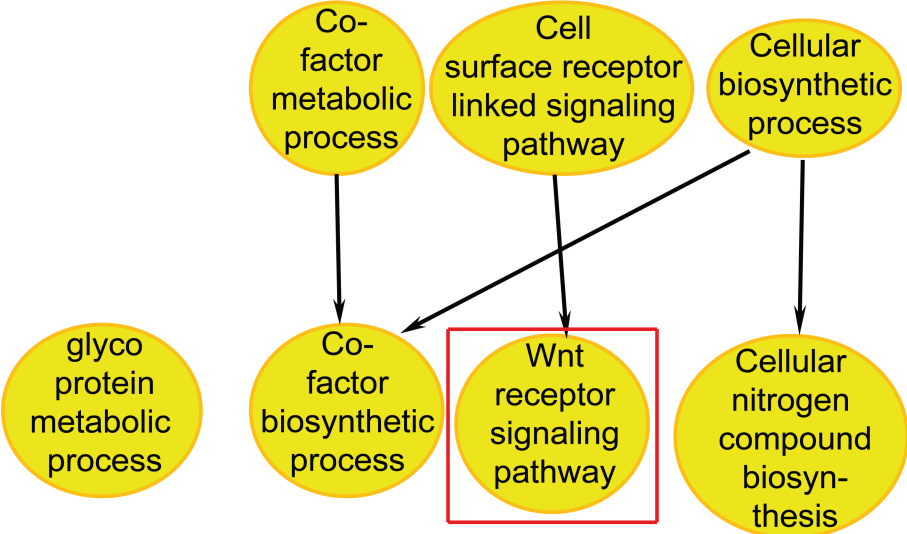
I used three independent deep-sequencing analysis softwares to analyze my results; Davids Gene Function Classification Tool©, Cytoscape© and The Panther Classification System©. Strikingly, two of three software analysis highlighted canonical Wnt signaling as most differentially regulated pathway in B3GNT8 LoF cells, and the third software analysis showed its significant differential regulation (fig. 24, all p-values<0.05 after Benjamini False Discovery Rate Correction BFDRC). My own analysis of known pathway specific target genes confirmed the predominant modulation of Wnt target genes (>93% vs. <43% from other pathways) (fig.



25 A). Down regulated Wnt target genes (all p-values<0.05 after BFDR) comprised e.g. Myc (-31%), SNAI2 (-60%), Cyclin D1 (-61%), Cited1 (-62%), and MMP-2 (-68%), all of which are well documented Wnt/ $\beta$ -catenin target genes that are upregulated in response to pathway activation. Axin2, which is one of the best characterized Wnt target genes, was also downregulated however Benjamini False Discovery Rate Correction judged it to be not significant. These data indicate that in HEK293 cells B3GNT8 mainly influences Wnt signaling.

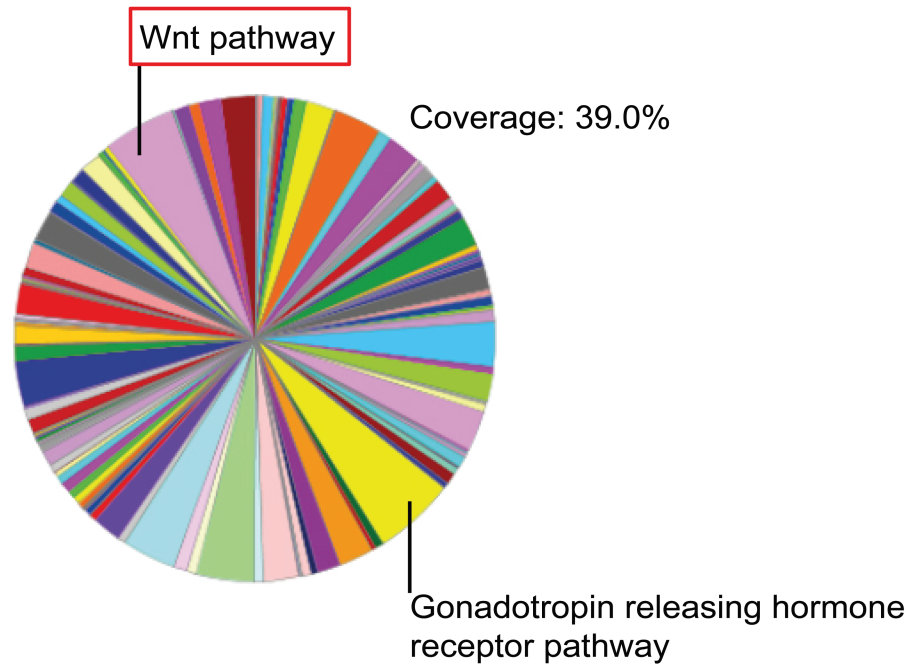
A

Cytoscape Software  
Gene Ontology Assignment



B

### Panther Classification System Pathway Assignment



C

### Dauids Gene Function Classification Tool KEGG-Pathway Assignment

Coverage: 27.2%

Category	Term	Genes	Count	%	Beniamini P-Value
KEGG_PATHWAY	<a href="#">MAPK signaling pathway</a>	83	1,8	1,8E-1	1,8E-1
KEGG_PATHWAY	<a href="#">Endocytosis</a>	65	1,4	4,3E-2	4,3E-2
KEGG_PATHWAY	<a href="#">Regulation of actin cytoskeleton</a>	63	1,4	3,5E-1	3,5E-1
KEGG_PATHWAY	<a href="#">Neurotrophin signaling pathway</a>	51	1,1	1,7E-2	1,7E-2
KEGG_PATHWAY	<a href="#">Wnt signaling pathway</a>	47	1,0	2,9E-1	2,9E-1
KEGG_PATHWAY	<a href="#">Insulin signaling pathway</a>	46	1,0	1,7E-1	1,7E-1
KEGG_PATHWAY	<a href="#">Tight junction</a>	44	0,9	2,0E-1	2,0E-1

**Figure 24: Three analysis identify Wnt signaling as differentially regulated by B3GNT8 LoF.**

A. Simplified Cytoscape result: Gene ontology terms that cover the 5234 genes differentially expressed in the B3GNT8 LoF. For differential gene expression analysis the default settings as described in the Cytoscape 3.0.1 users manual have been used. Cytoscape does not provide coverage data.

B. Simplified Panther Classification System result: 5234 differentially expressed genes assigned to KEGG-pathways. For differential expression analysis the default settings as described in Mi et al. (2013) have been used.

C. Simplified Davids Gene Function Classification Tool result: Assignment of 5234 differentially expressed genes after B3GNT8 LoF to KEGG-pathways. For differential gene expression analysis the default settings as described in DAVIDS bioinformatics resources 6.7 have been used.

A+B+C. Differentially expressed genes have a p-value <0.05 after BFDRC.

Using the Panther, Cytoscape and Davids analysis software I analyzed the differentially expressed set of genes from my RNAseq experiment (p-values<0.05 after BFDRC) for enriched gene sets (gene ontology terms or GO terms). E.g. my expectation was that silencing of B3GNT8 would lead to the up-regulation of other N-glycosyltransferase genes, due to compensatory mechanisms. I found however that the redundantly functioning family members of B3GNT8, B3GNT2 and -4, were not significantly up-regulated (+7% and +12% respectively). Indeed, all three software analyses showed that B3GNT8 silencing decreased the expression of 30 N-glycosyltransferases participating at different steps of the N-glycosylation process (fig. 25 B, lower Cytoscape graph, as one example). These glycosyltransferases include e.g. the dolichol-mannosyl-transferase ALG12 (from Panther, HGNC symbol), the galactosyltransferase B3GALT6, the GalNAc-transferase GALNT7, the sialyltransferase ST3GAL2, the fucosyl-transferase FUT4 and the GlcNAc-transferases B3GNT1 and B3GNT5.

It has been shown that B3GNT8 LoF leads to a down regulation of cell proliferation (Hua et al., 2012; Liu et al., 2010) and my results are in line with this. However, the mechanism by which B3GNT8 regulated cell proliferation is unclear. My GO term assignment of the differentially expressed genes found that a B3GNT8 knock down leads to upregulation of genes that take part in negatively regulating the cell cycle and in G1 phase arrest (fig. 25 B, upper Cytoscape graph). Genes that belong to the GO term “negatively regulating cell cycle” and that were up-regulated in my RNAseq experiment are (from cytoscape, HGNC symbols): GAS2L3, ING4, THAP5, RPRM, FOXO4, TCF7L2, LATS2, SART1, CYP27B1, CDKN2B, MTBP, PKD2, RHOB, BCL6, HBP1, RNF167, TCF4, NR2F2, DHCR24, PTPRK, PLA2G16, BMP2, TAF6, TP53BP2, WDR6, CDK6, GAS1, TP73, DDIT3, VASH1, EIF4G2, TRIM35, PRDM4, HDAC1, IRF6, RASSF1, BTG3, TBRG1, FOXC1, PRNP, PPP1R15A, HPGD, TP53INP1 and USP44. And genes that belong to the GO term “G1 phase arrest” and that were up-regulated in my RNAseq experiment are (from cytoscape, HGNC symbols): E2F1, TAF1, CDC6, MTBP, CDC23, CDK6, FOXO4 and TCF3.

To get a clearer look into the gene expression changes after the B3GNT8 silencing I plotted the number of differentially expressed genes against the protein family names (all p-values<0.05 after BFDRC). This analysis confirmed the down regulation of N-glycosyl transferases participating at different steps in the N-glycosylation process (fig. 25 C). My analysis also showed that collagens exhibited mainly reduced transcript numbers. The collagen sensing anthrax toxin receptor interacts with LRP6 to modulate Wnt signaling (Chen et al., 2013), which indicates an additional mechanism for B3GNT8s effects on Wnt signaling.

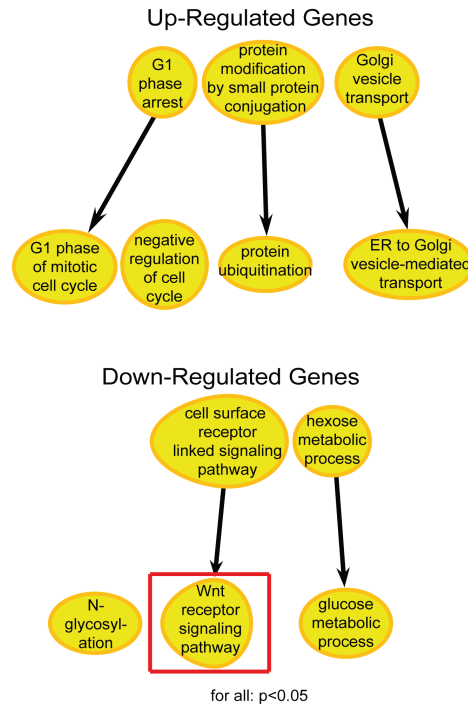
A

### Differentially Expressed Target Genes assigned to Signalling Pathways

	Wnt*	p53°	TGFβ°	Shh°	FGF°	MAPK°
Target genes	47	122	147	40	75	86
Differentially expressed (in percent)	93,6%	42,6%	38,1%	27,5%	26,7%	24,4%

B

### Assignment of Differentially Expressed Genes to Selected Gene Ontology Terms (Cytoscape)



C

### Selected Differentially Expressed Protein Families

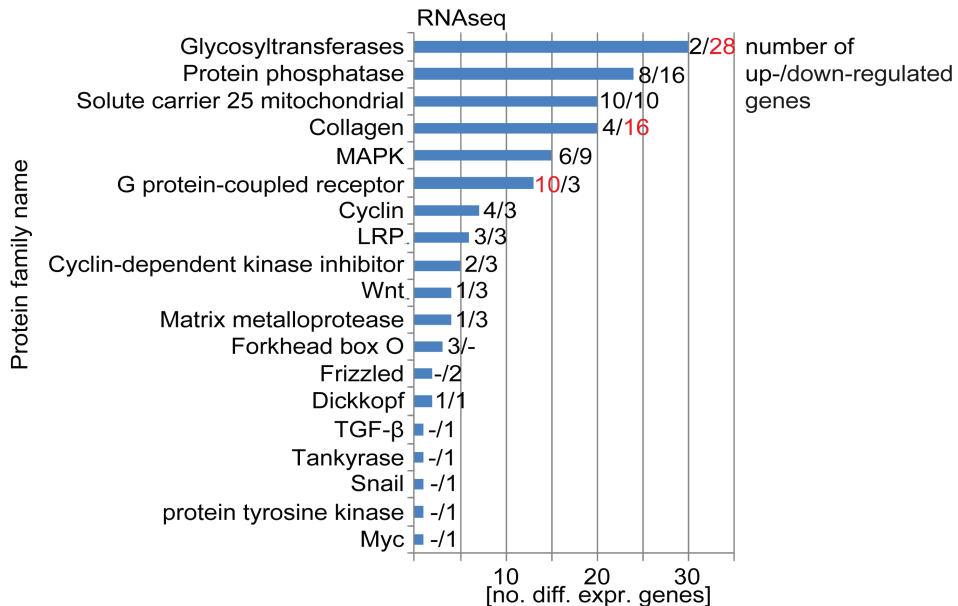


**Figure 25: RNAseq of Control siRNA vs. B3GNT8 siRNA treated HEK293T cells.**

RNAseq results of two conditions (triplets each): Control siRNA versus B3GNT8 siRNA. Cells were seeded at day one in 6 well plates and transfected with 100pmol of the siRNA (siControl or siB3GNT8). On day two the medium was exchanged. On day three, cells were lysed in peqGold RNA pure, and RNA was precipitated. RNA concentrations were adjusted with Nanodrop 1000 Spectrophotometer, and qPCR confirmed the knock down.

A. The level of influence of the B3GNT8 knock down on signaling pathway activities. For references about the target genes, please refer to the materials and methods section. Only genes have been selected with a p-value lower than 0.05. \* = target genes in HEK293T cells, ° = target genes from multiple cell lines due lack of HEK293T specific genes. Note the high percentage of differentially expressed target genes in the Wnt pathway.

B. Assignment of differentially expressed genes to gene ontology terms by the Cytoscape software (simplified). Note the down regulation of Wnt signaling and N-glycosylation. Note also the upregulation of G1 phase arrest effectors.  
 C. Number of differentially expressed genes per protein family. The number before the dash denotes the number of upregulated genes. The number after the dash denotes the number of down-regulated genes. Most of the families with low counts are not shown. Note the reduced numbers of glycosyl transferases and collagens.

### 3.13 B3GNT8 reduces Wnt/PCP signaling

After the RNAseq indicated that B3GNT8 mainly influences Wnt signaling I wanted to analyze the ability of B3GNT8 to regulate the different pathway branches of Wnt signaling. There are at least three different Wnt pathways known: the canonical  $\beta$ -catenin dependent pathway, and the two non-canonical  $\text{Ca}^{2+}$  and PCP (planar cell polarity) signaling pathways. PCP signaling is inhibited by Wnt/ $\beta$ -catenin signaling and is Activating Transcription Factor 2 (ATF2) dependent (Tahinci et al., 2007; Gray et al., 2013). I therefore tested the effect of B3GNT8 on non-canonical Wnt signaling using an ATF2-dependent luciferase reporter assay and a parallel TOPFLASH assay served as control for B3GNT8s activity in Wnt/ $\beta$ -catenin signaling. Wnt5a served as an activator for the ATF2 dependent luciferase reporter assay. In line with its ability to promote Wnt/ $\beta$ -catenin signaling, B3GNT8 dose-dependently decreased PCP signaling and the effect was augmented in the presence of exogenous Wnt5a (fig. 26). This indicates that exogenous B3GNT8 does not uncouple  $\beta$ -catenin signaling from its well documented cross talk with PCP signaling.

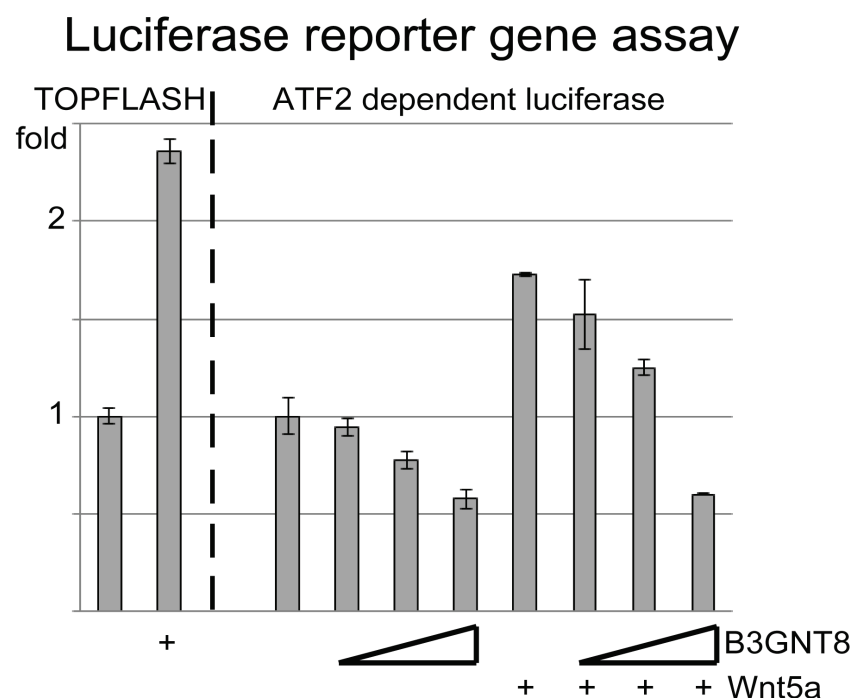


**Figure 26: B3GNT8 expression decreases Wnt/PCP signaling.**  
 B3GNT8 regulates PCP/Wnt signaling. Luciferase reporter assay using HEK293T cells and a canonical Wnt reporter (TOPFLASH) and a PCP reporter (ATF2 dependent luciferase). Cell lysates were harvested 24 hours post-transfection for Luciferase activity measurement. Amounts transfected per 96well: TOPFLASH 20ng, thymidine kinase renilla reporter 4ng, B3GNT8 15ng for TOPFLASH, ATF2 dependent luciferase 20ng, B3GNT8 3, 10, or 30ng for ATF2 dependent luciferase, Wnt5a 50ng. TOPFLASH confirms the functionality of the B3GNT8. Note that increasing concentrations of B3GNT8 dose-dependently decrease ATF2/PCP signaling. Wnt5a intensifies this effect.

### 3.14 B3GNT8 increases the cell surface levels of LRP6

Proper N-glycosylation is needed for LRP6 protein to proceed in the secretory route to the cell surface (Khan et al., 2007). I hypothesized that B3GNT8-modified N-glycans may regulate LRP6 cell surface levels and used cell surface biotinylation assays to look into this in more detail. In this assay, the Lysine residues of cell surface proteins are covalently coupled to a d-biotinyl-N-hydroxysuccinimid ester which is used together with avidin beads to enrich for biotin labeled cell surface proteins (Cole et al., 1987). Non-B3GNT8 modified LRP6 was used as negative control. The intracellular chaperone MESD aids transport of LRP6 to the cell surface (Khan et al., 2007) and was used as positive control. As expected, the B3GNT8 co-expression with LRP6 led to a dose-dependent increase of cell surface LRP6, as seen by the increased levels of biotinylated LRP6, which correlates well with the up-shift in the upper band of LRP6 (fig. 27). As expected, MESD caused an increase of cell surface LRP6 (compare lanes 1 and 5), however I did not increase the levels of B3GNT8-modified cell surface LRP6 (compare lanes 4 and 6). This suggests that B3GNT8 may be involved in the cell surface translocation of an LRP6 subspecies different from the subspecies promoted by MESD to reach the cell surface.

#### Cell Surface Biotinylation

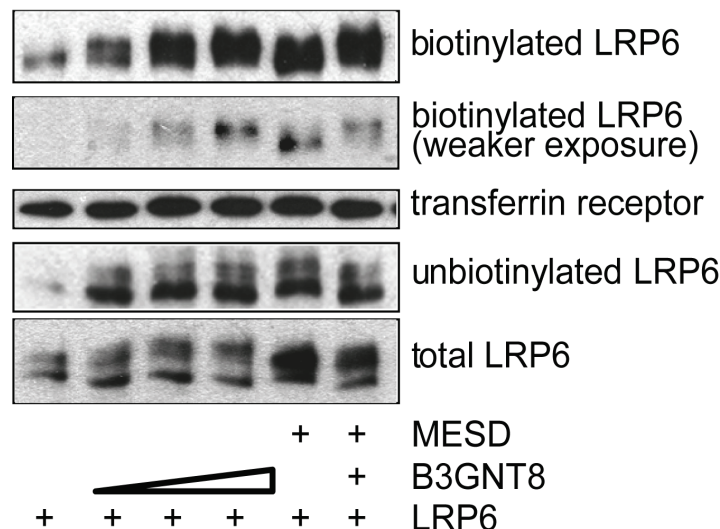


**Figure 27: B3GNT8 increases cell surface levels of LRP6.**

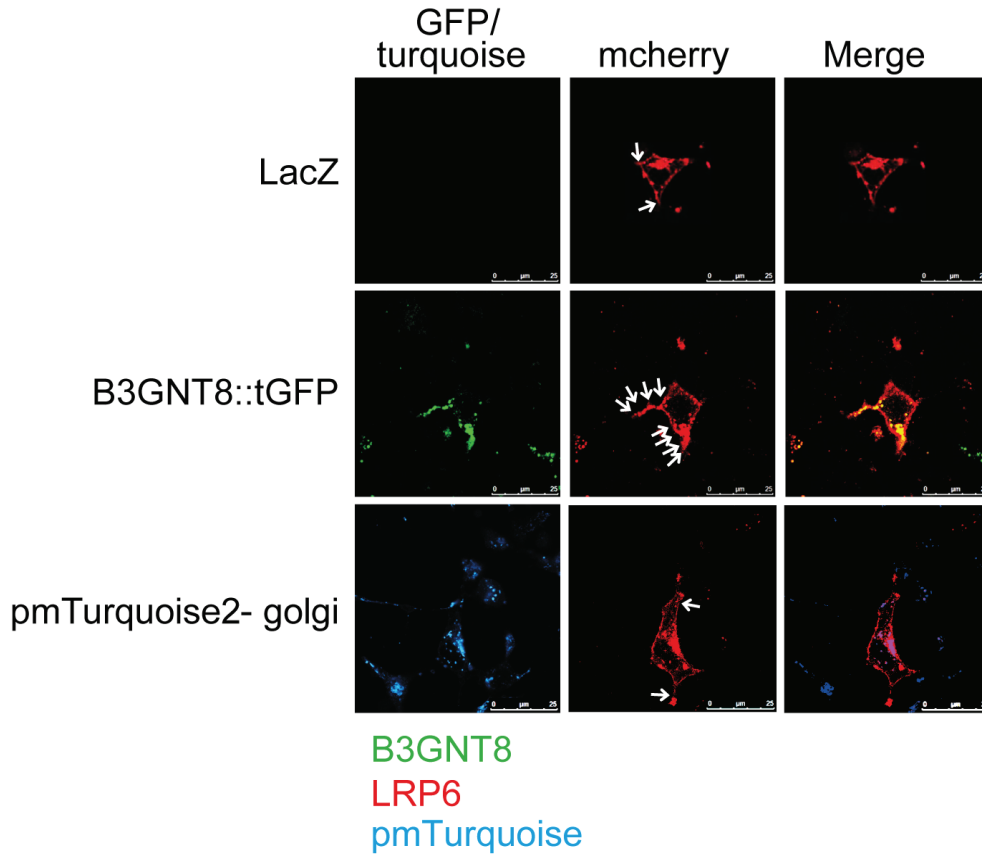
Western Blots of lysates from HEK293T cells co-transfected with LRP6 (20ng), B3GNT8 (0.5ng, 1ng, 5ng), and MESD (5ng), or MESD and B3GNT8 (both 5ng) per 96well. Labeling of cell surface proteins was done with Sulfo-NHS-SS-biotin at 4°C, and neutravidin beads were used for enrichment of biotinylated proteins. An anti-PCNA antibody was used for input lysate control (bottom panel), and the transferrin receptor (TfR) for biotinylated surface protein control. Note the dose-dependent increase in both LRP6 molecular weight and amount (top panel).

In order to analyze B3GNT8 promoted LRP6 cell surface transport using a different method I measured the distribution of mcherry-tagged LRP6 in the presence of B3GNT8::tGFP. Non-fluorescent LacZ and the golgi target sequence-containing pmTurquoise2-golgi protein

served as non-golgi resident and golgi-resident mock, respectively. B3GNT8 co-localized with LRP6 (fig. 28 B, middle panel) and the B3GNT8 transfected cells show a drastic increase in LRP6:mcherry containing vesicles in cellular protrusions compared to the non-golgi and the golgi mock (fig. 28 A, white arrows). To confirm that all vesicles have been counted, z-stacks of the cells were taken (fig. 28 B). In total, the cell number with a high number of LRP6::mcherry containing vesicles in cellular protrusions increased to approx. 3.5-fold in the B3GNT8::tGFP transfected cells compared to the controls. Since B3GNT8 is predicted to be located and function in the Golgi, these vesicles are presumably transporting LRP6 to the cell surface.

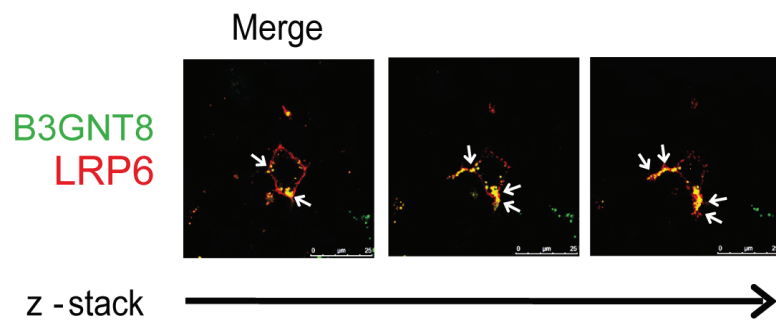
A

### Confocal microscopy Vesicles in Cell Protrusions



B

### Confocal microscopy B3GNT8::tGFP and LRP6::mcherry





C

### Percentage of cells with high numbers of LRP6::mcherry vesicles

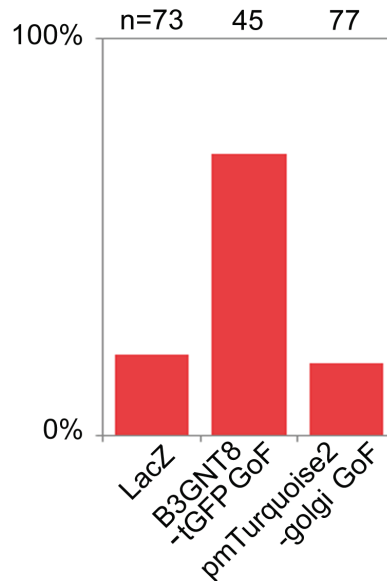


**Figure 28: B3GNT8 co-localizes with and increases cell surface levels of LRP6.**

A+B. Confocal microscopy of Hek293T cells overexpressing LRP6::mcherry, B3GNT8::GFP, and the golgi marker pmTurquoise2-golgi. LacZ was used as non-golgi resident mock, pmTurquoise2-golgi was used as golgi-resident mock. Transfections were made in a 3cm petri dish, photos were taken with SP5 Tandem DM6000. Note that B3GNT8::tGFP overexpression increases the LRP6::mcherry containing vesicles (B middle panel). Scanning via z-stacking through cells makes the increase of LRP6::mcherry containing vesicles more visible (C). Amounts transfected are as in fig. 26.

C. Statistical counting of one representative experiment of cells containing high numbers of LRP6::mcherry containing vesicles in three different conditions.

### **3.15 The first 2 conserved LRP6 N-glycans are able to contact ligands**

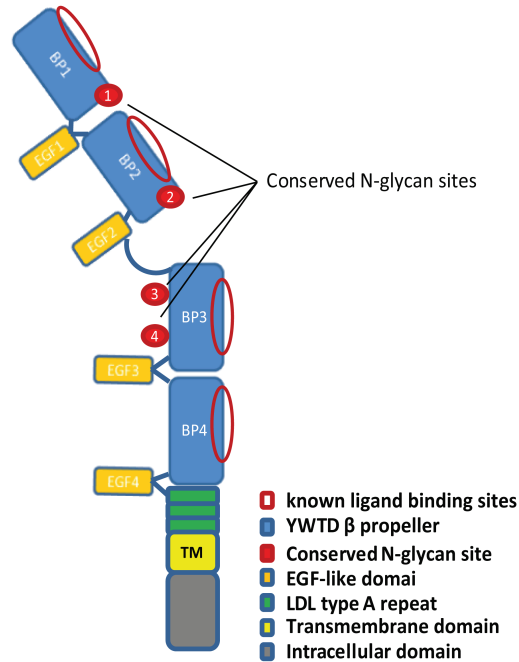
Within each BP there are 5 individual YWTD BP/ $\beta$ -sheet motifs and, interestingly, in both BP1 and BP3 the conserved N-glycan is immediately preceded by these YWTD/ $\beta$ -sheet motifs (see fig. 11, colored boxes). In BP2, the conserved N-glycan is however preceded by the YWTD/ $\beta$ -sheet motif plus an additional  $\beta$ -sheet. This positions the N-glycosylation site of BP2 in close proximity to known ligand binding sites, as it is the case for the conserved N-glycosylation site of BP1 (fig. 29 B, C and D). (The addition of a  $\beta$ -sheet in BP2 is conserved in LRP6 of all aforementioned species, and in homo sapiens LRP5; not shown).

I used the 3D modeling OpenGL based molecular visualization system PyMOL to try and understand whether the first two conserved N-glycan chains of LRP6 could potentially interact with known LRP6 ligands. Structural data of LRP6, MESD and N-glycans was obtained from: Pymol database ID: 4DG6 Holdsworth et al. 2012, 4FQC Mouquet et al. 2012, 2KMI Chen et al. 2010. I modelled two MESD ligands (LRP6 chaperone) on the first two  $\beta$ -propellers of LRP6 (fig. 29 B). Modeling of MESD binding to LRP6 was based on the molecular docking techniques of Chen et al. (2010). Additionally I modelled the first two conserved LRP6 N-glycans. Although I modelled rather short N-glycans both N-glycans were able to

contact a MESD ligand. This may hint to a functional relevance of the first two conserved LRP6 N-glycans in ligand binding.

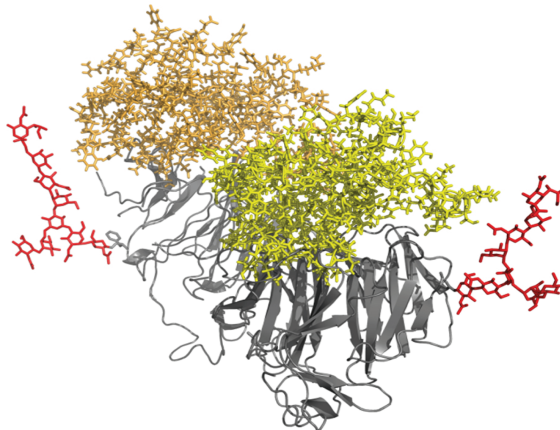
A

### Conserved N-glycans of LRP6



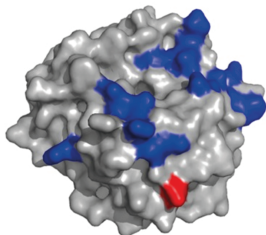
B

### Tertiary Structure of the first 2 β-propellers of LRP6 N-glycans on the first 2 β-propellers of LRP6 with two MESD



C

### Molecular Surface of the first LRP6 β-propeller MESD chaperone binding sites and conserved N-glycan site



D

### Molecular Surface of the first LRP6 β-propeller MESD escort binding sites and conserved N-glycan site

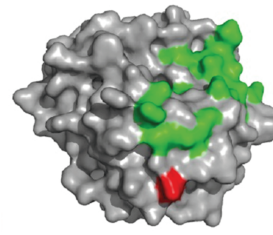


**Figure 29: The first two conserved LRP6 N-glycans are in close spatial proximity to known MESD binding sites.**

A, Scheme of LRP6, with red filled circles indicating the position of evolutionarily conserved LRP6 N-glycan sites (Asn81, 486, 692, and 865, #1 to 4 respectively). Dark red ovals show known ligand binding sites. Note the close spatial proximity of conserved N-glycan site #1 and 2 to ligand binding sites.

B. LRP6 beta propeller 1 and 2 are shown in gray cartoon, 2 MESD proteins are projected upon them in yellow sticks, both in chaperone domain binding position, LRP6' N-glycans are shown in red sticks. All N-glycans are modelled by using the pentasaccharide core plus two antennae: 1 N-acetylglucosamine and 1 N-acetylactosamine with a sialic acid cap.

C. LRP6 beta propeller 1 is shown in grey mesh, MESD chaperone domain binding sites are indicated in blue, the first conserved N glycosylation site is marked red.

D. As in C, but MESD escort domain bindings sites are indicated in green.

### **3.16 B3GNT8 acts in hexose induced Wnt signaling**

Wnt signaling is positively coupled with glucose and L-glutamine supply from cell culture media in J774.2 and RAW264.7 macrophage cell lines and the N-glycosylation process is involved (Anagnostou and Shepherd, 2008). I hypothesized that B3GNT8, which is dependent on hexose supply for its enzymatic activity, may be involved in this glucose dependent regulation of Wnt signaling. I made the assumption that hexose dependent modulation of Wnt signaling is a more general feature of cells and applies as well to HEK293 cells. To test if glucose supply changes Wnt signaling in HEK293T cells, cell culture media supplemented with different amounts of either D-glucose or L-glutamine were used for HEK293T cells that were transfected with TOPFLASH reporter plasmids. Different Fetal Bovine Serum (FBS) concentrations were first tested and from these experiments it could be shown that decreasing FBS concentrations increases Wnt signaling (fig. 30). A concentration of 5% FBS was chosen for the glucose/glutamine titration experiments because at this concentration Wnt signaling could be further enhanced or decreased and the endogenous LRP6 protein bands could be clearly detected by WB analysis (fig. 30, red arrows). In addition, dialyzed FBS and DMEM with low glucose (1000mg/l) and no L-glutamine were used as to remove glucose and L-glutamine and indeed it behaved in the same way as non-dialyzed FBS, thus validating the use of dialyzed FBS (fig. 30).

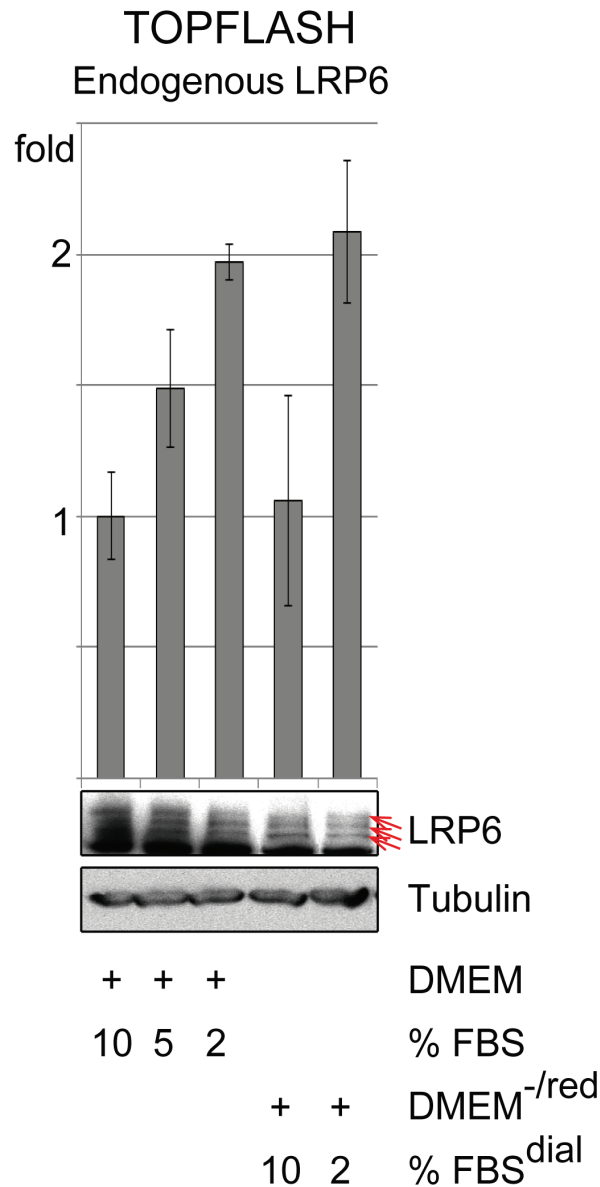


**Figure 30: FBS reduction increases TOPFLASH response and reduces LRP6 protein bands.**

TOPFLASH reporter assay (upper graph) and Western Blot (panels below) of cells stimulated with different FBS amounts. Cells were co-transfected with Wnt reporter TOPFLASH (20ng), thymidine kinase-renilla reporter (4ng), and LacZ (76ng) in 96well format in DMEM with 5% FBS and 1% Pen/Strep. After 6h, the DMEM was exchanged for the medium indicated. After 36h, the cells were harvested in passive lysis buffer for luciferase assays or in 1% triton lysis buffer for Western Blot. Note the increase in TOPFLASH response upon FBS reduction.  $\alpha$ -LRP6 (T1479) was used to detect total LRP6. All other antibodies recognized natural protein epitopes. Note the decrease in LRP6 Western Blot bands (red arrows) upon FBS reduction.

We then performed experiments using 5% dialyzed FBS to which different amounts of either D-glucose or L-glutamine was added and cell lysates were harvested after 36h for both Wnt reporter assays and Western Blot analysis of endogenous LRP6. We found that the reduction of glucose had no significant effect on Wnt signaling and that reduction of glutamine results in a slight decrease in Wnt signaling (fig. 30). From this we conclude that HEK293 cells share a part of the glucose/glutamine response mechanism with macrophage cells.

To test if LRP6 reacts to glucose and L-glutamine depletion we also performed Western Blot analysis of the endogenous LRP6 protein. Interestingly, when exposing cells to decreasing

amounts of glucose or glutamine the upper, cell surface LRP6 band changed dramatically (fig. 31, upper panel). With decreasing glucose concentration the upper LRP6 band migrated at first slower, showing a clear upshift, and then disappearing, together with the appearance of a new lower band just below the ER form of LRP6. The result of decreasing glutamine amounts was equally striking, with a clear and progressive upshift of the upper LRP6 band with decreasing glutamine. This indicates that cells respond to glucose or L-glutamine changes by synthesizing different LRP6 subspecies, which may account at least partially for the changes in Wnt signaling.

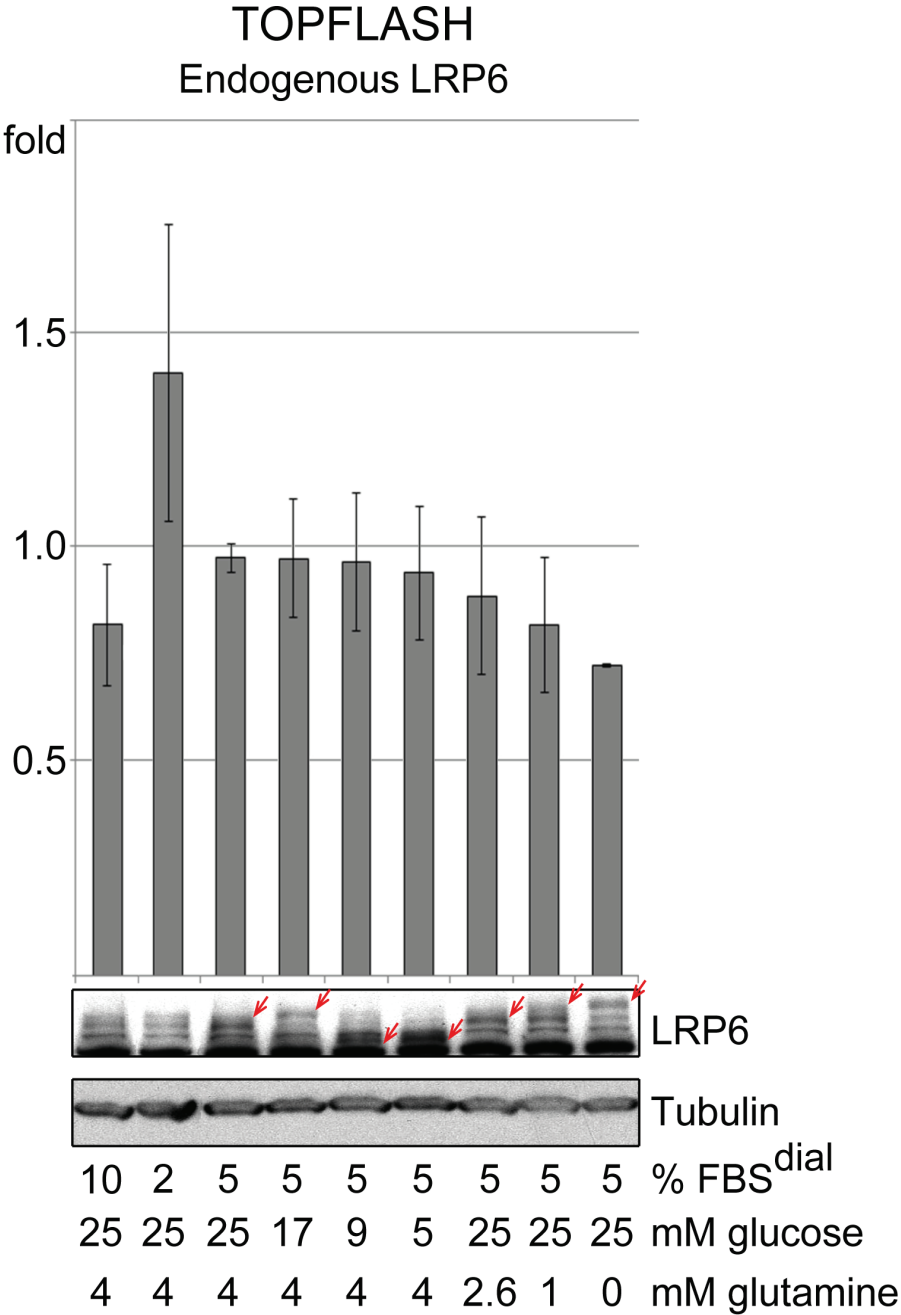


**Figure 31: Wnt-signaling and LRP6 react to glucose/glutamine reduction.** TOPFLASH reporter assay (upper graph) and Western Blot (panels below) of cells stimulated with different D-glucose/L-glutamine. Cells were co-transfected with Wnt reporter TOPFLASH (20ng), thymidine kinase-renilla reporter (4ng), and LacZ (76ng) in 96well format in DMEM (25mM D-glucose, 4mM L-glutamine), 5% FBS and 1% Pen/Strep. After 6h, the DMEM was exchanged for DMEM<sup>red</sup> (i.e. 5mM D-glucose/no L-glutamine) and the FBS-, D-glucose-, and L-glutamine-concentration indicated. After 36h, the cells were harvested in passive

lysis buffer for luciferase assays or in 1% triton lysis buffer for Western Blot. Note the decrease in TOPFLASH signaling upon glutamine reduction.  $\alpha$ -LRP6 (T1479) was used to detect total LRP6. All other antibodies recognized natural protein epitopes. Note the change of the upper LRP6 Western Blot band (red arrows) upon glucose and glutamine reduction.

I then asked if exogenous B3GNT8 can rescue LRP6 bands and Wnt signaling in glucose or glutamine titrations. I therefore exposed TOPFLASH-transfected HEK293 cells to the same glucose or glutamine titrated media as above, either with or without exogenous B3GNT8. I increased exposure time of media to 48h, which indeed enhance the TOPFLASH response. In glutamine titrated media, the composition of the upper LRP6 forms changed significantly, both with or without B3GNT8 (fig. 32, upper and third panel). The depletion of glutamine leads to a reduction of NDP-activated hexose forms (Nakaishi et al., 2009), one of which is likely to be the GlcNAc donor for B3GNT8, UDP-GlcNAc. In glucose reduced media however, B3GNT8 stabilized both upper LRP6 protein bands (fig. 32, red arrows).

The TOPFLASH assays confirmed the reduction of Wnt signaling upon lowering glutamine levels (fig. 32). Strikingly, together with the rescue of the upper LRP6 bands, B3GNT8 blocked the reduction in Wnt signaling caused by reduced glucose/glutamine. This may indicate that B3GNT8 can rescue the effects of hexose depletion and suggests that B3GNT8 might play a role in hexose induced Wnt signaling.

## TOPFLASH and Western Blot Glucose and Glutamine Reduction w/o B3GNT8

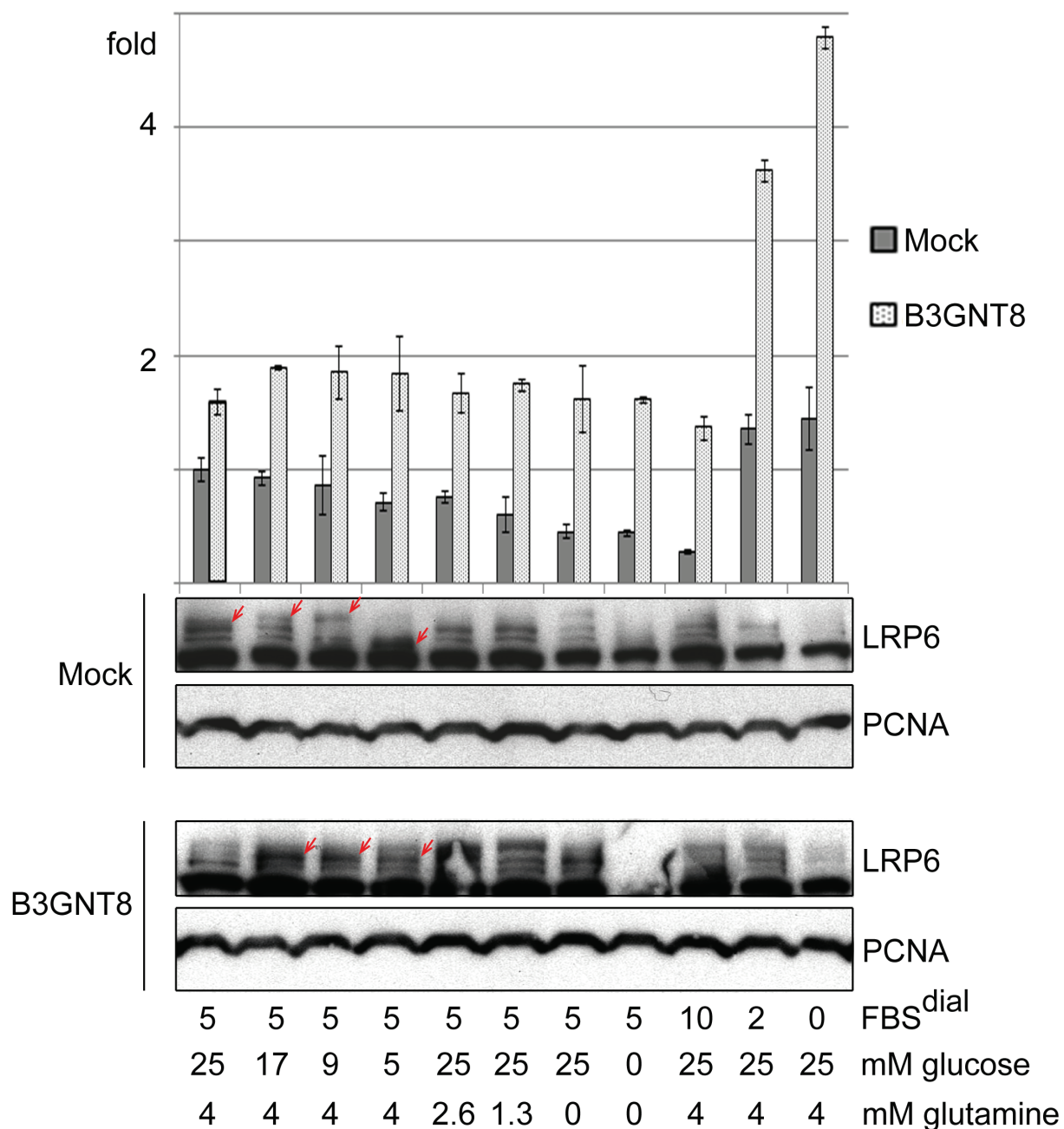


**Figure 32: B3GNT8 rescues upper LRP6 bands and TOPFLASH signaling in glucose/glutamine reduced media.**

TOPFLASH reporter assay and Western Blots of cells stimulated with different glucose/glutamine amounts in the presence or absence of B3GNT8. Glucose and glutamine amounts were varied as indicated. Cells were co-transfected with Wnt reporter TOPFLASH (20ng), thymidine kinase-renilla reporter (4ng), LacZ and w/o B3GNT8 (15ng) in 96well format in DMEM, 5% FBS and 1% Pen/Strep. After 6h, the DMEM was exchanged for DMEM<sup>red</sup> (i.e. 5mM D-glucose/no L-glutamine) and the FBS-, D-glucose-, and L-glutamine-concentration indicated. After 48h the cells were harvested in passive lysis buffer (from Promega) for luciferase assays or in 1%triton lysis buffer for Western Blot. Note the reduction of TOPFLASH signaling upon L-glutamine reduction. Note that B3GNT8 expression stops this.  $\alpha$ -LRP6 (T1479) was used to detect total LRP6.  $\alpha$ -PCNA antibody was used to detect the loading control PCNA. Note the change in LRP6 Western Blot bands (upper red arrows) upon glucose and glutamine reduction and the stabilization of the upper LRP6 bands by B3GNT8 (lower red arrows).

In a different approach to analyze the role of B3GNT8 in hexose induced Wnt signaling, I increased hexose levels by adding the readily available Azido-N acetylmannosamine. The azidosugar Azido-N acetylmannosamine (ManNAz) (a kind gift of Dr. Ute Schepers) is a

modified hexose analog that, when present in its more hydrophobic peracetylated form, can readily be taken up by cells and then epimerized by cellular esterases for incorporation into the glycosylation pathway. Increasing ManNAz supply in normal 5% FBS containing DMEM slightly increased TOPFLASH signaling (fig. 33). Overexpression of LRP6 activated Wnt signaling as expected, however under these conditions no increase of signaling was seen upon the addition of ManNAz. Only upon co-expression of B3GNT8 with LRP6 was the effect of ManNAz again seen (fig. 33), indicating that B3GNT8 may indeed play a role in hexose induced Wnt signaling at the level of LRP6.

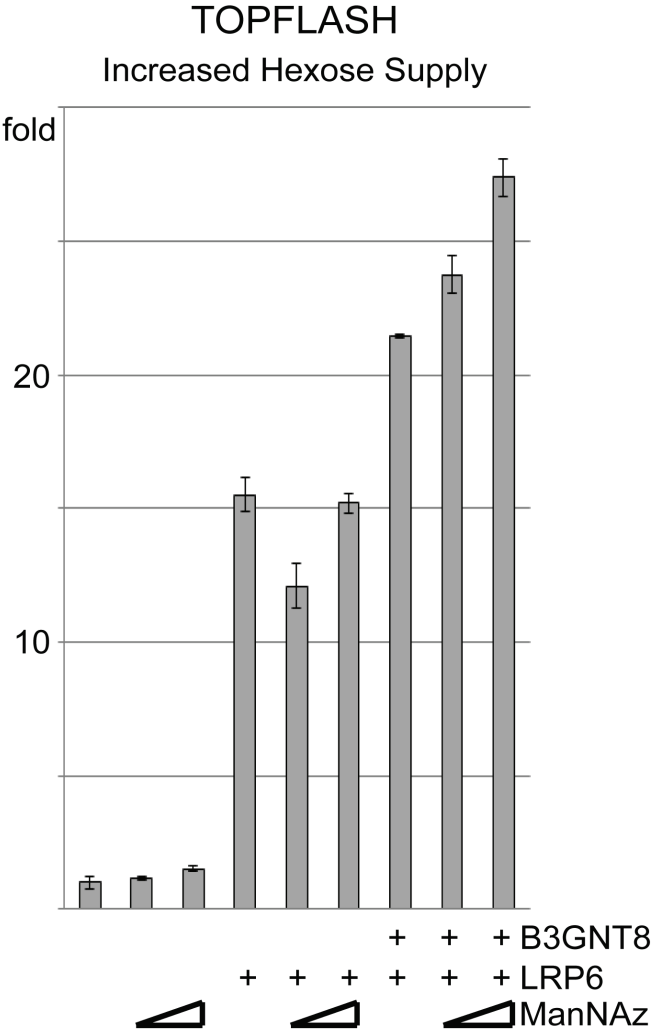


**Figure 33: Co-expression of B3GNT8 with LRP6 augments hexose sensitivity of TOPFLASH signaling in HEK293 cells.** TOPFLASH reporter assay using HEK293T cells treated with increasing amounts of the hexose ManNAz. 20ng LRP6 and 15ng B3GNT8 were transfected and either 80µM or 7mM ManNAz added 5h post transfection. Cell lysates were harvested 26 hours post-transfection for Luciferase activity measurement. Note that co-expression of B3GNT8 sensitizes LRP6 to hexose induced Wnt signaling.



## 4. Discussion

---

The main findings of this study are listed below:

1. B3GNT8 is a new modifier and regulator of LRP6 and Wnt signaling.
2. B3GNT8 modifies the complex LRP6 N-glycans to regulate Wnt signaling.
3. B3GNT8 modifies certain LRP6 subspecies to enhance Wnt signaling via promotion of Golgi-to-surface transport.
4. This B3GNT8 promoted LRP6 subspecies is different from the LRP6 forms that MESD helps to fold/transport in the secretory pathway.
5. B3GNT8 loss-of-function modulates mainly canonical Wnt signaling.
6. B3GNT8 plays a role in the metabolic regulation of Wnt signaling.

Here I discuss my experimental data in the context of our current understanding of Wnt signaling and the N-glycosylation pathway.

### **4.1 The decision criteria for pursuing the characterization of B3GNT8**

#### **4.1.1 Identification of B3GNT8**

Although it is known since more than a decade that LRP6 needs N-glycosylation to come to the cell surface (Khan et al., 2007; Hsieh et al., 2003), to date no LRP6 modifying N-glycosyltransferase has been identified. I screened a medaka cDNA expression library for LRP6 modifying N-glycosyltransferases and identified two glycosyltransferases in my screen, in addition to two that were identified in a previous screening experiment that used a different cDNA library as the source of potential modifiers. Out of these four LRP6 modifying glycosyltransferases, of which three have been further tested in titration experiments, only B3GNT8 modulated Wnt signaling in addition to modifying LRP6. B3GNT8 is one of 9 enzymes comprising the  $\beta$ -1,3-N-acetyl-glucosaminyltransferase family (B3GNT), however B3GNT8 is a recently identified member and relatively uncharacterized. It is involved in the poly-N-acetyllactosamine (polyLacNAc) synthesis, i.e. the alternating addition of GlcNAc and galactose on complex- or hybrid-type N-glycans (Seko and Yamashita, 2005), and may therefore be directly involved in the maturation of LRP6.

The effects of *homo sapiens* B3GNT8 expression on LRP6/Wnt signaling were less drastic (not shown) which is an effect that has been observed both with our medaka library clones

as well as with clones from a *Xenopus* library. This apparent higher specific activity may be due to the lower body temperature of medaka which may have resulted in the evolution of proteins that are more active than their mammalian counterparts under the cell culture conditions we are using. Although it can be argued that these are potentially artifactual conditions to select LRP6 modifiers, the fact that B3GNT8 siRNA silencing experiments showed a requirement of human B3GNT8 for Wnt signaling in HEK293 cells convinced me to pursue the further characterization of this LRP6 glycosyltransferase.

Wnt signaling is highly involved in cancer and in cancer metastasis (Guo et al., 2014). Polylactosamine and related structures play important roles in cell-cell interaction (Zhou, 2003), in cell-extracellular matrix (ECM) interaction (Varki et al., 2009), in immune response and thus in determining the metastatic capacity of cancer cells (Togayachi et al., 2008; Dennis and Laferte, 1987). Strikingly, in malignant transformed fibroblasts (Yamashita et al., 1984) and in tumor cells with high metastatic behavior (Dennis et al., 1987) the amount of poly-N-acetyllactosamine specifically on tetra-antennary N-glycans is increased. My hypothesis was that the known modulation of Wnt signaling via N-glycosylation (Anagnostou and Shepherd, 2008) may be linked to B3GNT8-mediated modification of the tetra-antennary N-glycans of LRP6, which may affect tumor cell proliferation and metastatic potential (Ihara et al., 2002; Granovsky et al., 2000; Seberger and Chaney, 1999; Pierce et al., 1997; Kobata, 1989; Dennis and Laferte, 1989).

## **4.2 Participation of B3GNT8 in Wnt signaling**

### **4.2.1 Direct or indirect modification of the LRP6 N-glycans by B3GNT8**

The N-glycans of LRP6 are all thought to be processed from high mannose precursors into complex- or hybrid-types (Hsieh et al., 2003) and substrates of B3GNT8 are complex-type N-glycans (Ishida et al., 2005), which my Endoglycosidase H and neuraminidase assays confirmed. Moreover, my data strongly suggests that B3GNT8 modifies the complex N-glycans on the ECD of LRP6 (figs. 13 and 18). Direct interaction between LRP6 and B3GNT8 is supported by co-immunoprecipitation experiments and co-localization experiments (figs. 14 and 28). Although the co-immunoprecipitation experiments also show a physical interaction of B3GNT8 with other proteins (ROR2, LRP5, Kremen1, Wnt3a, FGFR1, and FLRT3), none of them was modified (not shown). Considering that N-glycosyltransferases recognize carbohydrate moieties as well as amino acids in close proximity to the carbohydrate, N-glycosyltransferases are able to bind to non-substrate proteins (Baenziger, 1994). Thus, the substrate specificity of B3GNT8 may not solely come from its substrates but may be additionally conferred by other protein partners. The identification of such partners will be important for further research to establish the mechanisms by which B3GNT8 promotes Wnt signaling.

It will also be important to demonstrate clearly that B3GNT8 is able to incorporate GlcNAc into LRP6 N-glycans. One possibility to test this would be the development of an *in vitro* glycosylation assay. The activity of B3GNT8 towards tetra-antennary N-glycans has been demonstrated by galactosylating a tetraGP substrate (Gal $\beta$ 1 $\rightarrow$  4GlcNAc $\beta$ 1 $\rightarrow$  2(Gal $\beta$ 1 $\rightarrow$  4GlcNAc $\beta$ 1 $\rightarrow$  4)Man $\alpha$ 1 $\rightarrow$  3[Gal $\beta$ 1 $\rightarrow$  4GlcNAc $\beta$ 1 $\rightarrow$  2 (Gal $\beta$ 1 $\rightarrow$  4 GlcNAc $\beta$ 1 $\rightarrow$  6)Man $\alpha$ 1 $\rightarrow$  6]Man $\beta$ 1 $\rightarrow$  4GlcNAc) missing a peptide backbone (Seko and Yamashita 2005). This *in vitro* glycosylation assay has not been tested for glycan chains attached to peptides. For an *in vitro* glycosylation assay utilizing B3GNT8, LRP6 harboring N-glycan chains from intermediate steps of the N-glycosylation pathway would be helpful. However, as seen by clear and distinct bands in SDS-PAGE/Western Blot, LRP6 is found mostly either in immature or mature form but seldom with glycan chains from intermediate N-glycosylation steps. Thus, a purification of LRP6 protein from cellular lysates will likely not obtain adequate amounts of appropriate LRP6 forms. Another approach would be to obtain LRP6 proteins with unprocessed oligosaccharide precursor, such as the immature form LRP6 present in the ER. After tryptic digest and purification of the immature LRP6 protein by HPLC, the N-glycan processing can then experimentally be mimicked. To this end, subsequent N-glycan trimming by Glucosidase I, II, III, Mannosidase I, II and Endomannosidase as well as MGAT branching are needed (Roth, 2002; Roth et al., 2010). A check by Mass Spectrometry should verify the resulting glycan structure and then B3GNT8 can be applied.

Despite an *in vitro* glycosylation assay confirming the possibility of B3GNT8 adding GlcNAc to LRP6 glycan chains, it is possible that B3GNT8 does not directly modify growing LRP6 N-glycan chains in live cells. B3GNT8 could indirectly support the modification of the LRP6 N-glycan chains by attachment of other functional groups, as e.g. phosphate groups (Akeboshi et al., 2009). To address this question, I initiated collaboration with Ute Schepers here at KIT. We will use Mass Spectrometry to analyze the N-glycan chains of tryptic digested LRP6 in the absence or presence of B3GNT8. This work is currently ongoing.

Another approach to monitor the hypothesized B3GNT8-mediated elongation of LacNAc units on LRP6 N-glycans is by use of lectin assays. Lectins are carbohydrate-binding proteins that specifically bind sugar moieties and are grouped according to the monosaccharides for which they show the highest affinity. Lectins with particular monosaccharide specificity also vary in their affinities for different glycan structures (e.g. high-mannose, complex, bi-/tri-/tetra-antennary complex). To this purpose, I initiated collaboration with Christian Thiel from the Center for Child and Adolescent Medicine (AG glycosylation defects) of the University Heidelberg, who is an expert in the analysis of congenital disorders of glycosylation (CDG). B3GNT8 GoF and LoF COS-7 cell culture experiments will be performed using tagged LRP6, and lectins will then be used to analyze the glycan epitopes of immuno-purified LRP6. The lectins will be HRP-coupled to allow detection by SDS-PAGE/Western Blot. This work is in progress.

#### **4.2.2 Participation of the B3GNT8-modified LRP6 in Wnt signaling**

Both LRP6 activated and base-line/endogenous Wnt signaling dose-dependently responded to increasing B3GNT8 concentrations. Moreover, the increasing phosphorylation at the first PPSP site (serin 1490) on endogenous LRP6, which is generally regarded as the first sign of activated Wnt signaling (Chen et al., 2009; Davidson et al., 2005), confirms that the B3GNT8-modified LRP6 form participates in Wnt signaling (fig. 10). In support of this, B3GNT8-modified LRP6 was present in biotinylated cell surface fractions, thus being accessible to Wnt ligands. This is consistent with the ability of B3GNT8 to further promote Wnt signaling in cells that have been exposed to Wnt conditioned medium (fig. 15). Receptor sub-species can differ in N-glycan number (Lau and Dennis, 2008). Although differences in N-glycan number of cell surface LRP6 has not been reported, cells can equip the same cell surface protein with a varying number of N-glycans using UDP-GlcNAc to regulate differentiation programs (Lau et al., 2007). The variation of N-glycan number regulates the cell surface expression of glycoproteins. Glycoproteins that exhibit switchable cell surface expression generally include proteins with less than 5 N-glycosylation sites (e.g. TbR, CTLA-4, GLUT4), while glycoproteins with higher numbers lead to hyperbolic responses (e.g. EGFR, IGFR, FGFR, PDGFR) (Lau and Dennis, 2008). LRP6 harbors 10 such putative N-glycosylation sites (own sequence analysis, not shown). Reduction hexose concentration in the cell culture medium changes the SDS-PAGE migration pattern of the upper LRP6 protein band (fig. 31), suggesting that Wnt signaling reacts to hexose supply partially through LRP6. To answer if Wnt signaling reacts to hexose supply by changes of cell surface LRP6, LRP6 cell surface levels in hexose reduced media should be quantified using cell surface biotinylation assays. Furthermore, Mass Spectrometry analysis of LRP6 N-glycans from cells in hexose reduced media could elucidate how N-glycan number, localization and composition react.

#### **4.2.3 B3GNT8 and Wnt pathway members**

Of the N-glycosylated canonical Wnt pathway members LRP6, Wnt, and Frizzled, B3GNT8 only modified LRP6, suggesting that the modification of LRP6 ECD promotes Wnt signaling. In line with my expectation, a truncated LRP6 lacking all N-glycosylation sites was not affected by B3GNT8 (fig. 18). B3GNT8 failed to modify LRP5, which is highly similar to and functionally redundant with LRP6 (Kelly et al., 2004). Although LRP5 harbors only 6 putative N-glycosylation sites, LRP5 and LRP6 contain the same 4 conserved sites. This indicates a functional relevance for these conserved sites. Considering that B3GNT8 fails to modify LRP5 this suggests that B3GNT8 is highly specific for LRP6. Nevertheless, B3GNT8 protein levels decreased in the presence of overexpressed LRP5 and increased in the presence of overexpressed LRP6, indicating that there is a link to both LRP5 and LRP6. Although LRP5 expression levels appeared to be lower than LRP6, the decrease of B3GNT8 protein in the presence of LRP5 was significant (fig. 19). In HEK293 cells, LRP6 plays a dominant role over LRP5 (Ettenberg et al., 2010), probably due to stabilization by high numbers of N-glycans

(Shental-Bechor and Levy, 2008) that might be a reason for the low LRP5 levels. On the other hand, the results of this study may reflect the different functions of LRP5 and LRP6 in tissue growth and homeostasis. E.g. in embryogenesis, LRP6 but not LRP5 is indispensable. On the other hand, the function of LRP5 is indispensable in adult bone homeostasis (He et al., 2004). To analyze the effects of LRP5/6 on B3GNT8 protein levels in more detail, more complex co-expression experiments using different amounts of LRP5 and -6 in combination with and LRP5/6 LoF is needed. Another approach is to analyze the effects of LRP5/6 GoF and LoF on B3GNT8 protein in cell lines derived from different human tissues and from different stages of embryogenesis.

#### **4.2.4 B3GNT2 and the modification of LRP6 and Wnt signaling in HEK293 cells**

B3GNT8 has been shown to enhance the activity of B3GNT2 in COS-7 cells (Seko and Yamashita, 2008; Seko and Yamashita, 2005), however any effect this may have on Wnt signaling are unknown. Although B3GNT2 can activate Wnt signaling it does not modify LRP6, this effect may be due enhanced N-glycosylation of other targets that regulate Wnt signaling). Furthermore, the combination of B3GNT2 and B3GNT8 resulted merely in an additive and not in a synergistic TOPFLASH increase, indicating that the enhancement of B3GNT2 activity by B3GNT8 does not occur in HEK293 cells.

Reasons for the differences in the results from Seko and Yamashita compared to mine can be explained by the following: they tested the single and combined enzymatic activities of B3GNT2 and -8 using *in vitro* assays, which are missing all regulatory enzymes and binding partners naturally co-existing in live cells. This artificial environment can change protein-protein association. The successful co-immunoprecipitation of B3GNT8 and- 2 in COS-7 cells and the increase in cell surface polyLacNAc chains in HL60 cells is interpreted by the authors as a confirmation of B3GNT8 enhancing the activity of B3GNT2 *in vivo*. Another possible explanation is that B3GNT2 and -8 participate in subsequent steps of N-glycosylation and therefore associate, like many other glycosyltransferases to build LacNAc (Spessott et al., 2012; de Graffenried and Bertozzi, 2004; Giraudo and Maccioni, 2003; Bieberich et al., 2002). In my opinion, this experiment from Seko and Yamashita suggests that exogenous B3GNT8 functions by synthesizing poly-LacNAc chains in HL60 cells and that B3GNT8 is the main polyLacNAc synthesizing B3GNT family member in HL60 cells. In support for this, myelocytic lineage-differentiation of HL60 cells by DMSO, as used by the authors, up-regulates B3GNT8 more than B3GNT2 (Qiu et al., 2011). Furthermore, Qiu et al. also show that the expression levels of B3GNT2 and -8 in myelocytic lineage-differentiated HL60 cells highly depend on the differentiation-inducing chemicals as e.g. DMSO, ATRA, or PMA. Thus, rather than B3GNT8-activated B3GNT2 being the cause of up-regulated polyLacNAc chains in HL60 cells it may rather have been the exogenously added B3GNT8.

#### **4.2.5 B3GNT8 LoF in LRP6/Wnt signaling**

While LRP6 expression stabilizes B3GNT8 (fig. 19), B3GNT8 gene silencing reduces LRP6 protein levels (fig. 22). This suggests there are alternative mechanisms of how B3GNT8 regulates Wnt signaling and hints at the involvement of feedback regulation between B3GNT8 and LRP6. The B3GNT8 siRNA LoF did not decrease LRP6 transcriptional levels, thus excluding the reported decrease of LRP6 mRNA expression by siRNA-induced long term effects (Khan et al. 2007). The LRP6 protein decrease must therefore happen post-transcriptionally. Another possibility is an increased LRP6 turnover rate by the protein quality control mechanism because of miss-produced N-glycans as seen for many other proteins (Nakagawa et al., 2009) and as suggested for LRP6 in the presence of Mest (Jung et al., 2011). The predicted substrate specificity of B3GNT8 towards the  $\beta$ 1,2-branch on existing N-glycan chains suggests that it acts at later stages in the N-glycosylation pathway, and this would explain the downregulation of the upper LRP6 band after B3GNT8 siRNA transfection. This supports an increased LRP6 turnover rate. Furthermore, my RNAseq experiments indicate that B3GNT8 LoF leads to decreased expression of glycosyltransferases participating at all steps of the N-glycosylation process (fig. 25), thus influencing also the synthesis of the less N-glycosylated LRP6.

The RNAseq data also showed that B3GNT8 gene silencing reduced transcript numbers of collagen family members (fig. 25). Considering the collagen-sensing anthrax toxin receptor interacts with LRP6 and modulates Wnt signaling (Chen et al., 2013; Abrami et al., 2008), this could be an additional way of how B3GNT8 modulates Wnt signaling, although one cannot rule out down regulation of collagen expression due to siRNA long term effects.

### **4. 3 Functions of B3GNT8-modified LRP6 N-glycans**

Four out of ten LRP6 N-glycosylation sites are highly conserved (fig. 11). Although two of these conserved sites have not been reported to be modified by attachment of N-glycans (Cheng et al., 2012; Chen et al., 2011; Khan et al., 2007), this may be due to the difficulties associated with studying protein N-glycosylation or to reduced hexose supply (Winterhalter et al., 2013; Nie et al., 2013; Lau et al., 2008). However, the high conservation of four N-glycosylation sites indicates a functional relevance.

#### **4.3.1 B3GNT8 in LRP6 Golgi-to-surface transport**

Correct N-glycosylation is needed by almost all proteins in the secretory pathway to come to the cell surface (Scheiffele and Fullekrug, 2000; Gut et al., 1998; Nabi and Rodriguez-Boulan, 1993) and LRP6 is retained in the ER if it fails to undergo proper N-glycosylation (Jung et al.,



2011; Khan et al., 2007; Hsieh et al., 2003). As expected, B3GNT8 siRNA gene silencing changes the ratio of upper and lower LRP6 bands. The ratio change was subtle but reproducible (upper:lower-ratio changed from 7:1 to 6:1), in agreement with my prediction that B3GNT8 regulates LRP6 Golgi-to-surface transport. However, more experiments are needed for verification e.g. by applying high resolution SDS-PAGE (see results 3.2) to monitor changes both in the migration pattern and amounts of the different highly N-glycosylated LRP6 species.

The cell surface levels of LRP6 also depend on the intracellular chaperone MESD (Khan et al., 2007) and in the absence of MESD LRP6 forms aggregates in the ER (Koduri and Blacklow, 2007; Li et al., 2006; Li et al., 2005; Culi et al., 2004). All LDLR family members (like LRP6) consist of at least one beta propeller domain (BP), which is followed by an EGF-like repeat. MESD is required for the proper folding and maturation of these tandem BP-EGF-like repeats and aids in attachment of the oligosaccharide precursor to LRP6 (Culi et al., 2004), thus highlighting the importance of precursor attachment for LRP6 transport. Contrary to my expectations, MESD and B3GNT8 co-expression strengthens both non-modified and B3GNT8-modified LRP6 (fig. 27), suggesting that MESD promotes a species different than that promoted by B3GNT8. However, the MESD amino acid sequence contains an ER retention signal and MESD protein is indeed localized in the ER (Chen et al., 2011; Hsieh et al., 2003), whereas B3GNT8 is thought to localize in the Golgi (Seko and Yamashita, 2008). Hence, MESD aids the transport from ER to Golgi, where B3GNT8 is located. Thus, until LRP6 reaches B3GNT8 many intermediate N-glycosylation steps are necessary, and meanwhile the LRP6 protein can be subject to different molecular changes, like intracellular ligand binding (Li et al., 2005) or conformational changes of the immature N-glycan (Baenziger, 1994). Furthermore, the LRP6 protein consists of different splice variants and the LRP6 gene shows multiple single nucleotide polymorphisms (SNPs) that are known to play distinct roles in Alzheimer's disease and high- and low-bone-mass disease (Alarcon et al., 2013; Williams and Insogna, 2008). These steps could serve as priming events thereby determining the fate of the yet immature oligosaccharide.

#### **4.3.2 B3GNT8 in LRP6/ligand interaction**

The positioning of the conserved LRP6 N-glycan attachment sites 1 and 2 is located one additional  $\beta$ -sheet after the YWTD BP/ $\beta$ -sheet motifs and puts the corresponding N-glycan chains in close proximity to known ligand binding sites (fig. 29). My molecular visualization modeling confirmed that these additional amino acids between the YWTD BP/ $\beta$ -sheet motif and the N-glycan 2 are necessary for the proximity to the ligand binding sites (not shown) and the existence of this additional  $\beta$ -sheet is conserved in LRP6 and -5 (fig. 11). This suggests a functional relevance in ligand binding, either for ER/Golgi-located LRP6 (e.g. by binding MESD; Liu et al., 2009) or at the cell surface (e.g. by binding Wnt1, Wnt9b, Dkk1 and SOST, which bind to the first two LRP6  $\beta$ -propellers; Ettenberg et al., 2010; Bourhis et al.,

2010; Ahn et al., 2011; Bourhis et al., 2011). My TOPFLASH assays showed significantly enhanced Wnt signaling by B3GNT8 in Wnt3-CM treated cells (fig. 15). Although this enhancement may arise from increased LRP6 cell surface expression (fig. 27), the possibility of stronger binding of Wnts and/or Frizzleds to LRP6 remains a plausible explanation for the enhancement. In support of this, Dkk1-CM inhibits B3GNT8 TOPFLASH synergies (not shown), indicating the necessity of Wnt-accessible signalosome members for B3GNT8-mediated Wnt enhancement. To further elucidate the function of the LRP6 N-glycans in LRP6/ligand interactions, TOPFLASH reporter assays with ligands binding to LRP6 BP1 and/or BP2 in the presence or absence of B3GNT8 could be used. In addition, LRP6/ligand binding assays, e.g. dual-color dual-focus line scanning fluorescence correlation spectroscopy (Dörlich et al., 2015), can be employed.

### **4.3.3 B3GNT8 in signalosome endocytosis**

Proper Wnt signaling is thought to require Rab5-dependent endocytosis and recycling of the receptors back to the cell surface (Hagemann et al., 2009). For signaling maintenance the signalosome is transported into endosomes or multi-vesicular bodies (MVBs) (Dobrowolski et al., 2012; Taelman et al., 2010). Considering that B3GNT8 acts at the level of the LRP6 signalosome and shows synergy with Rab5 expression, my data support a transport of signalosomes in endosomes (fig. 17). Although clathrin- and/or caveolin-mediated endocytosis are thought to be involved in signalosome endocytosis, B3GNT8 did not show synergies with clathrin and caveolin expression (not shown). Clathrin and caveolin involvement in Wnt signaling is however still a matter of debate and depends on the cell type being analyzed (Demir et al., 2013; Kikuchi et al., 2009). Also galectin-3 conditioned medium, a polyLacNAc binding protein which modulates Wnt signaling presumably by forming a non-endocytosable receptor:galectin-lattice (depending on the cellular context) (Garner and Baum, 2008; Shi et al., 2007; Demetriou et al., 2001), did not affect the B3GNT8-mediated Wnt enhancement (not shown). In my experiments B3GNT8 rather enhanced Wnt signaling by increasing the cell surface levels of certain LRP6 subspecies (fig. 27). To me this suggests that Wnt stimulation upon B3GNT8 expression results mainly from the enhanced LRP6 Golgi-to-surface transport.

## **4.4 B3GNT8 and other pathways**

### **4.4.1 B3GNT8 and Wnt/PCP signaling**

The non-canonical PCP signaling is inhibited by Wnt/ $\beta$ -catenin signaling and is Activating Transcription Factor 2 (ATF2) dependent (Tahinci et al., 2007; Gray et al., 2013). Although B3GNT8 mainly influenced Wnt signaling in our RNAseq experiment, B3GNT8 dose-



dependently decreased PCP signaling and the effect was augmented in the presence of exogenous Wnt5a (figs. 25 and 26). This indicates that exogenous B3GNT8 does not uncouple  $\beta$ -catenin signaling from its well documented cross talk with PCP signaling.

#### **4.4.2 B3GNT8 and the N-glycosylation pathway**

The RNAseq data shows that the redundantly functioning family members B3GNT2 and B3GNT4 (Seko and Yamashita, 2005) were non-significantly up-regulated upon silencing of B3GNT8 (not shown). On the other hand, all three bioinformatic software analysis that I performed show decreased expression levels of N-glycosyltransferases participating at all steps of the N-glycosylation process. Although I cannot formally rule out that this is due long term siRNA treatment, this suggests feedback mechanisms for N-glycosyltransferases from different steps of the N-glycosylation process, in addition to co-localization mechanism for successively acting glycosyltransferases (Spessott et al., 2012; Ishida et al., 2005; de Graffenried and Bertozzi, 2004).

#### **4.4.3 B3GNT8 and cell cycle**

B3GNT8 regulates the proliferation of cells in culture (Hua et al., 2012; Liu et al., 2010) and tumor growth in nude mice (Hua et al., 2012), however the mechanism is unclear. Although I used non-synchronized cells, my RNAseq data suggest that the regulation of proliferation is due to upregulation of G1-phase arrest effectors (fig. 25). Thus, future RNAseq experiments can use cells with synchronized cell cycles to confirm and extend these findings. Furthermore, there is a known connection between cell cycle control and Wnt-signalling (Davidson., 2009), so the effect of B3GNT8 on the cell cycle and vice versa should also be investigated in more detail.

#### **4.4.4 B3GNT8 siRNA gene silencing and Wnt, p53, TGF $\beta$ , Shh, FGF, and MAPK signaling pathway**

In order to gain a more global picture of how cellular signaling pathways are regulated by B3GNT8, I specifically looked for differential expression of known transcriptional target genes in our RNAseq experiment. Although, in good agreement with my prediction, B3GNT8 silencing mainly effects the transcription of Wnt target genes, the effect on other signaling pathways, as e.g. Shh, FGF and MAPK, was also seen. However, considering the complex nature and cross-talk between cellular signaling pathways it is perhaps not surprising that additional signaling pathways are also affected. Reporter gene assays specific for different signaling pathways would be necessary to address this in more detail. The greater effect on Wnt signaling is likely due to a preference of B3GNT8 for LRP6; although B3GNT8 is involved

in the elongation of polyLacNAc present on all complex-type N-glycans (Seko and Yamashita, 2005), B3GNT8 does not modify the N-glycosylated EGF-R, TF-R, ROR2, LRP5, Kremen1, Wnt3a, Dkk3, FGFR1, and Fzd5 (figs. 14, 18, 19, 22 and 27). This suggests that B3GNT8 is a GlcNAc transferase with a certain specificity for LRP6 and therefore Wnt signaling. Protein specific N-glycosyltransferases are involved in conferring unique N-glycan structures to specific proteins and recognize both the N-glycan moiety and the surrounding amino acid residues, thereby creating very specific protein subspecies (Baenziger, 1994). The exact mechanism of how protein specific glycosyltransferases recognize their unique substrate is complex and just emerging (Lee et al., 2014). To date, only a few protein specific glycosyltransferases are known, such as e.g. UDP-Glc:glycoprotein glucosyltransferase, UDP-N-acetylglucosamine:lysosomal enzyme N-acetylglucosamine-1-phosphotransferase, and UDP-GalNAc:glycol-protein hormone N-acetylgalactosaminyltransferase (Manzella et al., 1996; Baenziger, 1994; Rosen, 1993; Troy, 1992; Rutishauser, 1992). To test if B3GNT8 is a protein specific glycosyltransferase, large scale protein modification screens would be necessary. If B3GNT8 is indeed an LRP6 specific GlcNAc transferase a clinical relevant research field would likely be established for the targeted inhibition of LRP6 Golgi-to-surface translocation in LRP6-misregulated diseases such as Alzheimer (Liu et al, 2014) and certain breast cancer subtypes (Liu et al., 2010).

Our RNAseq experiment also verified reports that B3GNT8 LoF reduces MMP2 expression and increases TIMP-2 expression, -32% and +26% respectively (Hua et al., 2012; Li et al., 2011). Although the authors failed to report a mechanism for these observations, it is most likely mediated by Wnt signaling, considering MMP-2 is a Wnt target gene (Wu et al., 2007).

#### **4.5 LRP6 and B3GNT8 in metabolic regulation of Wnt signaling**

##### **4.5.1 LRP6 and hexose induced Wnt signaling**

The regulation of Wnt signaling by metabolic processes is currently not well understood. However, both the Wnt pathway is significantly involved in many tumor types (Clevers, 2006; Gordon and Nusse, 2006) and one characteristic of tumors is elevated levels of hexose uptake and metabolism by the hexosamine biosynthetic pathway (Milewski, 2002; Gatenby and Gillies 2004; Bironaite et al., 2000). In the two macrophage tumor cell lines J774.2 and RAW264.7, Wnt signaling is significantly altered when D-glucose and L-glutamine levels are changed (Anagnostou and Shepherd, 2008). Like these macrophage cell lines, I could confirm that HEK293 cells share part of this glucose/glutamine-dependent regulation mechanism. Both glutamine and glucose are used in the hexosamine biosynthetic pathway (HBP) to produce nucleotide diphosphate-activated hexoses (NDP-hexoses), e.g. for N-glycosylation, and indeed, the glucose/glutamine mediated change in Wnt signaling utilizes N-glycosylation (Anagnostou and Shepherd, 2008). The authors reason that this mechanism adjusts cellular

growth to nutrient supply. Furthermore, they found evidence that metabolism-mediated change in Wnt signaling is elicited by pathway members that are upstream of GSK3. On Wnt receiving cells, only two members of the canonical Wnt pathway are known to be both N-glycosylated and upstream of GSK3: Frizzleds and LRPs, with LRPs inheriting a greater number of conserved N-glycosylation sites than Frizzleds (4 vs. 1, respectively, own alignment, not shown). My experiments indeed suggest there is an influence of glucose/glutamine levels on LRP6 maturation however do not clearly show a regulation of cell surface transport of LRP6 upon glucose/glutamine changes (fig. 31). More detailed experiments are required to specifically analyze the cell surface levels of LRP6 upon glucose/glutamine reduction, such as e.g. cell surface biotinylation assays or fluorescence microscopy assays. The existence of different LRP6 subspecies harboring different N-glycan modifications and their involvement in the regulation of Wnt signaling is an interesting future research topic. The investigation of the different phosphorylation events for each subspecies in the presence of Wnt ligands may get an indication about the contribution of each species to Wnt signaling.

It will be also important to study which LRP6 N-glycosylation sites play a role in hexose induced Wnt signaling. Considering glucose/glutamine-mediated changes in Wnt signaling utilize N-glycosylation (Anagnostou and Shepherd, 2008) mutation of specific LRP6 N-glycosylation sites and the effect this has on LRP6 function and Wnt signaling would be an interesting topic to study. Since the likelihood for precursor attachment to any N-glycosylation site depends on both the site distance to the C-terminus and the site preceding amino acid (Bano-Polo et al., 2011), my hypothesis is that the most N-terminal N-glycosylation sites are likely to be equipped with glycan chains and thus to be involved in hexose induced Wnt signaling.

#### **4.5.2 B3GNT8 and hexose induced Wnt signaling**

B3GNT8 promotes the stabilization of LRP6 upper bands that are otherwise reduced when glucose levels are lowered, however this effect is not seen when glutamine levels are lowered (fig. 32). L-glutamine is needed by the rate-limiting enzyme of the hexosamine pathway, glutamine:fructose-6-phosphate amido transferase (GFAT) (Nakaishi et al., 2009), thus, depletion of glutamine leads to a shortage of multiple NDP-activated hexose forms. Although exogenously added B3GNT8 has increased chances to utilize GlcNAc from the donor UDP-GlcNAc as compared to endogenous N-glycosyltransferases, in glutamine reduction B3GNT8 could not modify LRP6. Thus, B3GNT8 appeared to be depleted of its GlcNAc-donor, UDP-GlcNAc. In contrast to glutamine reduction, cells can partially compensate glucose reduction by interconverting hexoses via epimerization (Boyce et al., 2011; Holden et al., 2003; Hinderlich et al. 2000). And indeed, B3GNT8 stabilizes both upper LRP6 bands in glucose titrated media (fig. 32), suggesting that B3GNT8 compensates the effects of the glucose loss on LRP6 by drawing UDP-GlcNAc from cellular hexose pools (Seko

and Yamashita, 2008). Furthermore, the RNAseq data suggest that this compensatory effect on LRP6 by B3GNT8 may additionally result from a coupled expression of N-glycosyltransferases participating at all steps of N-glycosylation. In support of this, LRP6 stabilizes B3GNT8 protein levels, suggesting a feedforward mechanism. Interestingly, together with the rescue of the upper LRP6 bands, B3GNT8 both blocked the reduction in Wnt signaling caused by reduced glutamine (fig. 32) and augmented hexose sensitivity caused by increased ManNAz (fig. 33), indicating that B3GNT8 may indeed play a role in hexose induced Wnt signaling at the level of LRP6. Consistently, synthesis of tetra-antennary N-glycans (a substrate of B3GNT8) is highly sensitive to hexosamine flux (Lau et al., 2007). Detailed structural analysis of the N-glycans of LRP6 by Mass Spectrometry is therefore an important part of the future work to understand better the role of B3GNT8 and hexose induced Wnt signaling. Furthermore, sequence analysis revealed that  $\beta$ -catenin has one putative O-glycosylation site and that Frizzleds have more than three putative N-glycosylation sites (not shown).  $\beta$ -catenin and Frizzled may therefore be dependent on cellular hexose levels in addition to LRP6 and should be included in future research.

#### **4.6 Consequences of my study**

An unsolved issue in the field of Wnt/ $\beta$ -catenin signaling concerns the N-glycosylation of Wnt ligands and their transmembrane receptors Frizzled and LRP. While it has been clearly shown that Wnts, LRPs and Frizzleds need N-glycosylation to reach the cell surface and that this process modulates Wnt signaling (MacDonald and He 2012; Janda et al., 2012; Khan et al., 2007; Yamamoto et al., 2005; Hsieh et al., 2003; Tanaka et al., 2002) only little is known about the N-glycosyltransferases involved.

Recently the N-glycan branching enzyme MGAT-V was shown to modulate Wnt signaling. MGAT-V acts at an early step of N-glycan diversification by inducing  $\beta$ 1,6-branching of the trimmed oligosaccharide (Guo et al., 2014). MGAT-V induces synthesis of tetra-antennary N-glycans, and considering the known roles that tetra-antennary N-glycans and Wnt signaling play in cancer (Joiner et al., 2013; Chen et al., 2011; Ihara et al., 2002; Granovsky et al., 2000; Seberger and Chaney, 1999; Pierce et al., 1997; Kobata, 1989; Dennis and Laferte, 1989) it is likely that Wnt ligands and their receptors harbor tetra-antennary N-glycans. However a direct connection between the N-glycosylated pathway members Wnts, Frizzleds, LRPs and the MGATV remains to be shown. In addition, the main diversifying N-glycosyl transferases which contribute to the length of the N-glycan antennae (GlcNAc transferases and galactose transferases) remain unknown. The reason for this is partly due to the difficulty associated with the study of protein glycosylation (Winterhalter et al., 2013; Nie et al., 2013; Leymarie and Zaia, 2012).

My study shows for the first time an N-glycan antenna elongating GlcNAc transferase to regulate canonical Wnt signaling and emphasizes the importance of cellular metabolism for both glycoprotein and cell surface receptor studies. My data opens an interesting new research field with regard to putative protein-specificity of this new LRP6 modifier. Furthermore, my data may provide insight into the B3GNT8-mediated regulation of tumor growth in nude mice (Hua et al., 2012). To investigate into a connection between tumor growth and B3GNT8-modulated Wnt signaling will be of great interest to explore. This data may also provide insights into the tumor signaling pathways that are supported by the generally elevated levels of glucose and glucose flux through the hexosamine biosynthetic pathway (Gatenby and Gillies, 2004; Milewski, 2002; Bironaite, 2000). Finally, this may lead to therapies where B3GNT8 is targeted to regulate LRP6 Golgi-to-surface transport. LRP6 misregulatory diseases include Alzheimer's disease (Liu et al., 2014; Alarcon et al., 2013), high- and low-bone-mass disease (Williams and Insogna, 2008) and certain breast cancer subtypes (Liu et al., 2010). To investigate into B3GNT8s involvement in these diseases will be of great interest.

My work supports a model where B3GNT8 modifies certain LRP6 subspecies to modulate their Golgi-to-surface transport. In addition, my study identifies for the first time a GlcNAc transferase that is involved in the metabolic regulation of Wnt signaling. A model in which B3GNT8 promotes LRP6 Golgi-to-surface transport under the influence of metabolic processes is therefore proposed (fig. 34). This model is based on my work using cultured cells and will therefore require *in-vivo* verification in the future.

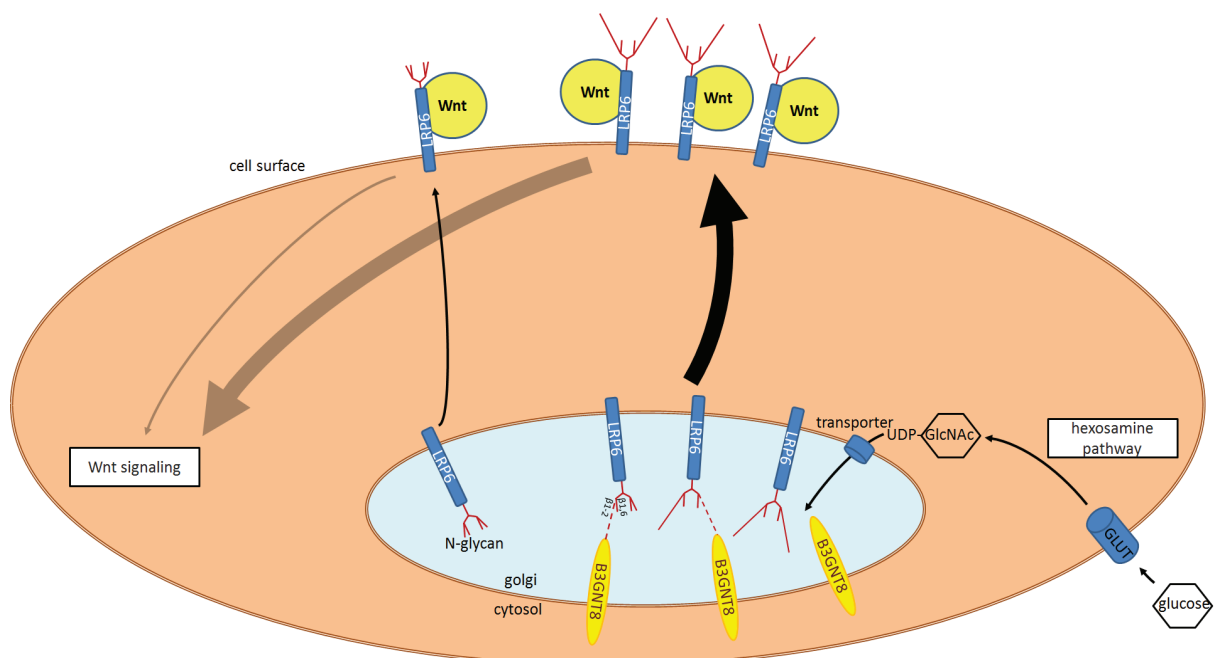


**Figure 34: B3GNT8 adds modifications to and enhances the cell surface transport of LRP6 under the influence of metabolic processes.** B3GNT8 modifies the N-glycans on LRP6 (red lines), which aids the LRP6 Golgi-to-surface transport. This leads to enhanced Wnt signaling in the presence of the Wnt ligand compared to non-modified LRP6. Hexoses (e.g. glucose) are taken up by hexose transporters (e.g. the glucose transporter GLUT) and are utilized by the hexosamine biosynthetic pathway to build up UDP-GlcNAc (or are epimerized from intracellular hexose pools, not shown). UDP-GlcNAc is the hexose donor of B3GNT8 and supports B3GNT8s enzymatic activity on LRP6 thereby increasing Wnt signaling.

## 5. Materials and Methods

---

### **5.1 Methods**

For reasons of accuracy and comprehensibility are the catalog numbers of consumables and equipment as well as the ingredients of pre-mixed solutions to be found in the Materials section.

#### **5.1.1 Maintenance of Cells**

The cell medium contained 1x Dulbecco's Modified Eagle Medium (DMEM) (+4,5g glucose, +pyruvate, +L-glutamine) (GIBCO) with 5% Fetal Bovine Serum (FBS) (Sigma Aldrich Co.) and 1% Penicillin/Streptomycin (Pen/Strep) (GIBCO) unless otherwise stated. 5% BSA was chosen because of the more equal ratio of upper vs. lower LRP6 band. For siRNA inhibition experiments the same DMEM medium with 5% FBS without Pen/Strep was used to enhance knock down efficiency. Incubation was done at 37°C (5% CO<sub>2</sub>). For passaging the HEK293T cells were washed in Phosphate Buffered Saline (PBS) (without CaCl<sub>2</sub> and MgCl<sub>2</sub>) (GIBCO) 1ml 0,25% trypsin-EDTA (GIBCO) was applied for 3min at 37°C (5%CO<sub>2</sub>) to detach cells from a 75cm<sup>2</sup> Cellstar Cell Culture flask (greiner bio-one). For 96well Cellstar Cell Culture Plates (greiner bio-one) the volume of trypsin was adjusted to cell growth area. Subsequently, they were taken up into new medium and counted in a Neubauer cell counting chamber for experiments and for cell culture stock.

#### **5.1.2 Transient ScreenfectA Transfection of Cell Lines for Overexpression Experiments**

For 96well plates 0,35µl/well ScreenfectA (InCella) was mixed with 9,65µl dilution buffer (InCella). 100ng of the transfecting plasmid DNA were filled up with DNA EB elution buffer (QIAGEN) to 10µl. Both mixes were combined and incubated 30min at RT without any mechanical disturbance to ensure proper lipoplex formation. Finally 80µl cell suspension was added to the mix and 95µl of the mix plated onto 96well plates (one step transfection). Or 80µl of DMEM+10%FBS+1%Pen/Strep medium was added and 95µl was given to already settled cells in 96well plates (two step transfection). For other well plate formats the volumes have been adjusted according to cell growth area.

#### **5.1.3 Transient Promofectin Transfection of Cell Lines for Overexpression Experiments**

For most overexpression experiments Promofectin (Promocell) was chosen because it showed a more equal ratio of upper vs. lower LRP6 band. For 96well plates 0,35µl/well Promofectin was mixed with 9,65µl OPTI-MEM Reduced Serum Medium (GIBCO) to enhance transfection efficiency. 100ng of the transfecting plasmid DNA were filled up with DNA EB elution buffer (QIAGEN) to 10µl. Both mixes were combined and incubated 30min at RT



without any mechanical disturbance to ensure proper lipoplex formation. Finally 80µl cell suspension was added and 95µl of the mixture plated onto 96well plates (one step transfection). Or 80µl medium was added and 95µl was given to already settled cells in 96well plates (two step transfection). For other well plate formats the volumes have been adjusted according to cell growth area. Where necessary the transfection mix was exchanged for DMEM cell growth medium+10%FBS+1%Pen/Strep after 6h.

#### **5.1.4 ScreenfectA Transfection of Cell Lines for siRNA Experiments**

For 24 well plates (greiner bio-one) 1µl/well ScreenfectA (InCella) was combined with 40µl dilution buffer (InCella). 20pmol siRNA was taken up into 40µl dilution buffer. Both mixes were combined and incubated 30min at RT without any mechanical disturbance to ensure proper lipoplex formation. Finally 400µl HEK293T cells were added, and 450µl of the mixture was plated in a 24well Cellstar Cell Culture Plate (greiner bio-one). The plate was left for 10min to ensure homogenous distribution of cells.

#### **5.1.5 Cell Lysis for SDS-PAGE / Western Blotting**

After removal of the growth medium 40µl/96well of 1% triton lysis buffer (TLB) was added to the cells. To ensure protein stability the following steps were done at 4°C or on ice. The lysis was allowed to proceed for 3min with intermediate vortexing. The lysate was centrifuged with 12.000rpm for 5min. 30µl of the lysate was taken into a new vessel without disturbing the cell debris pellet. The lysate was added 10µl 4xLaemmli buffer and boiled at 95°C for 5min to ensure protein denaturation. Until usage lysates were stored at -20°C.

#### **5.1.6 Bradford Assay**

3µl of a HEK293T cell lysate (in 1% TLB) was mixed with 12µl 0.15M NaCl solution and 100µl Bradford solution (Sigma Aldrich Co.) in Elisa Reader 96well Microplates (greiner bio-one). Samples were measured on ELX-808IU Absorbance Microplate Reader from BioTek Instruments. Standard curve was made with 1mg/ml Bovine Serum Albumin Fraction V pH7.0 (BSA) (GE Healthcare) solution.

#### **5.1.7 Sodium Dodecyl Sulfate – Polyacrylamide Gel Electrophoresis (SDS-PAGE)**

The separating gel (percentage dependent on the proteins of interest) was poured in a caster (BIO-RAD), covered with saturated n-butanol or isopropanol to get an even surface, and left for polymerization for about 30min. The top of the gel was washed with ddH<sub>2</sub>O, filled with the stacking gel, and a comb was inserted to create the loading pockets. After 30min, the comb was taken out carefully, and the pockets were washed with ddH<sub>2</sub>O 1-2times. The gel was put into a MINI-PROTEAN Tetra Systems gel running unit (BioRad), which was filled with 1xSDS-PAGE running buffer. A maximum of 10µl (for 0.75mm thick gels) or 20µl (for 1.5mmthick gels) of each sample was loaded according to Bradford measurement.

The gel electrophoresis was done for 30min at 80V and then 1-2h at 120V, depending on the separation needed.

#### **5.1.8 Semi-Dry Western Blotting**

The blot papers were soaked with transfer buffer. PVDF Immobilon-P 0.45 $\mu$ m Transfer Membrane (MerckMillipore Co.) was first activated with methanol, Protran BA 85 Nitrocellulose 0.45 $\mu$ m membrane (Whatman) with ethanol. The transfer stack was placed in a Western Blotting TransBlot SD cell (BIO-RAD) from bottom (anode) to top (cathode) in the following order: thick Whatman gel blotting paper, thin Whatman gel blotting paper (both Sigma Aldrich Co.), membrane, gel, thin Whatman gel blotting paper, thick Whatman gel blotting paper. Each layer was pressed carefully to remove air bubbles. Blotting was done at 0.1A (per 40cm<sup>2</sup> gel) for 1hour.

#### **5.1.9 Western Blotting with Trans Blot Turbo System**

The blot paper stacks were wetted with transfer buffer (BIO-RAD). The membrane was activated with ethanol. The transfer stack was placed in a TransBlotTurbo transfer system (BIO-RAD) from bottom (anode) to top (cathode) in the following order: blotting paper stack (supplied by manufacturer), membrane (supplied by manufacturer), gel, blotting paper stack. Each layer was pressed carefully to remove air bubbles. The blotting was run for 7min at 1.3A for one 40cm<sup>2</sup> gel (or 2.5A for two 40cm<sup>2</sup>) or 30min for high molecular weight proteins.

#### **5.1.10 Blocking, Incubation with Primary and Secondary Antibodies, and Washing with the BioLane InSitu Hybridization Mashine**

The procedure in the BioLane HTI (intavis) was as follows: Blocking was done in 5% (w/v) BSA solution for 1.5h at RT. Primary antibody incubation was done for 10hours at 4°C. Then the blots were washed 5x in TBS-T solution, the first wash for 15 sec, the following for 8min each. Secondary antibody incubation was done for 1hour at 4°C. Again, the blot was washed according to the just mentioned procedure. Storage of the membrane was at 4°C. The protein was visualized with the ECL Western Blotting Substrate (Promega Co.).

#### **5.1.11 Blocking, Incubation with Primary and Secondary Antibodies, and Washing the SNAP i.d.**

A 40cm<sup>2</sup> membrane was blocked in 30ml 1% (w/v) BSA solution by sucking the BSA solution through the membrane with the SNAP i.d. 2.0 protein detection system (MerckMillipore Co.). Primary antibody incubation was done overnight at 4°C on a shaker ( $\alpha$ -LRP6total-T1479d61 1:5000,  $\alpha$ -B3GNT8rb2 1:500,  $\alpha$ -EGFR 1:5000,  $\alpha$ -TfR 1:20000,  $\alpha$ -PCNA 1:20000,  $\alpha$ -Sp1490-CS Wnt-dependent 1:5000,  $\alpha$ -Myc 1:20000,  $\alpha$ -FLAG 1:5000,  $\alpha$ -V5 1:5000,  $\alpha$ -tubulin 1:5000,  $\alpha$ -Axin 1:5000,  $\alpha$ -GFP 1:10000,  $\alpha$ -Wnt3a 1:3000). The blots were washed with 120-250ml TBS-T in the SNAP i.d. 2.0. Secondary antibody incubation was done for 1-4hours at



4°C on a shaker ( $\alpha$ -rabbit,  $\alpha$ -mouse both 1:2000). Again, the blot was washed as just mentioned. Storage of the membrane was at 4°C. The protein was visualized with the ECL Western Blotting Substrate (Promega Co.).

#### **5.1.12 Transformation of Electro-competent *Escherichia coli* Strains**

20-50ng plasmid DNA in 1-3 $\mu$ l and 50-100 $\mu$ l of electro-competent XL1 blue *Escherichia coli* suspension was pipetted into an electro-cuvette with an electrode distance of 1mm. The electroporation was done at 1.8Kilovolt with a time constant of approximately 5millisec. After immediate addition of 1ml SOC medium the bacteria were incubated in a 1.5ml Eppendorf tube (Eppendorf AG) at 37°C on a shaker. After 1h, 10-20 $\mu$ l of the bacterial suspension was plated in a 10cm petri dish, or 6-12 $\mu$ l in a 6cm petri dish.

#### **5.1.13 Transformation of Chemo-Competent *Escherichia coli* Strains**

10-100ng plasmid DNA or 5 $\mu$ l of a ligation mix was added to 50-100 $\mu$ l of chemo-competent TOP10 *Escherichia coli* suspension and left on ice for 30min. Chemo-transformation was done at 42°C for 45-50sec with a subsequent rest for 2min on ice. After addition of 900 $\mu$ l SOC medium the bacterial suspension was incubated in a 1.5ml Eppendorf reaction tube at 37°C on a shaker. After 1h, 10-20 $\mu$ l of the bacterial suspension was plated in a 10cm petri dish, or 6-12 $\mu$ l in a 6cm petri dish.

#### **5.1.14 Plasmid Preparation with the PEQlab Mini-Prep Kits (peqlab)**

5ml over night culture of an electro- or chemo-transformed single clone *Escherichia coli* XL1 blue colony was centrifuged at 5000g for 10min. The bacterial pellet was resuspended in 250 $\mu$ l solutionI (part of the kit). Subsequently, 250 $\mu$ l solutionII, and 350 $\mu$ l solutionIII (both part of the kit) were added with inverting of the Eppendorf reaction tubes after each step. The mixture was loaded onto a peqlab mini-prep column (part of the kit) and centrifuged at 10.000g for 1min. 500 $\mu$ l PW plasmid buffer (part of the kit) was added to the column, and it was centrifuged again at 10.000g for 1min. Washing was done 2x with 75 $\mu$ l DNA wash buffer (part of the kit), and an additional centrifuging at 10.000g for 2min removed liquids from the column. The plasmid was eluted with 50 $\mu$ l elution buffer (part of the kit) by centrifugation at 5000g for 2min. For higher plasmid yields, the corresponding prep kits were used.

#### **5.1.15 Endonuclease Digestion of Plasmids and DNA**

A minimum of 200ng DNA was added to 10% 10x Fast Digest Green Buffer (Fermentas) and 5% DNA digestion enzyme. The final volume was adjusted to 20 $\mu$ l. Digestion was done 37°C for 5-15min for fast digest enzymes or longer depending on the DNA concentration.

### **5.1.16 Luciferase Assays**

For luciferase assays, one 96 well was lysed in 40µl Passive Lysis Buffer (PLB) (Promega Co.). Then 10µl of sample was mixed with 10µl of PLB in a white walled 96well plate. For firefly luciferase, glycylglycine buffer with DTT and ATP (both 1:100) or with firefly substrate solution (1:5 in glycylglycine buffer) was prepared. For renilla luciferase coelenterazine was prepared 1:10000 in coelenterazine buffer. The mixing and the measurement was done on Victor Light luminescence counter (PerkinElmer) for 2sec by well. All TOPFLASH (firefly luciferase) values were normalized against renilla luciferase values.

### **5.1.17 Cell Surface Biotinylation**

To inhibit endocytosis, the cells were constantly kept on ice during the following procedure. 40min before harvest cell were carefully scraped into 2ml Eppendorf tubes and washed with ice cold PBS (pH8.0). Immediately before use, a 5mg/ml Sulfo-NHS-SS-biotin (Thermo Scientific Inc.) solution was prepared. The working concentration was 1mg/ml and was added to the cells carefully. After shaking for 2h at 4°C, the cells were pelleted. To remove unreacted biotin, the cells were washed 3 times with quenching buffer and then centrifuged at 500g for 2min. Lysis was done in 150µl 1% triton lysis buffer for 3min with intermediate vortexing. A centrifuging step at 12000g removed cell debris. The supernatant was transferred to a new Eppendorf tube and an aliquot of 30µl was taken as “input”. The NeutrAvidin Agarose Resin beads (Thermo Scientific Inc.) were washed 2x in PBS (pH7.2) and were suspended 1:1 in PBS to make 50% slurry solution. 20µl slurry and 100µl supernatant were mixed and the precipitation was done 2hours or overnight at 4°C, depending on the protein of interest. The next day the beads were centrifuged at 500g for 1min, and an aliquot of 30µl of the supernatant was marked as “flowthrough/unbound”. After washing of the beads 3x with TBS-T, 25µl PBS was added together with 10µl laemmli buffer. The samples were boiled at 95°C for 5min and centrifuged at maximum speed. The supernatant was labelled as “biotinylated”.

### **5.1.18 Immunoprecipitation**

Cell were harvested from 6well Cellstar Cell Culture plates (greiner bio-one) in 500µl 1% triton lysis buffer, kept on ice for 3min, and by addition of 400µl 1%triton lysis buffer transferred into a 1.5ml Eppendorf tube. After centrifuging at maximum speed for 5min, the lysate was transferred to a new Eppendorf tube and a 30µl aliquot was taken as “input”. Bradford assay ensured equal total protein concentrations for SDS-PAGE. 25µl 2mg/ml anti-T1479 antibody (own production) was added to the lysate and samples rotated at 4°C for 4hours. Meanwhile 15µl of agarose A beads and agarose G beads (both Roche Diagnostics GmbH) were mixed and washed twice with PBS. The beads were resuspended in 300µl 1% triton lysis buffer and added to the sample for overnight rotation at 4°C. The next day the beads were carefully centrifuged and 30µl of the supernatant was labelled as “unbound”. The beads were washed 3 times in 1% TBS (0.3M salt) and once in 500µl of Tris-HCl-MgCl<sub>2</sub> solution. For elution, 30µl of 2x Laemmli was added. The samples were boiled at 55°C at 1100rpm for 15min and the supernatant was labelled as “IP”.

### **5.1.19 Polymerase Chain Reaction (PCR)**

4µl of 5x Green GoTaq Reaction buffer (Promega Co.) was mixed with 0.5µl dNTP mix (10mM), 1µl forward primer (10µM), 1µl reverse primer (10µM), 9.25µl PCR grade water, 0.25µl 5U/µl GoTaq DNA polymerase (Promega Co.), and 4µl cDNA to 20µl total volume. After initial denaturation at 95°C for 2min, for GAPDH primers 40cycles of denaturation (95°C, 1min), primer annealing (55°C, 1min), and elongation (72°C, 1.5min) were applied with a terminal elongation at 72°C for 10min on a peQSTAR 2x Gradient PCR machine (peQLab). For LRP6 or B3GNT8 the said PCR cycled 30 times.

### **5.1.20 RNA Extraction**

The cells were pelleted and dissolved in 500µl peqGold RNA pure (peqlab). An equivalent volume of a phenol:chloroform:isopropylalcohol (25:24:1, pH 5.0) was added and mixed by inverting. After centrifugation at maximum speed for 5min the upper aqueous phase was transferred into a new 1.5ml Eppendorf tube. 0.1 volumes of sodium acetate (3M, pH 4.8) and 2.5 volumes of pure ethanol were added. To facilitate precipitation samples were stored for more than 30min at 4°C. After centrifuging for 20min at 4°C at maximum speed the pellet was washed with 75% ethanol and air dried. Reconstitution of RNA was done in 20µl of nuclease free water at 55°C for 10min.

### **5.1.21 DNase I Digestion**

600ng RNA was mixed with 1µl 1U/µl DNaseI (Fermentas), 1µl 10x Reaction buffer for DNaseI (Fermentas), and filled up with nuclease free water to a total volume of 10µl. After 1 hour at 37°C 1µl 25mM EDTA (Fermentas) was added to the digestion mix und put to 65°C for 10min to stop digestion.

### **5.1.22 Reverse Transcriptase PCR (RT-PCR)**

For Reverse Transcriptase (RT)<sup>+</sup> samples 6µl of DNase I digest was mixed with 14µl RT<sup>+</sup> mix. For RT<sup>-</sup> samples 3µl digest was mixed with 7µl RT<sup>-</sup> mix. The RT<sup>+</sup> mix consisted of: 1µl MMLV RT Rnase H Point Mutant (Promega Co.), 4µl 5x RT buffer (Promega Co.), 2µl dNTP mix (2.5mM each), 1µl 200ng/µl random hexamer primer (Life Technologies), 1.6µl 25mM MgCl<sub>2</sub> (Promega), 3,9µl PCR grade water, and 0.5µl 40U/µl RiboLock RNase Inhibitor (Fermentas). The RT<sup>-</sup> mix consisted of: 2µl 5x RT buffer, 1µl dNTP mix, 1µl random hexamer primer, and 3µl PCR grade water. The sample/RT mix was then incubated 10min at 25°C, 60min at 42°C, and 10min at 70°C. To RT<sup>+</sup> samples 80µl PCR grade water was added, to RT<sup>-</sup> samples 40µl. The samples were stored at -20C.

### **5.1.23 Real Time PCR (qPCR)**

10µl of 2x GoTaq qPCR Master Mix (Promega Co.) was mixed with 1µl forward primer (10µM), 1µl reverse primer (10µM), 2µl cDNA, and 6µl water. For B3GNT8 1.5µl of each

primer (10 $\mu$ M) together with 7 $\mu$ l template ensured consistent results. The qPCR was run on a StepOnePlus Real-Time PCR System (AB applied Biosystems).

#### **5.1.24 RNAseq**

Total RNA extraction was performed with Trizol (Invitrogen) following the manufacturer's protocol. Extracted total RNA samples were tested on RNA nanochips (Agilent). Sequencing libraries were generated from 1  $\mu$ g of RNA samples with the TruSeq stranded mRNA kit (Illumina). Size and concentration of sequencing libraries were determined with DNA-chip (Agilent) and the concentrations adjusted to 7 pM. Multiplexed samples were loaded on a single sequencing lane. Paired end reads (2 x 50 nucleotides) were obtained on a HiSeq1500 using SBS v3 kits (Illumina). Cluster detection and base calling were performed using RTAv1.13 and quality of reads assessed with CASAVA v1.8.1 (Illumina). The reads were mapped against the human genome (GRCh37) using tophat version 2.0.11 1 with the options -r 180 --mate-std-dev 80 --b2-sensitive --no-novel-juncs -a 5 --library-type fr-unstranded and using known exon junctions (Ensembl release 75). Gene expression was determined with HTSeq version 0.5.3p3 2 by counting for each gene the number of reads that overlapped with the annotation location obtained from Ensembl release 75. Differential expression was calculated using the R package DESeq 2, thereby following the workflow as described by Trapnell et al. (2009) and Anders & Huber (2010). Genes with an adjusted p-value (FDR) less than 0.05 were considered as differentially expressed.

#### **5.1.25 Fixation of Cells in Formaldehyde**

Cells were washed with PBS and fixed in 4% formaldehyde for 10min. 3 times washing with PBS removed unbound formaldehyde.

#### **5.1.26 Peptide-N-Glycosidase F (PNGaseF) Digestion of LRP6**

After the cell lysis proteins were taken up in Laemmli buffer and boiled at 95°C for 4min. 4 $\mu$ l 500U/ $\mu$ l PNGaseF (New England BioLabs GmbH) was added to 40 $\mu$ l sample. The digest took place for 2h at 37°C and was stopped at 95°C for 5min.

#### **5.1.27 Endoglycosidase H Digestion of LRP6**

After the cell lysis proteins were taken up in Laemmli buffer and boiled at 95°C for 4min. 1 $\mu$ l 500U/ $\mu$ l Endoglycosidase H (New England BioLabs GmbH) was added to 10 $\mu$ l sample. The digest took place for 2h at 37°C and was stopped at 95°C for 5min.

#### **5.1.28 Co-Immunoprecipitation**

Cells from 6well Cellstar Cell Culture plates (greiner bio-one) were lysed for 3min on ice in 500 $\mu$ l 1% triton lysis buffer with intermediate vortexing. By adding 400 $\mu$ l 1% triton lysis

buffer the cells were taken into a new 1.5ml Eppendorf tube and centrifuged on maximum speed for 5min. 800µl were transferred into a new Eppendorf tube and an aliquot of 45µl was labelled as input. Bradford assay ensured equal total protein concentrations for SDS-PAGE. 20µl ANTI-FLAG M2 Affinity Gel beads (Sigma-Aldrich Co.) per well were washed 3 times in TBS (0.3M salt) and once in 1% triton lysis buffer. The beads were resuspended in an appropriate volume and added to the cell lysates for overnight rotation at 4°C. Next day 45µl of the supernatant was labelled as “unbound” and the beads were washed 3 times with TBS (0.3M salt) by 10min rotating. The beads were eluted by addition of 30µl of TBS (0.3M salt) and 17µl Laemmli Western Blot buffer and subsequent shaking at 55°C for 15min.

## **5.2 Materials**

### **5.2.1 Consumables**

Table 2: Description of consumables

<u>Consumable</u>	<u>Company</u>	<u>Catalog Number</u>
1.5ml 3810X Eppendorf tube	Eppendorf AG	0030 125 150
10cm petri dish		
10cm Petri Dishes	greiner bio-one	632102
10xFast Digest Green Buffer	Fermentas	
10xFastDigest buffer	Fermentas	
145mm CellStar Cell Culture Dishes	greiner bio-one	639160
175cm <sup>2</sup> Cellstar Cell Culture flask	greiner bio-one	660160
1x DMEM (+4,5g glucose, +pyruvate, +L-glutamine)	GIBCO	41966-029
2.0ml Eppendorf Safe-Lock Tubes	Eppendorf AG	0030 120 049
24 well Cellstar Cell Culture plates	greiner bio-one	662160
2x GoTaq qPCR Master Mix	Promega Co.	A6001
5x Green GoTaq Reaction buffer	Promega Co.	M791A
5x RT buffer	Promega Co.	M531A
60mm CellStar Cell Culture Dishes	greiner bio-one	628160
6cm petri dish		
6well Cellstar Cell Culture plates	greiner bio-one	657160
75cm <sup>2</sup> Cellstar Cell Culture flask	greiner bio-one	658170
96well Cellstar Cell Culture	greiner bio-one	655180

Plates		
agarose A beads	Roche Diagnostics GmbH)	11719408001
agarose G beads	Roche Diagnostics GmbH	11719416001
ANTI-FLAG M2 Affinity Gel beads	Sigma-Aldrich Co.	A2220
Bradford solution	Sigma Aldrich Co.	36916-500
BSA Bovine Serum Albumin Fraction V pH7.0	GE Healthcare	K41-001
Coelenterazin Renilla	Biosynth AG	C7000
cOmplete Protease Inhibitor Cocktail Tablets	Roche Diagnostics GmbH	11697498001
D-Luciferin Firefly	Biosynth AG	L-8200
DNA EB elution buffer from QIAprep Spin Miniprep Kit (250)	QIAGEN	27106
DNA-chips Bioanalyser 2100	Agilent	
DNaseI 1U/ $\mu$ l	Fermentas	EN0521
ECL Western Blotting Substrate	Promega Co.	W1015
electroporation-cuvette 1mm	VWR International GmbH	71-2010
Elisa Reader 96well Microplates	greiner bio-one	655101
Endoglycosidase H 500U/ $\mu$ l	New England BioLabs GmbH	P0702S
FBS Fetal Bovine Serum	Sigma Aldrich Co.	F7524
Galectin-3	ProSpec-Tany TechneGene Ltd.	cyt-606
GoTaq DNA polymerase 5U/ $\mu$ l	Promega Co.	M830B
HEK293T cells	DSMZ	ACC 635
MgCl <sub>2</sub> 25mM	Promega Co.	A351B
MMLV RT Rnase H Point Mutant	Promega Co.	M170A
Neuraminidase	New England BioLabs, Inc.	P0720S
NeutrAvidin Agarose Resin beads	Thermo Scientific Inc.	29200
OPTI-MEM Reduced Serum Medium	GIBCO	31985-062
Page Ruler™ Prestained Protein Ladder	Thermo Scientific Inc.	26616
PBS Phosphate Buffered Saline	GIBCO	14190-094
Penicillin/Streptomycin (Pen/Strep)	GIBCO	15140-122
peqGold RNA pure	peQLab	30-1010
PEQlab Mini-Prep Kits	peQLab	12-6943-02
PLB Passive Lysis Buffer	Promega Co.	E194A

PNGaseF 500U/μl	New England BioLabs GmbH	P0704S
Promofectin	Promocell	PK-CT-2000-100
Protran BA 85 Nitrocellulose 0.45μm membrane	Whatman	10 401 197
PVDF Immobilon-P 0.45μm Transfer Membrane	MerckMillipore Co.	IPVH00010
RiboLock RNase Inhibitor 40U/μl	Fermentas	EO0381
RNA nano-chips Bioanalyser 2100	Agilent	
Rotiphorese Gel 30	Roth GmbH & Co. KG	3029.1
SBS v3 kits	Illumina	FC-401-3001
Screenfect dilution buffer	InCella	15-5277-03/B
ScreenfectA	InCella	S-3001
Sulfo-NHS-SS-biotin	Thermo Scientific Inc.	21331
Trans Blot Turbo 5x Transfer Buffer	BIO-RAD	200007676
Trizol	Life Technologies	15596-026
TruSeq stranded mRNA kit	Illumina	
trypsin-EDTA 0,25%	GIBCO	25200-056
Whatman gel blotting paper	Sigma Aldrich Co.	10426994
β <sub>1,4</sub> Galactosidase	New England BioLabs, Inc.	P0730S
β-N-Acetyl glucosaminidase	New England BioLabs, Inc.	P0732S

### **5.2.2 Equipment**

Table 3: Description of equipment

<u>Purpose</u>	<u>Equipment (Order Number)</u>	<u>Company</u>
Antibody incubation	BioLane HTI (5110)	intavis
Antibody incubation	SNAP i.d. 2.0 protein detection system (5001184)	MerckMillipore Co.
Balance	AB265-S/FACT	Mettler Toledo
Biosafety Clean Bench	CleanAir	Clean Air Techniek B.V.
Cell Culture Incubator	C150	Binder
Confocal Microscope	SPE	Leica
DNA/RNA/protein measurements	nanodrop ND-1000 Spectrophotometer	peQLab
Electroporation of <i>E. coli</i>	Micro Pulser (411BR6062)	BIO-RAD
Elisa Reader	ELX-808IU Absorbance Microplate Reader	BioTek Instruments
Luciferase Assay	Victor Light luminescence counter 1420	PerkinElmer
PCR	peQSTAR 2x Gradient	peQLab
qPCR	StepOnePlus Real-Time PCR System	AB Applied Biosystems
RNAseq Assessment of the	CASAVA v1.8.1	Illumina



quality of reads		
RNAseq Cluster detection and base calling	RTAv1.13	
RNAseq Differential Gene Expression	R package DESeq 2	
RNAseq Gene Expression	HTSeq version 0.5.3p3 2	
RNAseq Mapping against human genome	tophat version 2.0.11 1	
RNAseq Paired End Reads	Hiseq1500	illumina
SDS-PA gel electrophoresis	MINI-PROTEAN Tetra Systems gel running unit (552BR071005)	BIO-RAD
SDS-PA gel electrophoresis power supply	PowerPac basic (041BR 585 14)	BIO-RAD
Semi-Dry Western Blotting	TransBlot SD cell (221BR40878)	BIO-RAD
TransBlotTurbo Western Blotting	TransBlotTurbo transfer system (690BR008176)	BIO-RAD
X-ray film development	X-OMAT 2000 Processor	Kodak

### **5.2.3 Buffers and Premixed Solutions**

Table 4: Description of Buffers and Premixed Solutions

1% TBS (0.3M salt)	1,576g Tris-HCl, 3,5064g NaCl pH 7.4, 1 protease inhibitor (Roche), fill to 200ml with ddH <sub>2</sub> O
1% triton lysis buffer	Triton X-100 1%, 0.15M NaCl, 50mM Tris-HCl pH7.4, 5mM Na <sub>3</sub> VO <sub>4</sub> , 25mM NaF, 0,2% NP-40, 1mM EDTA pH8.0, 1M EGTA, 0.3%Na-deoxychoate, add protease inhibitor from Roche,adjust pH to 7.0.
10x LB medium for bacteria	10g tryptone, 5g yeast extract, 10g NaCl, fill to 1l with ddH <sub>2</sub> O
10x SDS-PAGE running buffer	Glycin 144g, Tris 30,3g, 10g SDS for 1liter
20x TBS and TBS-T	Tris base 120g, NaCl 320g, KCl 8g for 2liter, adjust pH to 7.6. For TBS-T add 0.1% Tween-20 to 1xTBS
4x Laemmli Western Blot sample buffer	For 10ml: 2.6ml ddH <sub>2</sub> O, 1ml β-mercaptoethanol, 0.01% bromphenol blue, 4ml Glycerol (86%), 0.8g SDS, 2.4ml 1M Tris pH6.8.
Coelenterazine buffer	0.4M K <sub>2</sub> HPO <sub>4</sub> , 0.4M KH <sub>2</sub> PO <sub>4</sub> , 0.5M NaCl, 1mM EDTA, adjust pH to 7.6
Glycylglycine buffer	glycylglycine 25mM, MgSO <sub>4</sub> 15mM, EGTA 4mM, adjust pH to 7.8
quenching buffer	50mM glycine (0,1877g) in 50ml PBS/CaCl <sub>2</sub> /MgCl <sub>2</sub> pH7.4
SDS-Page solution B	1.5M Tris-HCl, 0.4% SDS (pH 8.8)
SDS-Page solution C	0.5M Tris-HCl, 0.4% SDS (pH 6.8)



Semi Dry Western Blotting Buffer	25 mM Tris base (5.8g), 192 mM glycine pH 8.3 (2.9g), 0,037% SDS (0.37g), 20% Methanol (200 ml), make up to 1 liter with ddH <sub>2</sub> O
SOB medium and SOC medium	SOB medium: 2% Bactotryptone, 0.5% yeast extract, 10mM NaCl, 2,5mM KCl, 10mM MgCl, 10mM MgSO <sub>4</sub> . For SOC medium add 20mM glucose
Tris-HCl-MgCl <sub>2</sub> solution	25nM Tris-HCl, 2mM MgCl <sub>2</sub>

### **5.2.4 siRNA**

Table 5: Description of siRNAs

<u>Name siRNA</u>	<u>Target Sequence</u>	<u>Company</u>	<u>Catalog No.</u>
siGENOME Non-Targeting siRNA #3	AUG UAU UGG CCU GUA UUA G	Dharmacon, GE Healthcare	D-001210-03-20
siGlo Red		Dharmacon, GE Healthcare	D-001630-02-05
siGENOME Human LRP6 (4040), Set of 4, #1	CAG AUG AAC UGG AUU GUU A	Dharmacon, GE Healthcare	D-003845-02
siGENOME Human LRP6 (4040), Set of 4, #2	GAA CUA UGA UUC AGA ACC U	Dharmacon, GE Healthcare	D-003845-05
siGENOME Human LRP6 (4040), Set of 4, #3	CCA GGA AUG UCU CGA GGU A	Dharmacon, GE Healthcare	D-003845-21
siGENOME Human LRP6 (4040), Set of 4, #4	GCA GAU AUC AGA CGA AUU U	Dharmacon, GE Healthcare	D-003845-22
siGENOME Human B3GNT8, SMARTpool #1	GAC GAU GCC UUU GUA CAC A	Dharmacon, GE Healthcare	D-031757-04
siGENOME Human B3GNT8, SMARTpool #2	GCU GUU GGC CGU CAA GUC A	Dharmacon, GE Healthcare	D-031757-03
siGENOME Human B3GNT8, SMARTpool #3	GCA UUC GGC UCU GGA AAC A	Dharmacon, GE Healthcare	D-031757-02
siGENOME Human B3GNT8, SMARTpool #4	GGA GAG CCG UCG CUA CAG U	Dharmacon, GE Healthcare	D-031757-01

### 5.2.5 Antibodies

Table 6: Description of primary antibodies

<u>Antibody Name</u>	<u>Clone/Batch/Comment</u>	<u>Isotype</u>	<u>Company</u>	<u>Catalog No.</u>	<u>Dilution</u>
$\alpha$ -Axin1	C76H11	Rabbit	Cell Signaling	#2087	1:5000
$\alpha$ -B3GNT8	YLLLAVKSEPGRFAERQAVR, rabbit2	Rabbit	Custom made	-	1:500
$\alpha$ -EGFR	-	Rabbit	Merck Millipore	06-847	1:5000
$\alpha$ -Flag	M2	Mouse	Sigma	#F1804	1:5000
$\alpha$ -Flag	M2 Affinity Gel	-	Sigma-Aldrich	A2220	
$\alpha$ -GFP	-	-	-	-	1:10000
$\alpha$ -LRP6 Sp1490-CS	Wnt dependent	Rabbit	Cell Signaling	#2568	1:5000
$\alpha$ -LRP6 T1479	d61	Rabbit	Custom made	Davidson et al., 2005	1:5000
$\alpha$ -Myc	9E10	Mouse	-	-	1:20000
$\alpha$ -PCNA	PC10	mouse	Santa Cruz	sc-56	1:20000
$\alpha$ -Transferrin receptor	-	mouse	Invitrogen	#136800	1:20000
$\alpha$ -Tubulin	TU-02	Mouse	Santa Cruz	#sc8035	1:5000
$\alpha$ -V5	V5-10	Mouse	Sigma-Aldrich	#V8012	1:5000
$\alpha$ -Wnt3a	-	Rabbit	abcam	ab28472	1:3000

Table 7: Description of secondary antibodies

<u>Antibody Name</u>	<u>Isotype</u>	<u>Company</u>	<u>Catalog No.</u>	<u>Dilution</u>
Polyclonal Anti-Mouse Immunoglobulins/HRP	Goat	Dako Denmark A/S	P0447	1:2000
Polyclonal Anti-Rabbit Immunoglobulins/HRP	Goat	Dako Denmark A/S	P0448	1:2000

### 5.2.6 RNAseq - target genes of different pathways

Table 8: Description of target genes from different pathways

<u>Wnt signaling:</u>		<u>TGF-<math>\beta</math> signaling:</u>	
<u>Ensembl identifier:</u>	<u>HGNC name:</u>	<u>Ensembl identifier:</u>	<u>HGNC name:</u>
ENSG00000168646	AXIN2	ENSG00000142208	AKT1
ENSG00000110092	CCND1	ENSG00000130429	ARPC1B
ENSG00000039068	CDH1	ENSG00000198668	CALM3
ENSG00000125931	CITED1	ENSG00000070831	CDC42
ENSG00000163347	CLDN1	ENSG00000187498	COL4A1
ENSG00000176102	CSTF3	ENSG00000134871	COL4A2
ENSG00000125266	EFNB2	ENSG00000204262	COL5A2
ENSG00000134531	EMP1	ENSG00000072803	FBXW11
ENSG00000142227	EMP3	ENSG00000115414	FN1
ENSG00000171617	ENC1	ENSG00000150907	FOXO1
ENSG00000133216	EPHB2	ENSG00000172380	GNG12
ENSG00000115414	FN1	ENSG00000082701	GSK3B
ENSG00000115738	ID2	ENSG00000104812	GYS1
ENSG00000117318	ID3	ENSG00000185950	IRS2
ENSG00000101384	JAG1	ENSG00000091136	LAMB1
ENSG00000213626	LBH	ENSG00000172037	LAMB2
ENSG00000139292	LGR5	ENSG00000106683	LIMK1
ENSG00000157227	MMP14	ENSG00000197442	MAP3K5
ENSG00000087245	MMP2	ENSG00000142733	MAP3K6
ENSG00000120149	MSX2	ENSG00000147065	MSN
ENSG00000136997	MYC	ENSG00000120149	MSX2
ENSG00000007171	NOS2	ENSG00000136997	MYC
ENSG00000124813	RUNX2	ENSG00000119630	PGF
ENSG00000135587	SMPD2	ENSG00000077157	PPP1R12B
ENSG0000019549	SNAI2	ENSG00000113575	PPP2CA
ENSG00000041982	TNC	ENSG00000106617	PRKAG2
ENSG00000122691	TWIST1	ENSG00000188191	PRKAR1B
ENSG00000038427	VCAN	ENSG00000183943	PRKX
ENSG00000085563	ABCB1	ENSG00000136238	RAC1
ENSG00000089685	BIRC5	ENSG00000155903	RASA2
ENSG00000166167	BTRC	ENSG00000117676	RPS6KA1
ENSG00000142871	CYR61	ENSG00000177189	RPS6KA3
ENSG00000090776	EFNB1	ENSG00000141968	VAV1
ENSG00000136960	ENPP2	ENSG00000132142	ACACA
ENSG00000182580	EPHB3	ENSG00000135503	ACVR1B
ENSG00000102678	FGF9	ENSG00000117020	AKT3
ENSG00000177606	JUN	ENSG00000129675	ARHGEF6

ENSG00000072071	LPHN1		ENSG00000115966	ATF2
ENSG00000196628	TCF4		ENSG00000058404	CAMK2B
ENSG00000065717	TLE2		ENSG00000148660	CAMK2G
ENSG00000106829	TLE4		ENSG00000055130	CUL1
ENSG00000127863	TNFRSF19		ENSG00000159023	EPB41
ENSG00000173511	VEGFB		ENSG00000006607	FARP2
ENSG00000153487	ING1		ENSG00000120063	GNA13
			ENSG00000140443	IGF1R
			ENSG00000140575	IQGAP1
			ENSG00000077943	ITGA8
			ENSG00000144668	ITGA9
			ENSG00000177606	JUN
			ENSG00000061676	NCKAP1
			ENSG00000139174	PRICKLE1
			ENSG00000166501	PRKCB
			ENSG00000100504	PYGL
			ENSG00000141564	RPTOR
			ENSG00000148737	TCF7L2
			ENSG00000165699	TSC1

<u>MAPK signaling:</u>		<u>p53 signaling:</u>	
<u>Ensembl identifier:</u>	<u>HGNC name:</u>	<u>Ensembl identifier:</u>	<u>HGNC name:</u>
ENSG00000125845	BMP2	ENSG00000181026	AEN
ENSG00000163347	CLDN1	ENSG00000029534	ANK1
ENSG00000176971	FIBIN	ENSG00000100852	ARHGAP5
ENSG00000197892	KIF13B	ENSG00000162772	ATF3
ENSG00000119138	KLF9	ENSG00000173575	CHD2
ENSG00000186868	MAPT	ENSG00000147257	GPC3
ENSG00000099953	MMP11	ENSG00000150457	LATS2
ENSG00000168743	NPNT	ENSG00000049323	LTBP1
ENSG00000143878	RHOB	ENSG00000198625	MDM4
ENSG00000144136	SLC20A1	ENSG00000168288	MMADHC
ENSG00000157514	TSC22D3	ENSG00000138386	NAB1
ENSG00000187955	COL14A1	ENSG00000148200	NR6A1
ENSG00000175197	DDIT3	ENSG00000110048	OSBP
ENSG00000134769	DTNA	ENSG00000106443	PHF14
ENSG00000125968	ID1	ENSG00000080839	RBL1
ENSG00000115461	IGFBP5	ENSG00000138771	SHROOM3
ENSG00000130522	JUND	ENSG00000008294	SPAG9
ENSG00000131437	KIF3A	ENSG00000026025	VIM
ENSG00000157227	MMP14	ENSG00000170425	ADORA2B
ENSG00000135919	SERPINE2	ENSG00000141376	BCAS3

ENSG00000069702	TGFBR3	ENSG00000122786	CALD1
		ENSG00000124762	CDKN1A
		ENSG00000187498	COL4A1
		ENSG00000134574	DDB2
		ENSG00000168209	DDIT4
		ENSG00000050165	DKK3
		ENSG00000136048	DRAM1
		ENSG00000172071	EIF2AK3
		ENSG00000178568	ERBB4
		ENSG00000138685	FGF2
		ENSG00000120254	FTHFSDC1
		ENSG00000048052	HDAC9
		ENSG00000049130	KITLG
		ENSG00000049759	NEDD4L
		ENSG00000087303	NID2
		ENSG00000148400	NOTCH1
		ENSG00000132646	PCNA
		ENSG00000106617	PRKAG2
		ENSG00000132334	PTPRE
		ENSG00000151490	PTPRO
		ENSG00000185088	RPS27L
		ENSG00000048392	RRM2B
		ENSG00000089006	SNX5
		ENSG00000120889	TNFRSF10B
		ENSG00000153560	UBP1
		ENSG00000172667	WIG1
		ENSG00000154767	XPC
		ENSG00000181790	BAI1
		ENSG00000113328	CCNG1
		ENSG00000126001	CEP250
		ENSG00000115129	TP53I3
		ENSG00000182165	TP53TG1

<u>FGF signaling:</u>		<u>SHH signaling:</u>	
<u>Ensembl identifier:</u>	<u>HGNC name:</u>	<u>Ensembl identifier:</u>	<u>HGNC name:</u>
ENSG00000006468	ETV1	ENSG000000041982	TNC
ENSG000000054598	FOXC1	ENSG000000059804	SLC2A3
ENSG000000064042	LIMCH1	ENSG000000076258	FMO4
ENSG000000068028	RASSF1	ENSG00000102543	CDADC1
ENSG000000099194	SCD	ENSG00000107796	ACTA2
ENSG00000101361	MIR1292	ENSG00000110092	CCND1
ENSG00000101868	POLA1	ENSG00000111087	GLI1

ENSG00000102760	RGCC		ENSG00000140350	ANP32A
ENSG00000109534	GAR1		ENSG00000180730	SHISA2
ENSG00000111186	WNT5B		ENSG00000185551	NR2F2
ENSG00000120738	EGR1		ENSG00000185920	PTCH1
ENSG00000132623	ANKEF1			
ENSG00000136158	SPRY2			
ENSG00000136960	ENPP2			
ENSG00000148677	ANKRD1			
ENSG00000152078	TMEM56			
ENSG00000161800	RACGAP1			
ENSG00000166033	HTRA1			
ENSG00000171848	RRM2			
ENSG00000180817	PPA1			

### **5.2.7 qPCR primer**

Table 9: Description of qPCR primers

<u>Name</u>	<u>Sequence</u>
q-GAPDH-for	5'-CGA TTT CTC CTC CGG GTG AT-3'
q-GAPDH-rev	5'-GCC CAA TAC GAC CAA ATC AGA-3'
q-B3GNT8-for	5'-CCC TGA CTT CGC CTC CTA C-3'
q-B3GNT8-rev	5'-GGT CTT TGA GCG TCT GGT TGA-3'
q-LRP6-for	5'-TTT GGA TGG GAC AGA ACG GG-3'
q-LRP6-rev	5'-TCC GGT TAG CAC CTG AGA GA-3'

### **5.2.8 Plasmids**

Table 10: Description of plasmids used in this study

<u>Name:</u>	<u>Reference:</u>
ATF2-luciferase	
Axin1B-HA	Davidson et al., 2005
B3GNT2-ol-pCMV-Sport6.1	see: medaka cDNA library clone
B3GNT7-ol-pCMV-Sport6.1	see: medaka cDNA library clone
B3GNT8::FLAG-ol-pCS2+	cloned in this project
B3GNT8::tGFP-hs-pCMV6-AC-GFP	OriGene Technologies
B3GNT8-ol-pCMV-Sport6.1	see: medaka cDNA library clone
CK1 $\gamma$ 2-xt-pRKW2	Davidson et al., 2005
Dvl1-hs-pCS2+	Davidson et al., 2005
Frizzled5-V5	
GSK3 $\beta$ -myc-pCS2+	Zeng et al., 2005
LacZ-pCMV2	Davidson et al., 2005
LRP5-myc	Mao et al., 2002

LRP6 $\Delta$ E1-4-hs-FLAG-pCS2+	Davidson et al., 2005
LRP6::6myc-hs-pCS2+	Davidson et al., 2005
LRP6::mcherry-hs-pCS2+	Dörlich et al., 2015
LRP6 $\Delta$ C-myc-hs-pCS2+	
MESD2-mm-pCMV-Sport6.1	Davidson et al., 2005
pEGFP-N1	
pmTurquoise2-N1-golgi	Gift from Steffen Scholpp
pThymidin-Kinase-Renilla	Promega
Rab11	see: medaka cDNA library clone
Rab4	see: medaka cDNA library clone
Rab5	see: medaka cDNA library clone
TOPFLASH	Davidson et al., 2005
transmembrane-GSK3v2-hs	
V5-DKK3x1-xt-pCS	
Wnt3a-V5	
Wnt5a	
$\beta$ -catenin-xt	Davidson et al., 2005
medaka cDNA library clone	Chen et al., 2014

## References:

---

- Abrami, L., Kunz, B., Deuquet, J., Bafico, A., Davidson, G., & Van Der Goot, F. G. (2008). Functional interactions between anthrax toxin receptors and the WNT signalling protein LRP6. *Cellular microbiology*, 10(12), 2509-2519.
- Ahn, V. E., Chu, M. L. H., Choi, H. J., Tran, D., Abo, A., & Weis, W. I. (2011). Structural basis of Wnt signaling inhibition by Dickkopf binding to LRP5/6. *Developmental cell*, 21(5), 862-873.
- Akeboshi, H., Kasahara, Y., Tsuji, D., Itoh, K., Sakuraba, H., Chiba, Y., & Jigami, Y. (2009). Production of human  $\beta$ -hexosaminidase A with highly phosphorylated N-glycans by the overexpression of the *Ogataea minuta* MNN4 gene. *Glycobiology*, 19(9), 1002-1009.
- Alarcón, M. A., Medina, M. A., Hu, Q., Avila, M. E., Bustos, B. I., Pérez-Palma, E., ... & De Ferrari, G. V. (2013). A novel functional low-density lipoprotein receptor-related protein 6 gene alternative splice variant is associated with Alzheimer's disease. *Neurobiology of aging*, 34(6), 1709-e9.
- Anagnostou, S., & Shepherd, P. (2008). Glucose induces an autocrine activation of the Wnt/beta-catenin pathway in macrophage cell lines. *Biochem. J*, 416, 211-218.
- Anders, S., & Huber, W. (2010). Differential expression analysis for sequence count data. *Genome biology*, 11(10), R106.
- Angers, S., & Moon, R. T. (2009). Proximal events in Wnt signal transduction. *Nature reviews Molecular cell biology*, 10(7), 468-477.
- Baenziger, J. U. (1994). Protein-specific glycosyltransferases: how and why they do it!. *The FASEB journal*, 8(13), 1019-1025.
- Baenziger, J. U., & Green, E. D. (1988). Pituitary glycoprotein hormone oligosaccharides: structure, synthesis and function of the asparagine-linked oligosaccharides on lutropin, follitropin and thyrotropin. *Biochimica et Biophysica Acta (BBA)-Reviews on Biomembranes*, 947(2), 287-306.
- Bafico, A., Liu, G., Yaniv, A., Gazit, A., & Aaronson, S. A. (2001). Novel mechanism of Wnt signalling inhibition mediated by Dickkopf-1 interaction with LRP6/Arrow. *Nature cell biology*, 3(7), 683-686.
- Bannykh, S. I., Rowe, T., & Balch, W. E. (1996). The organization of endoplasmic reticulum export complexes. *The Journal of Cell Biology*, 135(1), 19-35.
- Bañó-Polo, M., Baldin, F., Tamborero, S., Marti-Renom, M. A., & Mingarro, I. (2011). N-glycosylation efficiency is determined by the distance to the C-terminus and the amino acid



preceding an Asn-Ser-Thr sequon. *Protein Science*, 20(1), 179-186.

Bieberich, E., MacKinnon, S., Silva, J., Li, D. D., Tencomnao, T., Irwin, L., ... & Yu, R. K. (2002). Regulation of ganglioside biosynthesis by enzyme complex formation of glycosyltransferases. *Biochemistry*, 41(38), 11479-11487.

Bilić, J., Huang, Y. L., Davidson, G., Zimmermann, T., Cruciat, C. M., Bienz, M., & Niehrs, C. (2007). Wnt induces LRP6 signalosomes and promotes dishevelled-dependent LRP6 phosphorylation. *Science*, 316(5831), 1619-1622.

Bironaite, D., Nesland, J. M., Dalen, H., Risberg, B., & Bryne, M. (2000). N-Glycans influence the in vitro adhesive and invasive behaviour of three metastatic cell lines. *Tumor biology*, 21(3), 165-175.

Bourhis, E., Tam, C., Franke, Y., Bazan, J. F., Ernst, J., Hwang, J., ... & Hannoush, R. N. (2010). Reconstitution of a frizzled8· Wnt3a· LRP6 signaling complex reveals multiple Wnt and Dkk1 binding sites on LRP6. *Journal of Biological Chemistry*, 285(12), 9172-9179.

Bourhis, E., Wang, W., Tam, C., Hwang, J., Zhang, Y., Spittler, D., ... & Cochran, A. G. (2011). Wnt antagonists bind through a short peptide to the first  $\beta$ -propeller domain of LRP5/6. *Structure*, 19(10), 1433-1442.

Boyce, M., Carrico, I. S., Ganguli, A. S., Yu, S. H., Hangauer, M. J., Hubbard, S. C., ... & Bertozzi, C. R. (2011). Metabolic cross-talk allows labeling of O-linked  $\beta$ -N-acetylglucosamine-modified proteins via the N-acetylgalactosamine salvage pathway. *Proceedings of the National Academy of Sciences*, 108(8), 3141-3146.

Brada, D., & DUBACH, U. C. (1984). Isolation of a homogeneous glucosidase II from pig kidney microsomes. *European journal of biochemistry*, 141(1), 149-156.

Bretscher, M. S., & Munro, S. (1993). Cholesterol and the Golgi apparatus. *Science*, 261(5126), 1280-1281.

Burda, P., & Aebi, M. (1999). The dolichol pathway of N-linked glycosylation. *Biochimica et Biophysica Acta (BBA)-General Subjects*, 1426(2), 239-257.

Burns, D. M., & Touster, O. (1982). Purification and characterization of glucosidase II, an endoplasmic reticulum hydrolase involved in glycoprotein biosynthesis. *Journal of Biological Chemistry*, 257(17), 9991-10000.

Chavan, M., & Lennarz, W. (2006). The molecular basis of coupling of translocation and N-glycosylation. *Trends in biochemical sciences*, 31(1), 17-20.

Chen, D., Bhat-Nakshatri, P., Goswami, C., Badve, S., & Nakshatri, H. (2013). ANTXR1, a stem cell-enriched functional biomarker, connects collagen signaling to cancer stem-like cells and metastasis in breast cancer. *Cancer research*, 73(18), 5821-5833.

Chen, J., Liu, C. C., Li, Q., Nowak, C., Bu, G., & Wang, J. (2011). Two structural and functional domains of MESD required for proper folding and trafficking of LRP5/6. *Structure*, 19(3), 313-323.

Chen, M., Philipp, M., Wang, J., Premont, R. T., Garrison, T. R., Caron, M. G., ... & Chen, W. (2009). G Protein-coupled receptor kinases phosphorylate LRP6 in the Wnt pathway. *Journal of Biological Chemistry*, 284(50), 35040-35048.

Chen, Q., Su, Y., Wesslowski, J., Hagemann, A. I., Ramialison, M., Wittbrodt, J., ... & Davidson, G. (2014). Tyrosine phosphorylation of LRP6 by Src and Fer inhibits Wnt/ $\beta$ -catenin signalling. *EMBO reports*, e201439644.

Cheng, Z., Biechele, T., Wei, Z., Morrone, S., Moon, R. T., Wang, L., & Xu, W. (2011). Crystal structures of the extracellular domain of LRP6 and its complex with DKK1. *Nature structural & molecular biology*, 18(11), 1204-1210.

Cheng, Z., Biechele, T., Wei, Z., Morrone, S., Moon, R. T., Wang, L., & Xu, W. (2011). Crystal structures of the extracellular domain of LRP6 and its complex with DKK1. *Nature structural & molecular biology*, 18(11), 1204-1210.

Clevers, H. (2006). Wnt/ $\beta$ -catenin signaling in development and disease. *Cell*, 127(3), 469-480.

Cole, S. R., Ashman, L. K., & Ey, P. L. (1987). Biotinylation: an alternative to radioiodination for the identification of cell surface antigens in immunoprecipitates. *Molecular immunology*, 24(7), 699-705.

Cong, F., Schweizer, L., & Varmus, H. (2004). Wnt signals across the plasma membrane to activate the  $\beta$ -catenin pathway by forming oligomers containing its receptors, Frizzled and LRP. *Development*, 131(20), 5103-5115.

Culi, J., & Mann, R. S. (2003). Boca, an endoplasmic reticulum protein required for wingless signaling and trafficking of LDL receptor family members in *Drosophila*. *Cell*, 112(3), 343-354.

Culi, J., Springer, T. A., & Mann, R. S. (2004). Boca-dependent maturation of  $\beta$ -propeller/EGF modules in low-density lipoprotein receptor proteins. *The EMBO journal*, 23(6), 1372-1380.

Dann, C. E., Hsieh, J. C., Rattner, A., Sharma, D., Nathans, J., & Leahy, D. J. (2001). Insights into Wnt binding and signalling from the structures of two Frizzled cysteine-rich domains. *Nature*, 412(6842), 86-90.

Dasgupta, R., Kaykas, A., Moon, R. T., & Perrimon, N. (2005). Functional genomic analysis of the Wnt-wingless signaling pathway. *Science*, 308(5723), 826-833.

Davidson, G. (2010). The cell cycle and Wnt. *Cell Cycle*, 9(9), 1667-1668.

Davidson, G., Shen, J., Huang, Y. L., Su, Y., Karaulanov, E., Bartscherer, K., ... & Niehrs, C. (2009). Cell cycle control of wnt receptor activation. *Developmental cell*, 17(6), 788-799.

Davidson, G., Wu, W., Shen, J., Bilic, J., Fenger, U., Stannek, P., ... & Niehrs, C. (2005). Casein kinase 1  $\gamma$  couples Wnt receptor activation to cytoplasmic signal transduction. *Nature*, 438(7069), 867-872.

de Graffenried, C. L., & Bertozzi, C. R. (2004). The stem region of the sulfotransferase GlcNAc6ST-1 is a determinant of substrate specificity. *Journal of Biological Chemistry*, 279(38), 40035-40043.

Dell, A., Galadari, A., Sastre, F., & Hitchen, P. (2011). Similarities and differences in the glycosylation mechanisms in prokaryotes and eukaryotes. *International journal of microbiology*, 2010.

Demetriou, M., Granovsky, M., Quaggin, S., & Dennis, J. W. (2001). Negative regulation of T-cell activation and autoimmunity by Mgat5 N-glycosylation. *Nature*, 409(6821), 733-739.

Demir, K., Kirsch, N., Beretta, C. A., Erdmann, G., Ingelfinger, D., Moro, E., ... & Boutros, M. (2013). RAB8B is required for activity and caveolar endocytosis of LRP6. *Cell reports*, 4(6), 1224-1234.

Dennis, J. W., & Laferte, S. (1987). Tumor cell surface carbohydrate and the metastatic phenotype. *Cancer and Metastasis Reviews*, 5(3), 185-204.

Dennis, J. W., Laferte, S., & Vanderelst, I. (1989). Asparagine-linked oligosaccharides in malignant tumour growth. *Biochemical Society transactions*, 17(1), 29-31.

Dennis, J. W., Laferte, S., Waghorne, C., Breitman, M. L., & Kerbel, R. S. (1987). Beta 1-6 branching of Asn-linked oligosaccharides is directly associated with metastasis. *Science*, 236(4801), 582-585.

Dobrowolski, R., Vick, P., Ploper, D., Gumper, I., Snitkin, H., Sabatini, D. D., & De Robertis, E. M. (2012). Presenilin deficiency or lysosomal inhibition enhances Wnt signaling through relocalization of GSK3 to the late-endosomal compartment. *Cell reports*, 2(5), 1316-1328.

Dörlich, R. M., Chen, Q., Hedde, P. N., Schuster, V., Hippler, M., Wesslowski, J., ... & Nienhaus, G. U. (2015). Dual-color dual-focus line-scanning FCS for quantitative analysis of receptor-ligand interactions in living specimens. *Scientific reports*, 5.

Dong, Y., Lathrop, W., Weaver, D., Qiu, Q., Cini, J., Bertolini, D., & Chen, D. (1998). Molecular cloning and characterization of LR3, a novel LDL receptor family protein with mitogenic activity. *Biochemical and biophysical research communications*, 251(3), 784-790.

Doubravskaya, L., Krausova, M., Gradl, D., Vojtechova, M., Tumova, L., Lukas, J., ... & Korinek, V. (2011). Fatty acid modification of Wnt1 and Wnt3a at serine is prerequisite for lipidation at cysteine and is essential for Wnt signalling. *Cellular signalling*, 23(5), 837-848.

Drickamer, K. & Taylor, M. E. (2011). *Introduction to glycobiology*. Oxford university press.

Eckert, V., Blank, M., Mazhari-Tabrizi, R., Mumberg, D., Funk, M., & Schwarz, R. T. (1998). Cloning and functional expression of the human GlcNAc-1-P transferase, the enzyme for the committed step of the dolichol cycle, by heterologous complementation in *Saccharomyces cerevisiae*. *Glycobiology*, 8(1), 77-85.

Ellgaard, L., & Helenius, A. (2003). Quality control in the endoplasmic reticulum. *Nature reviews Molecular cell biology*, 4(3), 181-191.

Ettenberg, S. A., Charlat, O., Daley, M. P., Liu, S., Vincent, K. J., Stuart, D. D., ... & Cong, F. (2010). Inhibition of tumorigenesis driven by different Wnt proteins requires blockade of distinct ligand-binding regions by LRP6 antibodies. *Proceedings of the National Academy of Sciences*, 107(35), 15473-15478.

Fan, J. Y., Roth, J., & Zuber, C. (2003). Ultrastructural analysis of transitional endoplasmic reticulum and pre-Golgi intermediates: a highway for cars and trucks. *Histochemistry and cell biology*, 120(6), 455-463.

Fuerer, C., Habib, S. J., & Nusse, R. (2010). A study on the interactions between heparan sulfate proteoglycans and Wnt proteins. *Developmental Dynamics*, 239(1), 184-190.

Gabius, H. J. (Ed.). (2011). *The sugar code: fundamentals of glycosciences*. John Wiley & Sons.

Gao, C., & Chen, Y. G. (2010). Dishevelled: The hub of Wnt signaling. *Cellular signalling*, 22(5), 717-727.

Garner, O. B., & Baum, L. G. (2008). Galectin-glycan lattices regulate cell-surface glycoprotein organization and signalling. *Biochemical Society Transactions*, 36(Pt 6), 1472.

Gatenby, R. A., & Gillies, R. J. (2004). Why do cancers have high aerobic glycolysis?. *Nature Reviews Cancer*, 4(11), 891-899.

Geisler, C., & Jarvis, D. L. (2011). Letter to the Glyco-Forum: Effective glycoanalysis with *Maackia amurensis* lectins requires a clear understanding of their binding specificities. *Glycobiology*, 21(8), 988-993.

Giraud, C. G., & Maccioni, H. J. (2003). Endoplasmic reticulum export of glycosyltransferases depends on interaction of a cytoplasmic dibasic motif with Sar1. *Molecular biology of the Cell*, 14(9), 3753-3766.

Giraud, C. G., Daniotti, J. L., & Maccioni, H. J. (2001). Physical and functional association of glycolipid N-acetyl-galactosaminyl and galactosyl transferases in the Golgi apparatus. *Proceedings of the National Academy of Sciences*, 98(4), 1625-1630.

Gordon, M. D., & Nusse, R. (2006). Wnt signaling: multiple pathways, multiple receptors, and multiple transcription factors. *Journal of Biological Chemistry*, 281(32), 22429-22433.

Granovsky, M., Fata, J., Pawling, J., Muller, W. J., Khokha, R., & Dennis, J. W. (2000). Suppression of tumor growth and metastasis in *Mgat5*-deficient mice. *Nature medicine*, 6(3),

306-312.

Gray, J. D., Kholmanskikh, S., Castaldo, B. S., Hansler, A., Chung, H., Klotz, B., ... & Ross, M. E. (2013). LRP6 exerts non-canonical effects on Wnt signaling during neural tube closure. *Human molecular genetics*, 22(21), 4267-4281.

Gross, J. C., & Boutros, M. (2013). Secretion and extracellular space travel of Wnt proteins. *Current opinion in genetics & development*, 23(4), 385-390.

Gross, J. C., Chaudhary, V., Bartscherer, K., & Boutros, M. (2012). Active Wnt proteins are secreted on exosomes. *Nature cell biology*, 14(10), 1036-1045.

Guo, H., Nagy, T., & Pierce, M. (2014). Post-translational Glycoprotein Modifications Regulate Colon Cancer Stem Cells and Colon Adenoma Progression in *Apcmin/+* Mice through Altered Wnt Receptor Signaling. *Journal of Biological Chemistry*, 289(45), 31534-31549.

Gustavson, Mark D., et al. "Tcf binding sequence and position determines  $\beta$ -catenin and Lef-1 responsiveness of MMP-7 promoters." *Molecular carcinogenesis* 41.3 (2004): 125-139.

Gut, A., Kappeler, F., Hyka, N., Balda, M. S., Hauri, H. P., & Matter, K. (1998). Carbohydrate-mediated Golgi to cell surface transport and apical targeting of membrane proteins. *The EMBO Journal*, 17(7), 1919-1929.

Hagemann, A. I., Kurz, J., Kauffeld, S., Chen, Q., Reeves, P. M., Weber, S., ... & Scholpp, S. (2014). In vivo analysis of formation and endocytosis of the Wnt/ $\beta$ -Catenin signaling complex in zebrafish embryos. *Journal of cell science*, 127(18), 3970-3982.

Hammond, C., Braakman, I., & Helenius, A. (1994). Role of N-linked oligosaccharide recognition, glucose trimming, and calnexin in glycoprotein folding and quality control. *Proceedings of the National Academy of Sciences*, 91(3), 913-917.

Hao, H. X., Xie, Y., Zhang, Y., Charlat, O., Oster, E., Avello, M., ... & Cong, F. (2012). ZNRF3 promotes Wnt receptor turnover in an R-spondin-sensitive manner. *Nature*, 485(7397), 195-200.

Harvey, D. J. (2005). Proteomic analysis of glycosylation: structural determination of N- and O-linked glycans by mass spectrometry. *Expert review of proteomics*, 2(1), 87-101.

He, T. C., Sparks, A. B., Rago, C., Hermeking, H., Zawel, L., da Costa, L. T., ... & Kinzler, K. W. (1998). Identification of c-MYC as a target of the APC pathway. *Science*, 281(5382), 1509-1512.

He, X., Semenov, M., Tamai, K., & Zeng, X. (2004). LDL receptor-related proteins 5 and 6 in Wnt/ $\beta$ -catenin signaling: arrows point the way. *Development*, 131(8), 1663-1677.

Hebert, D. N., Foellmer, B., & Helenius, A. (1995). Glucose trimming and reglucosylation determine glycoprotein association with calnexin in the endoplasmic reticulum. *Cell*, 81(3), 425-433.

- HETTKAMP, H., LEGLER, G., & BAUSE, E. (1984). Purification by affinity chromatography of glucosidase I, an endoplasmic reticulum hydrolase involved in the processing of asparagine-linked oligosaccharides. *European Journal of Biochemistry*, 142(1), 85-90.
- Hey, P. J., Twells, R. C., Phillips, M. S., Nakagawa, Y., Brown, S. D., Kawaguchi, Y., ... & Hess, J. F. (1998). Cloning of a novel member of the low-density lipoprotein receptor family. *Gene*, 216(1), 103-111.
- Hinderlich, S., Berger, M., Schwarzkopf, M., Effertz, K., & Reutter, W. (2000). Molecular cloning and characterization of murine and human N-acetylglucosamine kinase. *European Journal of Biochemistry*, 267(11), 3301-3308.
- Hiruma, T., Togayachi, A., Okamura, K., Sato, T., Kikuchi, N., Kwon, Y. D., ... & Narimatsu, H. (2004). GLYCOBIOLOGY AND EXTRACELLULAR MATRICES-A Novel Human b1, 3-N-Acetylgalactosaminyltransferase That Synthesizes a Unique Carbohydrate Structure, GalNAc1-3GlcNAc. *Journal of Biological Chemistry*, 279(14), 14087-14095.
- Holden, H. M., Rayment, I., & Thoden, J. B. (2003). Structure and function of enzymes of the Leloir pathway for galactose metabolism. *Journal of Biological Chemistry*, 278(45), 43885-43888.
- Holdsworth, G., Slocombe, P., Doyle, C., Sweeney, B., Veverka, V., Le Riche, K., ... & Robinson, M. K. (2012). Characterization of the interaction of sclerostin with the low density lipoprotein receptor-related protein (LRP) family of Wnt co-receptors. *Journal of Biological Chemistry*, 287(32), 26464-26477.
- Holmen, S. L., Giambernardi, T. A., Zylstra, C. R., Buckner-Berghuis, B. D., Resau, J. H., Hess, J. F., ... & Williams, B. O. (2004). Decreased BMD and limb deformities in mice carrying mutations in both *Lrp5* and *Lrp6*. *Journal of Bone and Mineral Research*, 19(12), 2033-2040.
- Houston, D. W., & Wylie, C. (2002). Cloning and expression of *Xenopus Lrp5* and *Lrp6* genes. *Mechanisms of development*, 117(1), 337-342.
- Hsieh, J. C., Lee, L., Zhang, L., Wefer, S., Brown, K., DeRossi, C., ... & Holdener, B. C. (2003). *Mesd* encodes an LRP5/6 chaperone essential for specification of mouse embryonic polarity. *Cell*, 112(3), 355-367.
- Hua, D., Qin, F., Shen, L., Jiang, Z., Zou, S. T., Xu, L., ... & Wu, S. L. (2012).  $\beta$ 3GnT8 regulates laryngeal carcinoma cell proliferation via targeting MMPs/TIMPs and TGF- $\beta$ 1. *Asian Pacific Journal of Cancer Prevention*, 13(5), 2087-2093.
- Hwajin, J., Suk, K. L., & Eek-hoon, J. (2011). *Mest/Peg1* inhibits Wnt signalling through regulation of LRP6 glycosylation. *Biochemical Journal*, 436(2), 263-269.
- Ihara, S., Miyoshi, E., Ko, J. H., Murata, K., Nakahara, S., Honke, K., ... & Taniguchi, N. (2002). Prometastatic Effect of N-Acetylglucosaminyltransferase V Is Due to Modification and Stabilization of Active Matriptase by Adding  $\beta$ 1-6 GlcNAc Branching. *Journal of Biological Chemistry*, 277(19), 16960-16967.



- Ishida, H., Togayachi, A., Sakai, T., Iwai, T., Hiruma, T., Sato, T., ... & Narimatsu, H. (2005). A novel  $\beta$ 1, 3-N-acetylglucosaminyltransferase ( $\beta$ 3Gn-T8), which synthesizes poly-N-acetyllactosamine, is dramatically upregulated in colon cancer. *FEBS letters*, 579(1), 71-78.
- Itasaki, N., Jones, C. M., Mercurio, S., Rowe, A., Domingos, P. M., Smith, J. C., & Krumlauf, R. (2003). Wise, a context-dependent activator and inhibitor of Wnt signalling. *Development*, 130(18), 4295-4305.
- Iwai, T., Inaba, N., Naundorf, A., Zhang, Y., Gotoh, M., Iwasaki, H., ... & Narimatsu, H. (2002). Molecular cloning and characterization of a novel UDP-GlcNAc: GalNAc-peptide  $\beta$ 1, 3-N-acetylglucosaminyltransferase ( $\beta$ 3Gn-T6), an enzyme synthesizing the core 3 structure of O-glycans. *Journal of Biological Chemistry*, 277(15), 12802-12809.
- Jamal, B., Sengupta, P. K., Gao, Z. N., Nita-Lazar, M., Amin, B., Jalisi, S., ... & Kukuruzinska, M. A. (2012). Aberrant amplification of the crosstalk between canonical Wnt signaling and N-glycosylation gene DPAGT1 promotes oral cancer. *Oral oncology*, 48(6), 523-529.
- Janda, C. Y., Waghray, D., Levin, A. M., Thomas, C., & Garcia, K. C. (2012). Structural basis of Wnt recognition by Frizzled. *Science*, 337(6090), 59-64.
- Joiner, D. M., Ke, J., Zhong, Z., Xu, H. E., & Williams, B. O. (2013). LRP5 and LRP6 in development and disease. *Trends in Endocrinology & Metabolism*, 24(1), 31-39.
- Jung, H., Suk, K. L., & Eek-hoon, J. (2011). Mest/Peg1 inhibits Wnt signalling through regulation of LRP6 glycosylation. *Biochemical Journal*, 436(2), 263-269.
- Jungmann, J., & Munro, S. (1998). Multi-protein complexes in the cis Golgi of *Saccharomyces cerevisiae* with  $\alpha$ -1, 6-mannosyltransferase activity. *The EMBO Journal*, 17(2), 423-434.
- Jungmann, J., Rayner, J. C., & Munro, S. (1999). The *Saccharomyces cerevisiae* protein Mnn10p/Bed1p is a subunit of a Golgi mannosyltransferase complex. *Journal of Biological Chemistry*, 274(10), 6579-6585.
- Kagermeier-Schenk, B., Wehner, D., Özhan-Kizil, G., Yamamoto, H., Li, J., Kirchner, K., ... & Weidinger, G. (2011). Waif1/5T4 inhibits Wnt/ $\beta$ -catenin signaling and activates noncanonical Wnt pathways by modifying LRP6 subcellular localization. *Developmental cell*, 21(6), 1129-1143.
- Kalz-Füller, B., Bieberich, E., & Bause, E. (1995). Cloning and expression of glucosidase I from human hippocampus. *European Journal of Biochemistry*, 231(2), 344-351.
- Kataoka, K., & Huh, N. H. (2002). A novel  $\beta$ 1, 3-N-acetylglucosaminyltransferase involved in invasion of cancer cells as assayed in vitro. *Biochemical and biophysical research communications*, 294(4), 843-848.
- Kato, M., Patel, M. S., Levasseur, R., Lobov, I., Chang, B. H. J., Glass, D. A., ... & Chan, L. (2002). Cbfa1-independent decrease in osteoblast proliferation, osteopenia, and persistent embryonic eye vascularization in mice deficient in Lrp5, a Wnt coreceptor. *The Journal of cell biology*,

157(2), 303-314.

Kelleher, D. J., & Gilmore, R. (2006). An evolving view of the eukaryotic oligosaccharyltransferase. *Glycobiology*, 16(4), 47R-62R.

Kelly, O. G., Pinson, K. I., & Skarnes, W. C. (2004). The Wnt co-receptors Lrp5 and Lrp6 are essential for gastrulation in mice. *Development*, 131(12), 2803-2815.

Keramati, A. R., Liu, W., Nottoli, T., Faramarzi, S., Tellides, G., & Mani, A. (2009). The Cell Proliferative Effect of LRP6 Mutation is Mediated by Increased PDGF Dependent Cyclin D1 Expression. *Circulation*, 120(18 Supplement), S1097.

Khan, Z., Vijayakumar, S., de la Torre, T. V., Rotolo, S., & Bafico, A. (2007). Analysis of endogenous LRP6 function reveals a novel feedback mechanism by which Wnt negatively regulates its receptor. *Molecular and cellular biology*, 27(20), 7291-7301.

Kikuchi, A., Yamamoto, H., & Sato, A. (2009). Selective activation mechanisms of Wnt signaling pathways. *Trends in cell biology*, 19(3), 119-129.

Kim, I., Pan, W., Jones, S. A., Zhang, Y., Zhuang, X., & Wu, D. (2013). Clathrin and AP2 are required for PtdIns (4, 5) P2-mediated formation of LRP6 signalosomes. *The Journal of cell biology*, 200(4), 419-428.

Kim, S. E., Huang, H., Zhao, M., Zhang, X., Zhang, A., Semonov, M. V., ... & He, X. (2013). Wnt stabilization of  $\beta$ -catenin reveals principles for morphogen receptor-scaffold assemblies. *Science*, 340(6134), 867-870.

KOBATA, A. (1989). Altered glycosylation of surface glycoproteins in tumor cells and its clinical application. *Pigment Cell Research*, 2(4), 304-308.

Koduri, V., Blacklow, S. C. (2007). Requirement for natively unstructured regions of mesoderm development candidate 2 in promoting low-density lipoprotein receptor-related protein 6 maturation. *Biochemistry* 46:6570–6577.

Komekado, H., Yamamoto, H., Chiba, T., & Kikuchi, A. (2007). Glycosylation and palmitoylation of Wnt-3a are coupled to produce an active form of Wnt-3a. *Genes to Cells*, 12(4), 521-534.

König, H., & Müller, F. (2008). Minor splicing: Nuclear dogma still in question. *Proceedings of the National Academy of Sciences*.

König, H., Matter, N., Bader, R., Thiele, W., & Müller, F. (2007). Splicing segregation: the minor spliceosome acts outside the nucleus and controls cell proliferation. *Cell*, 131(4), 718-729.

Koo, B. K., Spit, M., Jordens, I., Low, T. Y., Stange, D. E., van de Wetering, M., ... & Clevers, H. (2012). Tumour suppressor RNF43 is a stem-cell E3 ligase that induces endocytosis of Wnt receptors. *Nature*, 488(7413), 665-669.

Kornfeld, R., & Kornfeld, S. (1985). Assembly of asparagine-linked oligosaccharides. *Annual*



review of biochemistry, 54(1), 631-664.

Kurayoshi, M., Yamamoto, H., Izumi, S., & Kikuchi, A. (2007). Post-translational palmitoylation and glycosylation of Wnt-5a are necessary for its signalling. *Biochem. J*, 402, 515-523.

Lau, K. S., & Dennis, J. W. (2008). N-Glycans in cancer progression. *Glycobiology*, 18(10), 750-760.

Lau, K. S., Partridge, E. A., Grigorian, A., Silvescu, C. I., Reinhold, V. N., Demetriou, M., & Dennis, J. W. (2007). Complex N-glycan number and degree of branching cooperate to regulate cell proliferation and differentiation. *Cell*, 129(1), 123-134.

Lee, L. Y., Lin, C. H., Fanayan, S., Packer, N. H., & Thaysen-Andersen, M. (2014). Differential site accessibility mechanistically explains subcellular-specific N-glycosylation determinants. *Frontiers in immunology*, 5.

Leymarie, N., & Zaia, J. (2012). Effective use of mass spectrometry for glycan and glycopeptide structural analysis. *Analytical chemistry*, 84(7), 3040-3048.

Li, V. S., Ng, S. S., Boersema, P. J., Low, T. Y., Karthaus, W. R., Gerlach, J. P., ... & Clevers, H. (2012). Wnt signaling through inhibition of  $\beta$ -catenin degradation in an intact Axin1 complex. *Cell*, 149(6), 1245-1256.

Li, Y., Chen, J., Lu, W., McCormick, L. M., Wang, J., & Bu, G. (2005). Mesd binds to mature LDL-receptor-related protein-6 and antagonizes ligand binding. *Journal of cell science*, 118(22), 5305-5314.

Li, Y., Lu, W., He, X., Bu, G. (2006). Modulation of LRP6-mediated Wnt signaling by molecular chaperone Mesd. *FEBS Lett* 580:5423–5428.

Lin, L., Huang, Q. X., Yang, S. S., Chu, J., Wang, J. Z., & Tian, Q. (2013). Melatonin in Alzheimer's disease. *International journal of molecular sciences*, 14(7), 14575-14593.

Liu, C. C., Pearson, C., & Bu, G. (2009). Cooperative folding and ligand-binding properties of LRP6  $\beta$ -propeller domains. *Journal of Biological Chemistry*, 284(22), 15299-15307.

Liu, C. C., Prior, J., Piwnica-Worms, D., & Bu, G. (2010). LRP6 overexpression defines a class of breast cancer subtype and is a target for therapy. *Proceedings of the National Academy of Sciences*, 107(11), 5136-5141.

Liu, C. C., Tsai, C. W., Deak, F., Rogers, J., Penuliar, M., Sung, Y. M., ... & Bu, G. (2014). Deficiency in LRP6-mediated Wnt signaling contributes to synaptic abnormalities and amyloid pathology in Alzheimer's disease. *Neuron*, 84(1), 63-77.

Liu, C., Li, Y., Semenov, M., Han, C., Baeg, G. H., Tan, Y., ... & He, X. (2002). Control of  $\beta$ -catenin phosphorylation/degradation by a dual-kinase mechanism. *Cell*, 108(6), 837-847.

- Liu, Y., Choudhury, P., Cabral, C. M., & Sifers, R. N. (1999). Oligosaccharide modification in the early secretory pathway directs the selection of a misfolded glycoprotein for degradation by the proteasome. *Journal of Biological Chemistry*, 274(9), 5861-5867.
- Lucocq, J. M., Brada, D., & Roth, J. (1986). Immunolocalization of the oligosaccharide trimming enzyme glucosidase II. *The Journal of cell biology*, 102(6), 2137-2146.
- Lustig, B., Jerchow, B., Sachs, M., Weiler, S., Pietsch, T., Karsten, U., ... & Behrens, J. (2002). Negative feedback loop of Wnt signaling through upregulation of conductin/axin2 in colorectal and liver tumors. *Molecular and cellular biology*, 22(4), 1184-1193.
- MacDonald, B. T., & He, X. (2012). Frizzled and LRP5/6 receptors for Wnt/ $\beta$ -catenin signaling. *Cold Spring Harbor perspectives in biology*, 4(12), a007880.
- Machamer, C. E. (1991). Golgi retention signals: do membranes hold the key?. *Trends in cell biology*, 1(6), 141-144.
- Manzella, S. M., Hooper, L. V., & Baenziger, J. U. (1996). Oligosaccharides containing  $\beta$ 1, 4-linked N-acetylgalactosamine, a paradigm for protein-specific glycosylation. *Journal of Biological Chemistry*, 271(21), 12117-12120.
- Mao, B., Wu, W., Davidson, G., Marhold, J., Li, M., Mechler, B. M., ... & Niehrs, C. (2002). Kremen proteins are Dickkopf receptors that regulate Wnt/ $\beta$ -catenin signalling. *Nature*, 417(6889), 664-667.
- Mao, B., Wu, W., Li, Y., Hoppe, D., Stannek, P., Glinka, A., & Niehrs, C. (2001). LDL-receptor-related protein 6 is a receptor for Dickkopf proteins. *Nature*, 411(6835), 321-325.
- Mason, J. O., Kitajewski, J., & Varmus, H. E. (1992). Mutational analysis of mouse Wnt-1 identifies two temperature-sensitive alleles and attributes of Wnt-1 protein essential for transformation of a mammary cell line. *Molecular biology of the cell*, 3(5), 521-533.
- McCormick, C., Duncan, G., Goutsos, K. T., & Tufaro, F. (2000). The putative tumor suppressors EXT1 and EXT2 form a stable complex that accumulates in the Golgi apparatus and catalyzes the synthesis of heparan sulfate. *Proceedings of the National Academy of Sciences*, 97(2), 668-673.
- Mellquist, J. L., Kasturi, L., Spitalnik, S. L., & Shakin-Eshleman, S. H. (1998). The amino acid following an asn-X-Ser/Thr sequon is an important determinant of N-linked core glycosylation efficiency. *Biochemistry*, 37(19), 6833-6837.
- Mi, H., Muruganujan, A., Casagrande, J. T., & Thomas, P. D. (2013). Large-scale gene function analysis with the PANTHER classification system. *Nature protocols*, 8(8), 1551-1566.
- Milewski, S. (2002). Glucosamine-6-phosphate synthase—the multi-facets enzyme. *Biochimica et Biophysica Acta (BBA)-Protein Structure and Molecular Enzymology*, 1597(2), 173-192.

Milhem, R. M., Ben-Salem, S., Al-Gazali, L., & Ali, B. R. (2014). Identification of the cellular mechanisms that modulate trafficking of frizzled family receptor 4 (FZD4) missense mutants associated with familial exudative vitreoretinopathy. *Invest Ophthalmol Vis Sci*, 55(6), 3423-3431.

Mitra, K., Ubarretxena-Belandia, I., Taguchi, T., Warren, G., & Engelman, D. M. (2004). Modulation of the bilayer thickness of exocytic pathway membranes by membrane proteins rather than cholesterol. *Proceedings of the National Academy of Sciences*, 101(12), 4083-4088.

Moremen, K. W. (2002). Golgi  $\alpha$ -mannosidase II deficiency in vertebrate systems: implications for asparagine-linked oligosaccharide processing in mammals. *Biochimica et Biophysica Acta (BBA)-General Subjects*, 1573(3), 225-235.

Mouquet, H., Scharf, L., Euler, Z., Liu, Y., Eden, C., Scheid, J. F., ... & Bjorkman, P. J. (2012). Complex-type N-glycan recognition by potent broadly neutralizing HIV antibodies. *Proceedings of the National Academy of Sciences*, 109(47), E3268-E3277.

Mulligan, K. A., Fuerer, C., Ching, W., Fish, M., Willert, K., & Nusse, R. (2012). Secreted Wingless-interacting molecule (Swim) promotes long-range signaling by maintaining Wingless solubility. *Proceedings of the National Academy of Sciences*, 109(2), 370-377.

Nabi, I. R., & Rodriguez-Boulan, E. (1993). Increased LAMP-2 poly(lactosamine) glycosylation is associated with its slower Golgi transit during establishment of a polarized MDCK epithelial monolayer. *Molecular biology of the cell*, 4(6), 627-635.

Naito, A. T., Sumida, T., Nomura, S., Liu, M. L., Higo, T., Nakagawa, A., ... & Komuro, I. (2012). Complement C1q activates canonical Wnt signaling and promotes aging-related phenotypes. *Cell*, 149(6), 1298-1313.

Nakagawa, H., Wakabayashi-Nakao, K., Tamura, A., Toyoda, Y., Koshihara, S., & Ishikawa, T. (2009). Disruption of N-linked glycosylation enhances ubiquitin-mediated proteasomal degradation of the human ATP-binding cassette transporter ABCG2. *FEBS journal*, 276(24), 7237-7252.

Nakaishi, Y., Bando, M., Shimizu, H., Watanabe, K., Goto, F., Tsuge, H., ... & Komatsu, M. (2009). Structural analysis of human glutamine: fructose-6-phosphate amidotransferase, a key regulator in type 2 diabetes. *FEBS letters*, 583(1), 163-167.

Nie, S., Lo, A., Zhu, J., Wu, J., Ruffin, M. T., & Lubman, D. M. (2013). Isobaric protein-level labeling strategy for serum glycoprotein quantification analysis by liquid chromatography-tandem mass spectrometry. *Analytical chemistry*, 85(11), 5353-5357.

Niehrs, C. (2004). Regionally specific induction by the Spemann-Mangold organizer. *Nature Reviews Genetics*, 5(6), 425-434.

Niehrs, C. (2012). The complex world of WNT receptor signalling. *Nature reviews Molecular cell biology*, 13(12), 767-779.

- Niehers, C., & Shen, J. (2010). Regulation of Lrp6 phosphorylation. *Cellular and Molecular Life Sciences*, 67(15), 2551-2562.
- Nilsson, T., & Warren, G. (1994). Retention and retrieval in the endoplasmic reticulum and the Golgi apparatus. *Current opinion in cell biology*, 6(4), 517-521.
- Nilsson, T., Slusarewicz, P., Hoe, M. H., & Warren, G. (1993). Kin recognition: a model for the retention of Golgi enzymes. *FEBS letters*, 330(1), 1-4.
- Norris, G. E., Stillman, T. J., Anderson, B. F., & Baker, E. N. (1994). The three-dimensional structure of PNGase F, a glycosyl asparaginase from *Flavobacterium meningosepticum*. *Structure*, 2(11), 1049-1059.
- Opat, A. S., Houghton, F., & Gleeson, P. A. (2000). Medial Golgi but Not Late Golgi Glycosyltransferases Exist as High Molecular Weight Complexes ROLE OF LUMINAL DOMAIN IN COMPLEX FORMATION AND LOCALIZATION. *Journal of Biological Chemistry*, 275(16), 11836-11845.
- Pan, W., Choi, S. C., Wang, H., Qin, Y., Volpicelli-Daley, L., Swan, L., ... & Wu, D. (2008). Wnt3a-mediated formation of phosphatidylinositol 4, 5-bisphosphate regulates LRP6 phosphorylation. *Science*, 321(5894), 1350-1353.
- Paulson, J. C. and Colley, K. J. (1989). Glycosyltransferases. Structure, localization, and control of cell type-specific glycosylation. *The Journal of Biological Chemistry*, 264 (30), 17615-17618.
- Piao, S., Lee, S. H., Kim, H., Yum, S., Stamos, J. L., Xu, Y., ... & Ha, N. C. (2008). Direct inhibition of GSK3beta by the phosphorylated cytoplasmic domain of LRP6 in Wnt/beta-catenin signaling. *PLoS one*, 3(12), e4046-e4046.
- Pierce, M., Buckhaults, P., Chen, L., & Fregien, N. (1997). Regulation of N-acetylglucosaminyltransferase V and Asn-linked oligosaccharide  $\beta$  (1, 6) branching by a growth factor signaling pathway and effects on cell adhesion and metastatic potential. *Glycoconjugate journal*, 14(5), 623-630.
- Pinhal, M. A., Smith, B., Olson, S., Aikawa, J. I., Kimata, K., & Esko, J. D. (2001). Enzyme interactions in heparan sulfate biosynthesis: uronosyl 5-epimerase and 2-O-sulfotransferase interact in vivo. *Proceedings of the National Academy of Sciences*, 98(23), 12984-12989.
- Pinson, K. I., Brennan, J., Monkley, S., Avery, B. J., & Skarnes, W. C. (2000). An LDL-receptor-related protein mediates Wnt signalling in mice. *Nature*, 407(6803), 535-538.
- Rhinn, M., Lun, K., Luz, M., Werner, M., & Brand, M. (2005). Positioning of the midbrain-hindbrain boundary organizer through global posteriorization of the neuroectoderm mediated by Wnt8 signaling. *Development*, 132(6), 1261-1272.
- Rives, A. F., Rochlin, K. M., Wehrli, M., Schwartz, S. L., & DiNardo, S. (2006). Endocytic trafficking of Wingless and its receptors, Arrow and DFrizzled-2, in the *Drosophila* wing. *Developmental biology*, 293(1), 268-283.

Rosen, S. D. (1993). Ligands for L-selectin: where and how many?. *Research in immunology*, 144(9), 699-703.

Roszkó, I., Sawada, A., & Solnica-Krezel, L. (2009, October). Regulation of convergence and extension movements during vertebrate gastrulation by the Wnt/PCP pathway. In *Seminars in cell & developmental biology* (Vol. 20, No. 8, pp. 986-997). Academic Press.

Roth, J. (1987). Subcellular organization of glycosylation in mammalian cells. *Biochimica et Biophysica Acta (BBA)-Reviews on Biomembranes*, 906(3), 405-436.

Roth, J. (2002). Protein N-glycosylation along the secretory pathway: relationship to organelle topography and function, protein quality control, and cell interactions. *Chemical reviews*, 102(2), 285-304.

Roth, J., Brada, D., Lackie, P. M., Schweden, J., & Bause, E. (1990). Oligosaccharide trimming Man9-mannosidase is a resident ER protein and exhibits a more restricted and local distribution than glucosidase II. *European journal of cell biology*, 53(1), 131-141.

Roth, J., Yam, G. H. F., Fan, J., Hirano, K., Gaplovska-Kysela, K., Le Fourn, V., ... & Zuber, C. (2008). Protein quality control: the who's who, the where's and therapeutic escapes. *Histochemistry and cell biology*, 129(2), 163-177.

Roth, J., Zuber, C., Park, S., Jang, I., Lee, Y., Kysela, K. G., ... & Cho, J. W. (2010). Protein N-glycosylation, protein folding, and protein quality control. *Molecules and cells*, 30(6), 497-506.

Rutishauser, U. (1992). NCAM and its polysialic acid moiety: a mechanism for pull/push regulation of cell interactions during development?. *Development*, 116(Supplement), 99-104.

Sasaki, K., Kurata-Miura, K., Ujita, M., Angata, K., Nakagawa, S., Sekine, S., ... & Fukuda, M. (1997). Expression cloning of cDNA encoding a human  $\beta$ -1, 3-N-acetylglucosaminyltransferase that is essential for poly-N-acetyllactosamine synthesis. *Proceedings of the National Academy of Sciences*, 94(26), 14294-14299.

Sayat, R., Leber, B., Grubac, V., Wiltshire, L., & Persad, S. (2008). O-GlcNAc-glycosylation of  $\beta$ -catenin regulates its nuclear localization and transcriptional activity. *Experimental cell research*, 314(15), 2774-2787.

Schachter, H. (2000). The joys of HexNAc. The synthesis and function of N-andO-glycan branches. *Glycoconjugate journal*, 17(7-9), 465-483.

Scheiffele, P., & Füllekrug, J. (2000). Glycosylation and protein transport. *Essays Biochem*, 36, 1-15.

Schmitt, M., Metzger, M., Gradl, D., Davidson, G., & Orian-Rousseau, V. (2015). CD44 functions in Wnt signaling by regulating LRP6 localization and activation. *Cell Death & Differentiation*, 22(4), 677-689.

Seberger, P. J., & Chaney, W. G. (1999). Control of metastasis by Asn-linked,  $\beta$ 1-6 branched

oligosaccharides in mouse mammary cancer cells. *Glycobiology*, 9(3), 235-241.

Seko, A., & Yamashita, K. (2004).  $\beta$ 1, 3-N-acetylglucosaminyltransferase-7 ( $\beta$ 3Gn-T7) acts efficiently on keratan sulfate-related glycans. *FEBS letters*, 556(1), 216-220.

Seko, A., & Yamashita, K. (2005). Characterization of a novel galactose  $\beta$ 1, 3-N-acetylglucosaminyltransferase ( $\beta$ 3Gn-T8): the complex formation of  $\beta$ 3Gn-T2 and  $\beta$ 3Gn-T8 enhances enzymatic activity. *Glycobiology*, 15(10), 943-951.

Seko, A., & Yamashita, K. (2008). Activation of  $\beta$ 1, 3-N-Acetylglucosaminyltransferase-2 ( $\beta$ 3Gn-T2) by  $\beta$ 3Gn-T8 POSSIBLE INVOLVEMENT OF  $\beta$ 3Gn-T8 IN INCREASING POLY-N-ACETYLLACTOSAMINE CHAINS IN DIFFERENTIATED HL-60 CELLS. *Journal of Biological Chemistry*, 283(48), 33094-33100.

Semenov, M. V., Zhang, X., & He, X. I. (2008). DKK1 antagonizes Wnt signaling without promotion of LRP6 internalization and degradation. *Journal of Biological Chemistry*, 283(31), 21427-21432.

Sengupta, P. K., Bouchie, M. P., & Kukuruzinska, M. A. (2010). N-glycosylation gene DPAGT1 is a target of the Wnt/ $\beta$ -catenin signaling pathway. *Journal of Biological Chemistry*, 285(41), 31164-31173.

Seto, E. S., & Bellen, H. J. (2006). Internalization is required for proper Wingless signaling in *Drosophila melanogaster*. *The Journal of cell biology*, 173(1), 95-106.

Shen, L., Liu, Z., Tu, Y., Xu, L., Sun, X., & Wu, S. (2011). Regulation of MMP-2 expression and activity by  $\beta$ -1, 3-N-acetylglucosaminyltransferase-8 in AGS gastric cancer cells. *Molecular biology reports*, 38(3), 1541-1550.

Shental-Bechor, D., & Levy, Y. (2008). Effect of glycosylation on protein folding: a close look at thermodynamic stabilization. *Proceedings of the National Academy of Sciences*, 105(24), 8256-8261.

Shi, Y., He, B., Kuchenbecker, K. M., You, L., Xu, Z., Mikami, I., ... & Jablons, D. M. (2007). Inhibition of Wnt-2 and galectin-3 synergistically destabilizes  $\beta$ -catenin and induces apoptosis in human colorectal cancer cells. *International journal of cancer*, 121(6), 1175-1181.

Shimomura, Y., Agalliu, D., Vonica, A., Luria, V., Wajid, M., Baumer, A., ... & Christiano, A. M. (2010). APCDD1 is a novel Wnt inhibitor mutated in hereditary hypotrichosis simplex. *Nature*, 464(7291), 1043-1047.

Shiraishi, N., Natsume, A., Togayachi, A., Endo, T., Akashima, T., Yamada, Y., ... & Sasaki, K. (2001). Identification and characterization of three novel  $\beta$ 1, 3-N-acetylglucosaminyltransferases structurally related to the  $\beta$ 1, 3-galactosyltransferase family. *Journal of Biological Chemistry*, 276(5), 3498-3507.

Spessott, W., Crespo, P. M., Daniotti, J. L., & Maccioni, H. J. (2012). Glycosyltransferase complexes improve glycolipid synthesis. *FEBS letters*, 586(16), 2346-2350.



- Spiro, R. G. (2002). Protein glycosylation: nature, distribution, enzymatic formation, and disease implications of glycopeptide bonds. *Glycobiology*, 12(4), 43R-56R.
- Stamos, J. L., & Weis, W. I. (2013). The  $\beta$ -catenin destruction complex. *Cold Spring Harbor perspectives in biology*, 5(1), a007898.
- Taelman, V. F., Dobrowolski, R., Plouhinec, J. L., Fuentealba, L. C., Vorwald, P. P., Gumper, I., ... & De Robertis, E. M. (2010). Wnt signaling requires sequestration of glycogen synthase kinase 3 inside multivesicular endosomes. *Cell*, 143(7), 1136-1148.
- Tahinci, E., Thorne, C. A., Franklin, J. L., Salic, A., Christian, K. M., Lee, L. A., ... & Lee, E. (2007). Lrp6 is required for convergent extension during *Xenopus* gastrulation. *Development*, 134(22), 4095-4106.
- Tamai, K., Semenov, M., Kato, Y., Spokony, R., Liu, C., Katsuyama, Y., ... & He, X. (2000). LDL-receptor-related proteins in Wnt signal transduction. *Nature*, 407(6803), 530-535.
- Tamai, K., Zeng, X., Liu, C., Zhang, X., Harada, Y., Chang, Z., & He, X. (2004). A mechanism for Wnt coreceptor activation. *Molecular cell*, 13(1), 149-156.
- Tanaka, K., Kitagawa, Y., & Kadowaki, T. (2002). *Drosophila* segment polarity gene product porcupine stimulates the posttranslational N-glycosylation of wingless in the endoplasmic reticulum. *Journal of Biological Chemistry*, 277(15), 12816-12823.
- Tang, X., Wu, Y., Belenkaya, T. Y., Huang, Q., Ray, L., Qu, J., & Lin, X. (2012). Roles of N-glycosylation and lipidation in Wg secretion and signaling. *Developmental biology*, 364(1), 32-41.
- Tetsu, O., & McCormick, F. (1999).  $\beta$ -Catenin regulates expression of cyclin D1 in colon carcinoma cells. *Nature*, 398(6726), 422-426.
- Tisserant, A., & Konig, H. (2008). Signal-regulated Pre-mRNA occupancy by the general splicing factor U2AF. *PLoS One*, 3(1), e1418-e1418.
- Togayachi, A., Akashima, T., Ookubo, R., Kudo, T., Nishihara, S., Iwasaki, H., ... & Narimatsu, H. (2001). Molecular cloning and characterization of UDP-GlcNAc: lactosylceramide  $\beta$ 1, 3-N-acetylglucosaminyltransferase ( $\beta$ 3Gn-T5), an essential enzyme for the expression of HNK-1 and Lewis X epitopes on glycolipids. *Journal of Biological Chemistry*, 276(25), 22032-22040.
- Togayachi, A., Kozono, Y., Sato, T., Kuno, A., Hirabayashi, J., Ikehara, Y., & Narimatsu, H. (2008). [Polylactosamine on glycoproteins regulates immune response]. *Tanpakushitsu kakusan koso. Protein, nucleic acid, enzyme*, 53(12 Suppl), 1590-1597.
- Trapnell, C., Pachter, L., & Salzberg, S. L. (2009). TopHat: discovering splice junctions with RNA-Seq. *Bioinformatics*, 25(9), 1105-1111.
- Trombetta, E. S. (2003). The contribution of N-glycans and their processing in the endoplasmic



reticulum to glycoprotein biosynthesis. *Glycobiology*, 13(9), 77R-91R.

Troy, F. A. (1992). Polysialylation: from bacteria to brains. *Glycobiology*, 2(1), 5-23.

Vagin, O., Kraut, J. A., & Sachs, G. (2009). Role of N-glycosylation in trafficking of apical membrane proteins in epithelia. *American Journal of Physiology-Renal Physiology*, 296(3), F459-F469.

Valenta, T., Hausmann, G., & Basler, K. (2012). The many faces and functions of  $\beta$ -catenin. *The EMBO journal*, 31(12), 2714-2736.

van Amerongen, R., & Nusse, R. (2009). Towards an integrated view of Wnt signaling in development. *Development*, 136(19), 3205-3214.

Van Damme, E. J., Peumans, W. J., Pusztai, A., & Bardocz, S. (1998). *Handbook of plant lectins: properties and biomedical applications*. John Wiley & Sons.

Varki, A., Cummings, R. D., Esko, J. D., Freeze, H. H., Stanley, P., Marth, J. D., ... & Etzler, M. E. (2009). Symbol nomenclature for glycan representation. *Proteomics*, 9(24), 5398-5399.

Walsh, C. (2006). *Posttranslational modification of proteins: expanding nature's inventory*. Roberts and Company Publishers.

Wassarman, P. M. (1992). Mouse gamete adhesion molecules. *Biology of reproduction*, 46(2), 186-191.

Wehrli, M., Dougan, S. T., Caldwell, K., O'Keefe, L., Schwartz, S., Vaizel-Ohayon, D., ... & DiNardo, S. (2000). *arrow* encodes an LDL-receptor-related protein essential for Wingless signalling. *Nature*, 407(6803), 527-530.

Williams, B. O., & Insogna, K. L. (2009). Where Wnts went: the exploding field of Lrp5 and Lrp6 signaling in bone. *Journal of Bone and Mineral Research*, 24(2), 171-178.

Winterhalter, P. R., Lommel, M., Ruppert, T., & Strahl, S. (2013). O-glycosylation of the non-canonical T-cadherin from rabbit skeletal muscle by single mannose residues. *FEBS letters*, 587(22), 3715-3721.

Wu, B., Crampton, S. P., & Hughes, C. C. (2007). Wnt signaling induces matrix metalloproteinase expression and regulates T cell transmigration. *Immunity*, 26(2), 227-239.

Wu, G., Huang, H., Garcia Abreu, J., & He, X. (2009). Inhibition of GSK3 phosphorylation of beta-catenin via phosphorylated PPPSPXS motifs of Wnt coreceptor LRP6. *PloS one*, 4(3), e4926-e4926.

Wuhrer, M., Deelder, A. M., & van der Burgt, Y. E. (2011). Mass spectrometric glycan rearrangements. *Mass spectrometry reviews*, 30(4), 664-680.

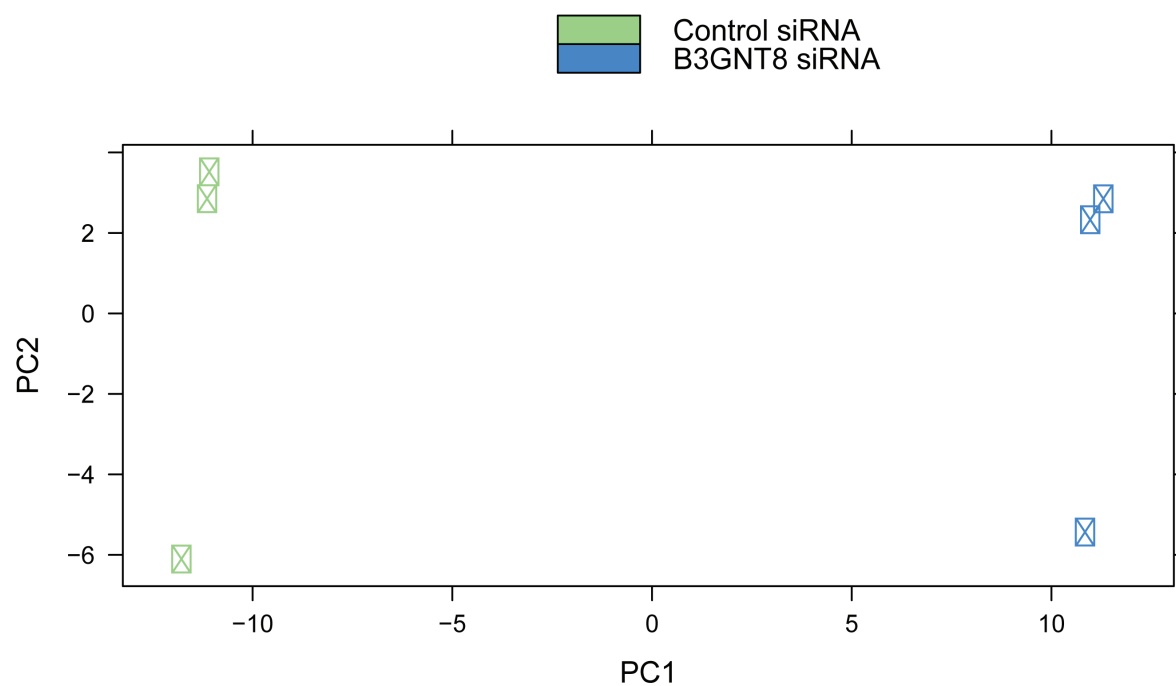
- Yamamoto, A., Nagano, T., Takehara, S., Hibi, M., & Aizawa, S. (2005). Shisa promotes head formation through the inhibition of receptor protein maturation for the caudalizing factors, Wnt and FGF. *Cell*, 120(2), 223-235.
- Yamamoto, H., Komekado, H., & Kikuchi, A. (2006). Caveolin is necessary for Wnt-3a-dependent internalization of LRP6 and accumulation of  $\beta$ -catenin. *Developmental cell*, 11(2), 213-223.
- Yamamoto, H., Sakane, H., Michiue, T., & Kikuchi, A. (2008). Wnt3a and Dkk1 regulate distinct internalization pathways of LRP6 to tune the activation of  $\beta$ -catenin signaling. *Developmental cell*, 15(1), 37-48.
- Yamashita, K., Ohkura, T., Tachibana, Y., Takasaki, S., & Kobata, A. (1984). Comparative study of the oligosaccharides released from baby hamster kidney cells and their polyoma transformant by hydrazinolysis. *Journal of Biological Chemistry*, 259(17), 10834-10840.
- Yeh, J. C., Hiraoka, N., Petryniak, B., Nakayama, J., Ellies, L. G., Rabuka, D., ... & Fukuda, M. (2001). Novel sulfated lymphocyte homing receptors and their control by a Core1 extension  $\beta$ 1, 3-N-acetylglucosaminyltransferase. *Cell*, 105(7), 957-969.
- Zhang, J., Schulze, K. L., Hiesinger, P. R., Suyama, K., Wang, S., Fish, M., ... & Scott, M. P. (2007). Thirty-one flavors of Drosophila rab proteins. *Genetics*, 176(2), 1307-1322.
- Zhang, P., Elabd, S., Hammer, S., Solozobova, V., Yan, H., Bartel, F., ... & Blattner, C. (2015). TRIM25 has a dual function in the p53/Mdm2 circuit. *Oncogene*.
- Zhou, D. (2003). Why are glycoproteins modified by poly-N-acetylglucosamine glycoconjugates?. *Current Protein and Peptide Science*, 4(1), 1-9.
- Zhou, S. M., Cheng, L., Guo, S. J., Zhu, H., & Tao, S. C. (2011). Lectin microarrays: a powerful tool for glycan-based biomarker discovery. *Combinatorial chemistry & high throughput screening*, 14(8), 711-719.
- Zhu, W., Shiojima, I., Ito, Y., Li, Z., Ikeda, H., Yoshida, M., ... & Komuro, I. (2008). IGFBP-4 is an inhibitor of canonical Wnt signalling required for cardiogenesis. *Nature*, 454(7202), 345-349.
- Zuber, C., & Roth, J. (2009). N-glycosylation. *The Sugar Code. Fundamentals of Glycosciences*, 87-110.
- Zuber, C., Fan, J. Y., Guhl, B., Parodi, A., Fessler, J. H., Parker, C., & Roth, J. (2001). Immunolocalization of UDP-glucose: glycoprotein glucosyltransferase indicates involvement of pre-Golgi intermediates in protein quality control. *Proceedings of the National Academy of Sciences*, 98(19), 10710-10715.
- Zuber, C., Spiro, M. J., Guhl, B., Spiro, R. G., & Roth, J. (2000). Golgi apparatus immunolocalization of endomannosidase suggests post-endoplasmic reticulum glucose trimming: implications for quality control. *Molecular biology of the cell*, 11(12), 4227-4240.

## Appendix:

Sample ID	Sample Ref	Index	Yield (Mbases)	% PF	# Reads	Mean Quality Score (PF)
11	Human	ATCACG	2.790	95,26	57.439.096	37,9
12	Human	TTAGGC	4.865	95,15	100.255.042	37,94
13	Human	ACTTGA	3.688	95,23	75.929.558	37,95
31	Human	GATCAG	2.939	95,52	60.319.302	37,94
32	Human	TAGCTT	2.343	95,44	48.131.594	37,99
33	Human	GGCTAC	3.758	95,53	77.127.878	37,98

**Supplementary Table 1: Quality of raw reads after base calling.**

Quality of raw reads has been assessed with RTAv1.13 (Illumina). Statistics for both reads are indicated. PF: cluster passing Illumina chastity filter.



**Supplementary Figure 1: Principal Component Analysis.**

Principal Component Analysis of biological triplicates of Control siRNA treated HEK 293T cells versus B3GNT8 siRNA treated HEK293T cells.

### Supplementary Table 2: Differentially regulated genes in B3GNT8 silenced HEK293 cells

The genes of this table reacted to B3GNT8 silencing with differential regulation. Genes were selected with p-values lower than 0.05 and differential regulation either more than 2.5fold or less than 0.4 fold. Upregulated genes are colored green, downregulated genes are colored red.

<b>Ensembl identifier</b>	<b>Wiki Gene Name</b>	<b>fold change</b>	<b>adjusted p-value</b>
ENSG00000256304	no name	8,91	5,70E-33
ENSG00000156096	UGT2B4	7,60	5,61E-20
ENSG00000119411	BSPRY	5,94	8,34E-31
ENSG00000126562	WNK4	5,19	4,79E-36
ENSG00000185070	LOC100506718	4,74	5,86E-11
ENSG00000204086	RPA4	4,71	3,69E-08
ENSG00000230002	ALMS1-IT1	4,48	1,06E-15
ENSG00000250091	no name	4,35	6,58E-10
ENSG00000188282	RUFY4	4,29	2,75E-06
ENSG00000224080	no name	3,85	3,12E-11
ENSG00000117595	IRF6	3,77	1,14E-07
ENSG00000166349	RAG1	3,77	3,04E-10
ENSG00000099399	MAGEB2	3,71	1,90E-14
ENSG00000248971	no name	3,71	1,72E-11
ENSG00000160588	MPZL3	3,64	1,50E-45
ENSG00000068028	RASSF1	3,62	3,85E-38
ENSG00000232630	no name	3,59	1,21E-18
ENSG00000267655	no name	3,44	1,58E-05
ENSG00000272373	no name	3,42	1,87E-11
ENSG00000260787	no name	3,31	2,22E-05
ENSG00000248498	no name	3,31	1,12E-07
ENSG00000213693	SEC14L1P1	3,30	3,74E-13
ENSG00000076554	TPD52	3,29	6,16E-52
ENSG00000104388	RAB2A	3,25	3,43E-63
ENSG00000228672	PROB1	3,25	5,17E-06
ENSG00000154479	CCDC173	3,19	9,78E-09
ENSG00000176933	TOB2P1	3,15	8,38E-10
ENSG00000112599	GUCA1B	3,15	1,41E-05
ENSG00000140835	CHST4	3,14	9,91E-05
ENSG00000204387	C6orf48	3,13	3,71E-52
ENSG00000154237	LRRK1	3,12	3,03E-15
ENSG00000025434	NR1H3	3,12	1,23E-27
ENSG00000180287	PLD5	3,11	5,24E-05
ENSG00000230069	no name	3,07	3,67E-09
ENSG00000137474	MYO7A	3,00	0,000158264
ENSG00000227184	EPPK1	2,98	6,50E-08
ENSG00000230873	STMND1	2,97	1,41E-05
ENSG00000188467	SLC24A5	2,89	2,30E-08
ENSG00000142675	CNKSR1	2,87	1,59E-12

<u>Ensembl identifier</u>	<u>Wiki Gene Name</u>	<u>fold change</u>	<u>adjusted p-value</u>
ENSG00000169031	COL4A3	2,87	2,34E-06
ENSG00000263235	no name	2,87	1,09E-10
ENSG00000204934	ATP6V0E2-AS1	2,86	8,74E-31
ENSG00000055732	MCOLN3	2,84	4,90E-55
ENSG00000162772	ATF3	2,82	4,53E-49
ENSG00000106404	CLDN15	2,79	2,15E-34
ENSG00000073605	GSDMB	2,79	3,06E-26
ENSG00000261589	no name	2,75	6,52E-16
ENSG00000184351	KRTAP19-1	2,75	0,000304951
ENSG00000102057	KCND1	2,74	2,47E-06
ENSG00000158815	FGF17	2,74	0,000567185
ENSG00000197748	WDR96	2,74	6,64E-08
ENSG00000228451	no name	2,72	8,44E-06
ENSG00000213385	no name	2,71	0,000255645
ENSG00000184545	LOC101927562	2,68	1,10E-11
ENSG00000259706	HSP90B2P	2,68	0,000522812
ENSG00000124602	UNC5CL	2,66	1,57E-07
ENSG00000272003	no name	2,64	9,52E-06
ENSG00000120675	DNAJC15	2,64	3,62E-05
ENSG00000113555	PCDH12	2,63	0,000226773
ENSG00000128567	PODXL	2,63	2,77E-41
ENSG00000158806	NPM2	2,62	0,001436297
ENSG00000171219	CDC42BPG	2,61	6,04E-09
ENSG00000185002	RFX6	2,61	8,27E-06
ENSG00000107829	FBXW4	2,60	1,09E-27
ENSG00000100156	SLC16A8	2,60	0,001071234
ENSG00000117586	TNFSF4	2,60	8,16E-06
ENSG00000179456	ZBTB18	2,58	2,25E-45
ENSG00000249641	HOXC-AS5	2,57	2,43E-05
ENSG00000163377	FAM19A4	2,56	0,000622485
ENSG00000185950	IRS2	2,55	3,09E-18
ENSG00000178381	ZFAND2A	2,55	7,32E-20
ENSG00000226180	no name	2,55	2,74E-08
ENSG00000270020	no name	2,54	0,000366311
ENSG00000175832	ETV4	2,54	8,68E-05
ENSG00000177519	RPRM	2,53	1,50E-07
ENSG00000231769	no name	2,52	3,62E-05
ENSG00000112812	PRSS16	2,51	1,93E-17
ENSG00000231738	TSPAN19	2,51	0,000863201
ENSG00000153093	ACOXL	2,51	0,000285579
ENSG00000255389	TRAF3IP2-AS1	2,50	7,37E-08
ENSG00000230524	COL6A4P1	2,50	5,02E-07

<u>Ensembl identifier</u>	<u>Wiki Gene Name</u>	<u>fold change</u>	<u>adjusted p-value</u>
ENSG00000137261	KIAA0319	2,50	1,07E-07
ENSG00000123124	WWP1	0,40	6,50E-38
ENSG00000109063	MYH3	0,40	4,30E-15
ENSG00000139292	LGR5	0,40	4,13E-06
ENSG00000119922	IFIT2	0,40	0,002569915
ENSG00000259511	UBE2Q2L	0,40	5,22E-05
ENSG00000100526	CDKN3	0,40	1,68E-33
ENSG00000263004	no name	0,39	3,02E-07
ENSG00000113658	SMAD5	0,39	2,55E-43
ENSG00000113356	POLR3G	0,39	2,51E-40
ENSG00000004139	SARM1	0,39	1,15E-09
ENSG00000188158	NHS	0,39	1,80E-14
ENSG00000110092	CCND1	0,38	9,29E-43
ENSG00000126016	AMOT	0,38	8,60E-44
ENSG00000134049	IER3IP1	0,38	2,02E-24
ENSG00000249395	CASC9	0,38	2,66E-07
ENSG00000134376	CRB1	0,38	0,000156232
ENSG00000125931	CITED1	0,38	7,71E-12
ENSG00000087116	ADAMTS2	0,38	1,65E-16
ENSG00000184985	SORCS2	0,38	0,000444268
ENSG00000149212	SESN3	0,37	2,82E-43
ENSG00000170396	ZNF804A	0,37	7,18E-12
ENSG00000130649	CYP2E1	0,37	6,47E-08
ENSG00000178343	SHISA3	0,37	1,46E-09
ENSG00000115252	PDE1A	0,37	1,78E-06
ENSG00000134531	EMP1	0,37	5,35E-05
ENSG00000179902	C1orf194	0,37	0,000589306
ENSG00000171522	PTGER4	0,37	0,000228211
ENSG00000236871	no name	0,37	3,20E-09
ENSG00000249992	TMEM158	0,36	1,58E-11
ENSG00000127870	RNF6	0,36	2,90E-26
ENSG00000253123	no name	0,36	1,18E-09
ENSG00000143320	CRABP2	0,36	1,26E-37
ENSG00000196104	SPOCK3	0,35	1,44E-10
ENSG00000261770	no name	0,35	4,63E-05
ENSG00000160801	PTH1R	0,35	0,000184165
ENSG00000011028	MRC2	0,35	5,04E-28
ENSG00000164466	SFXN1	0,35	1,32E-72
ENSG00000095713	CRTAC1	0,35	1,78E-06
ENSG00000130635	COL5A1	0,34	4,23E-27
ENSG00000138801	PAPSS1	0,34	1,25E-46
ENSG00000104490	NCALD	0,34	2,97E-11

<u>Ensembl identifier</u>	<u>Wiki Gene Name</u>	<u>fold change</u>	<u>adjusted p-value</u>
ENSG00000143494	VASH2	0,34	3,88E-32
ENSG00000110422	HIPK3	0,33	1,85E-49
ENSG00000174460	ZCCHC12	0,33	6,76E-45
ENSG00000253669	no name	0,32	9,80E-08
ENSG00000168621	GDNF	0,32	1,25E-09
ENSG00000087245	MMP2	0,32	1,52E-23
ENSG00000170961	HAS2	0,32	1,35E-07
ENSG00000140450	ARRDC4	0,32	2,97E-73
ENSG00000161681	SHANK1	0,31	9,53E-08
ENSG00000249328	RP11-26J3.1	0,31	1,71E-10
ENSG00000100292	HMOX1	0,30	1,79E-39
ENSG00000197467	COL13A1	0,30	1,27E-17
ENSG00000171388	APLN	0,30	2,10E-14
ENSG00000254290	no name	0,30	4,57E-19
ENSG00000102393	GLA	0,30	7,00E-55
ENSG00000198252	STYX	0,29	3,71E-53
ENSG00000184185	LOC100996843	0,29	5,53E-33
ENSG00000146070	PLA2G7	0,29	1,55E-09
ENSG00000155011	DKK2	0,29	8,73E-06
ENSG00000229404	LINC00858	0,28	9,51E-18
ENSG00000177469	PTRF	0,28	1,49E-56
ENSG00000115461	IGFBP5	0,28	6,63E-32
ENSG00000146250	PRSS35	0,27	4,00E-24
ENSG00000042493	CAPG	0,27	2,19E-14
ENSG00000273237	no name	0,27	9,05E-20
ENSG00000183691	NOG	0,26	2,10E-06
ENSG00000253414	no name	0,26	5,95E-27
ENSG00000104953	TLE6	0,25	3,24E-07
ENSG00000050030	KIAA2022	0,25	7,57E-19
ENSG00000203504	no name	0,24	6,69E-12
ENSG00000168542	COL3A1	0,23	2,33E-25
ENSG00000260837	no name	0,22	1,11E-08
ENSG00000166033	HTRA1	0,22	1,85E-50
ENSG00000188729	OSTN	0,21	2,61E-11
ENSG00000135046	ANXA1	0,17	7,73E-34



# Acknowledgements

---

My greatest thanks go to my wife Gabriela who greatly supported me: your love has carried me through this time. And I thank my daughter Isabella: with your smile you gave me cheerful mornings and evenings. Through you Gods love becomes apparent.

Special thanks also to Brigitte, Klaus, Hildegard, Hans, Adriana and Mircea for all their love and support.

I sincerely thank Dr. Gary Davidson for his constant intellectual input und advice with regard to my experiments and my presentations. I am thankful for his time he spent by commenting on this thesis and that I was allowed to enter this research field in his lab. I am especially thankful for his understanding and support after my daughter Isabella was born.

I thank my thesis advisory committee members Andrew Cato, Ute Schepers and Bastian Rapp. Their ideas, advice and cooperation have accompanied my work beyond the TAC meetings. And I thank Andrew Cato and Ute Schepers for evaluating this thesis.

I thank the Forschungsgruppe FOR1036 for helpful ideas and cooperation, especially Christian Thiel and Nastassja Himmelreich. Similarly I thank Olivier Armant for the RNAseq cooperation, Christoph Niehrs for the truncated LRP6 constructs and Joachim Wittbrodt for the medaka cDNA library.

I thank my lab members Janine Wesslowski, Yihang Wu, Yi Su, Ping Zang, Ching Chen, Sven Rosswag und Tanja Kuhn. Thanks also go to Nicole Sims for the help with the genomewide screen, Serge Lozowoj and Charlotte Sauerland for the help with the hexose experiments, Manuel Mannuss for the help with the exoglycosidase experiments, Serguei Bourov for the setup of a share at the Large Scale Data Facility and Steffen Scholpp for his ideas. I thank all the ITG members for their support and fun.

I also thank the former Wnt PhD student group for open discussions. The group consisted of Janine Wesslowski, Mark Schmitt, Eliana Stanganello und Marit Metzger.

My research was financed by the BioInterfaces Programme of the Helmholtz-Forschungsgemeinschaft (HFG). I thank the BioInterfaces Graduate School for interesting courses and the possibility to bring my ideas into the PhD programme by creating an own course and by setting up a PhD student retreat.

# Dank

---

Mein allergrößter Dank geht an meine Ehefrau Gabriela, die mich in dieser Zeit großartig unterstützt hat: Deine Liebe hat mich durch diese Zeit getragen. Und ich danke meiner Tochter Isabella: Mit Deinem Lächeln hast Du mir fröhliche Morgen und Abende geschenkt. Durch Euch wird Gottes Liebe sichtbar.

Ein besonderer Dank auch an Brigitte, Klaus, Hildegard, Hans, Adriana und Mircea für all Eure Liebe und Unterstützung.

Ich danke besonders Dr. Gary Davidson für seinen konstanten gedanklichen Input und seine Ratschläge bezüglich meiner Experimente und meiner Präsentationen. Ich bin dankbar für die Zeit, die er aufgewendet hat um diese Thesis zu kommentieren, und dass ich in seinem Labor in dieses interessante Forschungsgebiet eintreten durfte. Ich bin besonders dankbar für sein Verständnis und seine Unterstützung nach der Geburt meiner Tochter Isabella.

Ich danke meine Thesis Advisory Committee Mitgliedern Andrew Cato, Ute Schepers und Bastian Rapp. Sie haben mich mit ihren Ideen, Ratschlägen und Kooperationen auch über das TAC Meeting hinaus begleitet. Und ich danke Andrew Cato und Ute Schepers für das Evaluieren dieser Thesis.

Der Forschungsgruppe FOR1036 danke ich für hilfreiche Ideen und Kooperationen, besonders Christian Thiel und Nastassja Himmelreich. Genauso danke ich Olivier Armant für die Kooperation bei der RNAseq, Christoph Niehrs für die trunkierten LRP6 Konstrukte und Joachim Wittbrodt für die Medaka cDNA library.

Ich danke meinen Labormitgliedern Janine Wesslowski, Yihang Wu, Yi Su, Ping Zang, Ching Chen, Sven Rosswag und Tanja Kuhn. Dank geht auch an Nicole Sims für die Hilfe beim genomweiten Screen, Serge Lozowoj und Charlotte Sauerland für die Hilfe bei den Hexose-Experimenten, Manuel Mannuss für die Hilfe bei den Exoglycosidase-Experimenten, Serguei Bourov für die Einrichtung eines Shares bei der Large Scale Data Facility und Steffen Scholpp für seine Ideen. Ich danke allen Mitgliedern des ITG für Unterstützung und Spaß.

Ich danke auch der ehemaligen Wnt PhD student group für offene Diskussionen. Diese bestand aus Janine Wesslowski, Mark Schmitt, Eliana Stanganello und Marit Metzger.

Meine Forschung wurde möglich gemacht durch finanzielle Unterstützung des BioInterfaces Programmes der Helmholtz-Forschungsgemeinschaft. Ich danke der BioInterfaces Graduate School für interessante Kurse und die Möglichkeit meine eigenen Ideen in einem eigenen Kurs und in der Gestaltung des student retreats mit einbringen zu dürfen.

# Curriculum Vitae

---

## Persönliche Daten:

Name: Diplom-Biologe (KIT) Nico Andreas Braunegger  
Anschrift: Gothaer Straße 22  
76139 Karlsruhe  
Tel.: 015 15 / 88 24 187  
Nico.Braunegger@gmail.com

geboren am/in: 11. April 1982 in Baden-Baden  
Staatsangehörigkeit: Deutsch  
Familienstand: Verheiratet



## Berufs- und Bildungsweg:

Mär'12-Sep'15	Promotion
Sep'11-Feb'12	Fachliche Vorbereitung auf die Promotion
Jul'11-Aug'11	Berlin-Chemie AG
Jan'10-Jun'11	pharmexx GmbH
Okt'04-Okt'09	Studium Diplom-Biologie (KIT)
Apr'03-Okt'04	Studium Diplom-Betriebswirtschaftslehre (Universität Frankfurt am Main)
Sep'01-Jul'02	Zivildienst (ISB Karlsruhe)
Sep'98-Sep'01	Allgemeine Hochschulreife (HLA Rastatt)
Sep'88-Sep'98	Mittlere Reife (Realschule Kuppenheim)

Karlsruhe, den 09. September 2015